INTRINSIC GROUNDWATER POLLUTION VULNERABILITY OF MASAMA EAST WELL FIELD, KHURUTSHE AREA, BOTSWANA

Moshe Moses Kanaimba

200804449

A Thesis submitted to

GEOLOGY DEPARTMENT, FACULTY OF SCIENCE

UNIVERSITY OF BOTSWANA

In partial fulfilment of the requirements for the degree of
MASTER OF SCIENCE IN HYDROGEOLOGY

Supervisors:

Prof. Nata T. Tafesse

Dr. Kebabonye Laletsang

Gaborone

2019

APPROVAL

This project, Intrinsic Groundwater Pollution Vulnerability Assessment of Masama east well field, Khurutshe Area, Botswana, submitted to the Geology Department, University of Botswana, has been accepted as satisfactory for the partial fulfillment of the requirements for the degree of Master in Science and approved as to its style and contents.

……..

Prof. Nata T. Tafesse

Supervisor

Geology Department

Faculty of Science

University of Botswana

DECLARATION

I, Moshe Moses Kanaimba, declare that the thesis that I herewith submit for the Master Degree in Hydrogeology at the Geology Department, Faculty of Sciences, University of Botswana, is my independent work, and that I have not previously submitted it for a qualification at another institution of higher education. To the best of my knowledge and belief, the thesis contains no material previously published or written by another person except where due reference is made.

……

Moshe Moses Kanaimba

…….…….. 2019

ACKNOWLEDGEMENTS

I would like to express my heart-felt thanks to the following institutions and individuals for their contribution towards the completion of this thesis.

- Department of Water Affairs (DWA) for permitting me to conduct my research in Masama East well field, Khurutshe area, Botswana.
- Water Surveys Botswana for providing me with the data required for my thesis and sponsoring my data collection exercise. The experience and knowledge I acquired during my time in the field is valuable and I will forever be grateful for their support.
- The University of Botswana, Geology Department for providing a platform for me to pursue Master of Science in Hydrogeology. I appreciate the lectures and laboratory facilities availed to me.
- My supervisors, Prof. Nata T. Tafesse and Dr. Kebabonye Laletsang for their support and guidance during the course of the programme. They sacrificed their time and energy to ensure that I complete my studies and that is highly appreciated.
- My family, colleagues and friends for their occasional support and advice.
- Lastly and most important, God, for his grace. He is the reason I was able to overcome many obstacles and complete my thesis. Amen!!

ABSTRACT

An intrinsic groundwater pollution vulnerability assessment was conducted in Masama east well field, Botswana. The well field is located in close proximity to residential and agricultural land and might be exposed to the risk of groundwater pollution. The DRASTIC index model was applied to assess the groundwater pollution vulnerability of the study area. The technique combined a series of mathematical equations, physio-chemical properties of the study area and GIS to produce the standard groundwater pollution vulnerability map. The map was then calibrated using the sensitivity analysis to reduce the subjectivity associated with the DRASTIC index model and increase its accuracy. Additionally, the land use parameter was incorporated into the calibrated DRASTIC map to reflect the direct impact of human activities on the environment. These adjustments resulted in the production of the groundwater pollution vulnerability map of Masama east well field. This map was classified into four groundwater vulnerability classes labeled very low, low, moderate and high groundwater vulnerability. The very low, low, moderate and high groundwater vulnerability zones accounted for 39.0%, 19.9%, 27.5% and 13.6% of the total study area, respectively. Model validation was achieved using the spearman rank correlation coefficient and by visually comparing the nitrate distribution map of the study area and the land use map. The outcome of this study can be utilized as a guide by the land use planners, decision makers and the general public to divert activities that present greater risk of groundwater pollution to low vulnerability zones and preserve the water quality in the well field.

TABLE OF CONTENTS

LIST OF FIGURES

LIST OF TABLES

LIST OF EQUATIONS

LIST OF ABBREVIATIONS AND SYMBOLS

ADR	Advective-Dispersive-Reactive
AVI	Aquifer Vulnerability Index
BH	Borehole
BOS	Botswana Bureau of Standards Drinking Water
BRGM	Bureau de Recherche Geologiques et Minieres
$CaCO_3$	Calcium carbonate
Ca^{2+}	Calcium ion
Cd	Cadmium
Cl^-	Chloride ion
CMB	Chloride Mass Balance
Cr	Chromium
CRT	Constant Rate Test
Cu	Copper
DEM	Digital Elevation Model
DGS	Department of Geological Surveys
DI	DRASTIC Index
DRASTIC	Depth to groundwater, net Recharge, Aquifer media, Soil media, Topography, Impact of Vadose Zone, hydraulic Conductivity
DWA	Department of Water Affairs

EC	Electrical conductivity
ENE	East North East
ESE	East South East
F^-	Fluoride ion
FAO	Food and Agricultural Organization
Fe^{2+}	Iron (II) ion
GCS	Groundwater Consulting Services
GIS	Geographic Information System
GOD	Groundwater occurrence, Overall lithology of aquifer, Depth to groundwater table
HCO_3^-	Bicarbonate ion
HCS	Hydrogeological Complex and Setting
IDW	Inverse Distance Weighting
K^+	Potassium ion
km	Kilometer
km^2	Square kilometer
LULC	Land Use and Land Classification
m	Meter
Ma.	Million years ago
MDI	Modified DRASTIC Index
mg/l	Milligrams per liter

Mg^{2+}	Magnesium ion
mm	Millimeters
Mn^{2+}	Manganese ion
MRSA	Map Removal Sensitivity Analysis
m^2	Square meter
m^3	Cubic meter
m.a.s.l	Meters above sea level
m.b.g.l	Meters below ground level
Na^+	Sodium ion
Ni	Nickel
NNE	North North East
NNW	North North West
NO_3^-	Nitrate ion
Pb	Lead
pH	Potential hydrogen
r_s	Spearman Rank Correlation Coefficient
SO_4^{2-}	Sulphate ion
SPSA	Single Parameter Sensitivity Analysis
SRTM	Shuttle Radar Topographic Mission
SSE	South South East

SSW	South South West
SWL	Static Water Level
SWS	Schlumberger Water Services
TD	Total atmospheric chloride deposition from precipitation and dry fall out
TDS	Total Dissolved Solids
UNEP	United Nations Environment Programme
UNESC	United Nations Economic and Social Council
USA	United States of America
US EPA	United States Environmental Protection Agency
UTM	Universal Transverse Mercator
WGS	World Geodetic System
WHO	World Health Organization
WNW	West North West
WSW	West South West
WofE	Weights of Evidence
WSB	Water Surveys Botswana
µS	micro Siemens
^{0}C	Degrees Celsius
^{0}E	Degrees East
^{0}S	Degrees South

1. INTRODUCTION

1.1 Background

Freshwater is estimated to be 2.5% of all water on Earth and serves as an essential resource for global development and the survival of living things (Shiklomanov, 1993; cited from Sorichetta, 2010). However, this resource has become increasingly scarce over the last four decades leading to a safe drinking water deprived human population and the condition will be aggravated by detrimental human habits such as mining, infrastructural development, crop and livestock production (Oke, 2015; Li and Merchant, 2013). Kinzelbach et al. (2002) predicted that two out of three people will live in water-deprived areas and Africa will experience extreme water shortage in twenty countries by the year 2025. Desertification makes matters worse in the sense that majority of the land in Africa is covered by deserts which are gradually expanding (UNESC, 2007). This phenomenon is characterized by the limited number of surface water resources arising from low rainfall and skyrocketing evapotranspiration rates.

The Kalahari Desert, located in Southern Africa covers two thirds of Botswana limiting the surface water resources to the extreme north regions of Okavango and Chobe. The country experiences rainfall amounts ranging from 250 - 650 mm/annum with variation in both time and space. Low rainfall combined with high evapotranspiration rate and the existence of soil cover that has limited ability to retain water lead to the scarcity of water in most parts of the country hence the prevalence of successive long periods of droughts associated with the La Nina and El Nino phenomena (Wingqvist and Dahlberg, 2008). In the presence of limited surface water resources and an increasing population, the demand exceeds the supply of water in the country which makes groundwater a vital and reliable alternative resource.

Wingqvist and Dahlberg (2008) also state that 80% of all the water used in Botswana during the year 2005 was groundwater and this pile a lot of pressure on the resource hence the requirement for adequate protection and sustainable consumption. The same authors emphasized the importance of protecting a groundwater resource over long periods of time by stating that upon their introduction into an aquifer, the pollutants and their effects are expensive and near impossible to remove.

Groundwater pollution is referred to as loss of usable water due to its interaction with pollutants that infiltrated to the groundwater system from the surface (Kinzelbach et al., 2002) and it has resulted in limited groundwater resources in the country with regards to both quality and quantity. Both confined and unconfined aquifers are susceptible by some degree to groundwater pollution, even though deep confined aquifers may be deteriorated due to the more persistent pollutants over long periods of time (Robins et al., 2007). Therefore, it is essential to assess their vulnerability for the earliest identification of areas that are highly susceptible to pollution and their subsequent protection from the potential pollutants in order to conserve the groundwater quality.

Previous studies revealed the occurrence of groundwater contamination in Ramoutswa, Ghanzi, Mochudi and Serowe well fields among others in the country (Alemaw et al., 2004; Lewis et al., 1978). Minimization of groundwater pollution in Botswana is hindered by water governing laws such as the Water Act of 1968 and the Waterworks Act of 1962 which tend to be inadequate in their treatment of water pollution as well as monitoring and enforcement mechanisms hence the need for them to be reviewed (Centre for Applied Research, 2005). Another factor may be the lack of urgency towards the prevention and remediation of groundwater pollution occurrence by the relevant stakeholders entrusted with the role of governing the land and water resources (Robins et al., 2007).

This study is conducted in Masama east well field, Khurutshe area, Botswana. Masama east well field was commissioned as a back up to the North-South Water Carrier pipeline that supply freshwater to the greater Gaborone area from dams and well fields in the north parts of Botswana. The DRASTIC index model is used to evaluate the groundwater pollution vulnerability of the well field. The model was selected due to its ability to make use of readily available data and flexibility to combine with other methods (Jovanovic et al., 2006). The expected outcome was an overlay map indicating zones of high, moderate and low groundwater pollution vulnerability that can be utilized as a guide by the land use planners, decision makers and the general public to divert activities that present greater risk of groundwater system pollution to low vulnerability zones and preserve the water quality in the well field.

1.2 Statement of the Problem

Masama east well field is at risk of groundwater pollution by virtue of being located in close proximity with human settlements and agricultural activities. The continuous application of fertilizers and pesticides, improper disposal of waste or wastewater into the ground and spreading of manure constitute some of the activities that are more likely to introduce pollutants in to the groundwater system in the area. This poses a threat to the quality of the groundwater resources in the well field and it requires the implementation of a water management system that encourages sustainable development and caters for sensitivity of groundwater resources (Liggett and Gilchrist, 2013).

As a precautionary measure, DWA implemented the Botswana groundwater quality protection strategy to monitor groundwater quality and to ensure that the mandatory wellhead protection zones are established for every newly developed groundwater resource in the country (Stephenson et al., 2004). It is worth noting that wellhead protection zones account for small portions in relatively large well fields as they are established around boreholes only (Mclaren et al., 1996). It is imperative that a groundwater vulnerability assessment be conducted in such zones for early identification of high vulnerability areas and their subsequent protection from potential pollutants in order to prevent further loss of groundwater resources in Botswana. This research is proposed to evaluate the groundwater pollution vulnerability of the entire Masama east well field area, including portions omitted when establishing wellhead protection zones.

1.3 Research Questions

1.3.1 Primary Question

What is the potential groundwater pollution vulnerability of Masama east well field?

1.3.2 Specific Questions

- What are the potential pollutants in Masama east well field?
- What is the current state of groundwater quality in Masama east well field?
- How much is the amount of groundwater recharge per annum in Masama east well field?

- How many types of aquifers exist in Masama east well field and what are their characteristics?

1.4 Objectives

1.4.1 *General Objective*

The general objective of the study is to assess the potential groundwater vulnerability of the Masama east well field to pollution.

1.4.2 *Specific Objectives*

The specific objectives of the study include:

- To identify the potential pollutants in the study area;
- To determine the current quality of groundwater in the study area;
- To estimate the amount of recharge in the study area; and,
- To determine the aquifer types and their characteristics in the study area.

1.5 Description of the Study Area

1.5.1 Location and Accessibility

Masama east well field is used in this study to refer to a portion in the Khurutshe area that comprises two developed well fields namely Masama and Makhujwane in the Karoo Supergroup Formations (Figure 1.1). It is located approximately 100 km north of Gaborone along the south eastern margin of Botswana bounded between 26.339 to 26.614°E and 23.760 to 24.051°S and has an area of about 729.4 km^2. Masama east well field can be accessed using the main A1 road passing along its western edge, plus a network of unpaved roads and tracks (**Figure 1.1**). A few settlements such as Dibete, Artesia and Leshibitse exist within and around the study area.

1.5.2 Topography and drainage

Masama east well field lies within the Limpopo River Basin along the south eastern margin of Botswana. This basin is shared between four countries namely, Botswana, South Africa, Zimbabwe and Mozambique. It is divided into three portions known as the Upper, Middle and

Lower Limpopo River Reaches. Masama east well field falls within the Notwane river catchment, which is a tributary to the Limpopo River in the Upper Limpopo River Reach, an area known for its irregular flow patterns and high susceptibility to dry spells caused by successive drought periods (Petrie et al., 2015). The drainage of the area is influenced by the topography which conforms to the local geology and it follows a general south easterly direction into the Notwane River (Ashton et al., 2001; WSB, 2015). Masama east well field is a relatively flat plain that exhibits a gentle slope towards the Notwane River, except for the occurrence of ridges which follow the orientation of lineaments in the area. The highest elevation point is 995 m.a.s.l. in the northwestern parts of the well field near Dibete Village and the lowest point is at 885 m.a.s.l located towards the southeastern margin (Figure 1.1).

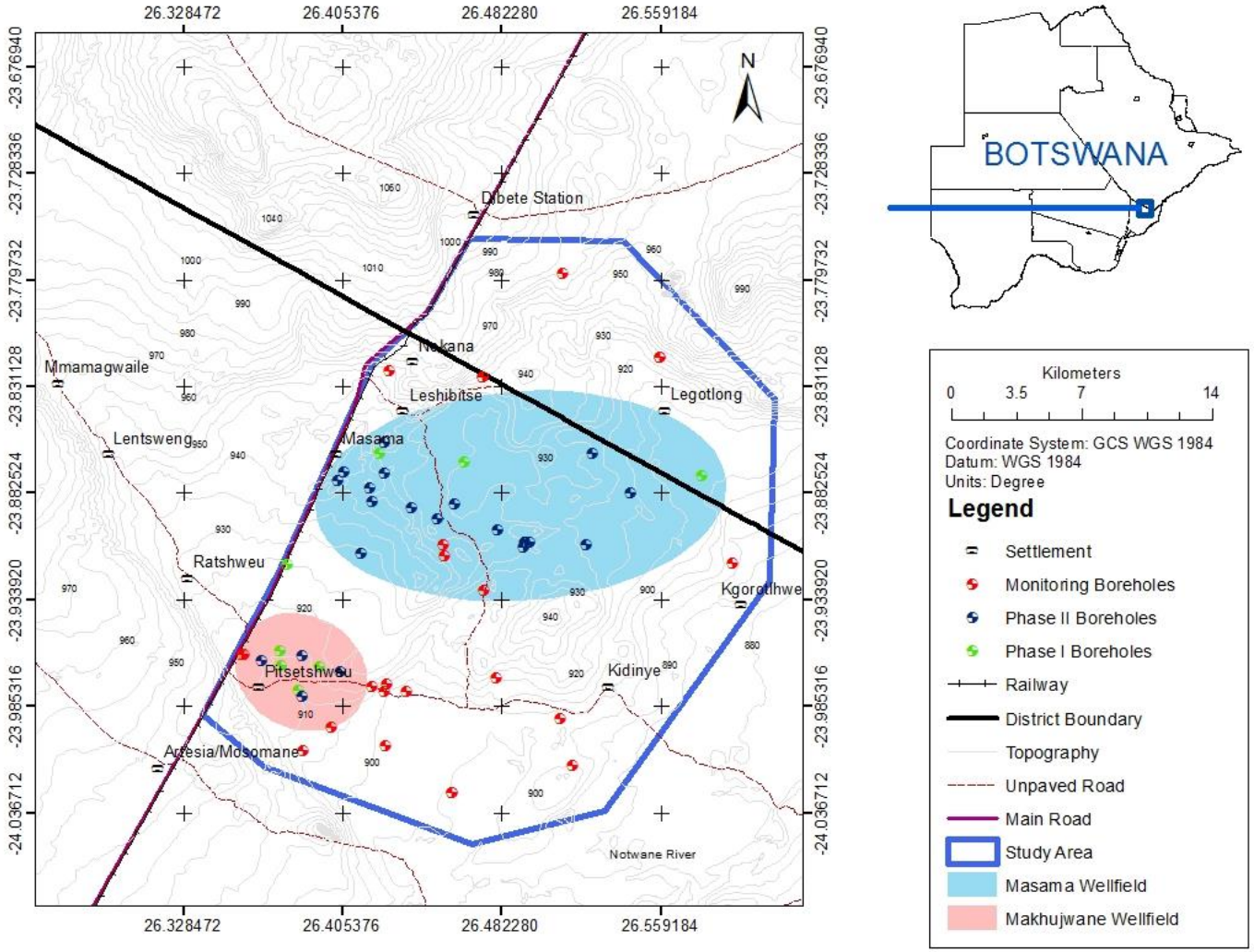

Figure 1.1. Location map of the study area (Source: DGS, 2009).

1.5.3 Climate

Due to its location on the fringes of the Kalahari Desert, the well field exhibits semi-arid climatic conditions characterized by hot summer and cold winter seasons with an average annual rainfall and temperature of 438 mm and 20.5^{o}C, respectively. The rainy season falls between November and March. The lowest temperature occurs during the months May to August, which is also the driest period of the year with rainfall reaching lows of 1mm (Acquah, 2007). High evapotranspiration rates are common in the study area, especially during the prolonged drought periods and they might be the reason why the occurrence of surface water resources is limited in both areal extent and quantity. Wingqvist and Dahlberg (2008) predicted a further increase in temperature in Botswana of 1 to 3 ^{o}C by the year 2050, thus exacerbating the scarcity of water in the region due to even higher evapotranspiration rates.

1.5.4 Soil

The well field has four different types of soils namely, ferralic arenosols (sandy), luvic arenosols (sandy loam), petric calcisols (gravel) and calcaric luvisols (loamy). Arenosols are deep sandy soils originating from weathered quartz-rich rocks that exhibit a course texture which explains their high permeability and low water retention capacity (Verbeek, 1990). They also have weak soil structure, they are normally non-plastic when wet and loose when dry (Mweso, 2003; Joshua, 1991). They comprise of 50-75% of fine sand and usually 5% of clay content and the occurrence of minimized run-off from rainfall events is common (Joshua, 1991). According to the soil map provided by the Ministry of Agriculture, two types of arenosols exist in the study area and they are ferralic and luvic arenosols. Luvic arenosols are characterized by the development of a layer of clay or the increment of clay within 125cm of the soil horizon. These are moderate to well drained brown sandy loam soils located in the extreme southwest portion of the study area (Joshua, 1991). Ferralic arenosols are fine to medium sands and they are found mostly in the central portion of the study area with some patches in the extreme NNE portion (Joshua, 1991).

Luvisols on the other hand can be defined as loamy soils exhibiting a variation in the amount of sand and clay, and they are associated with alluvial deposits. They have moderate to high permeability and usually form a crust which reduces the permeability because of higher clay content (Mweso, 2003). These are fertile soils which are best suited for various agricultural

activities and they occur mostly in flat or gentle slopes in areas with recognizable dry and wet periods (FAO, 2015). Calcareous luvisols located on the eastern margin, contain calcium carbonate and are the second most abundant soil type in the study area. Calcisols are common in arid and semi-arid regions on flat to hilly terrains, and they are characterized by presence of secondary carbonates in their structure. Petric calcisols are located on the southern portion of the well field and they can be distinguished by the presence of 40% or more oxidic solid mass or coarse rock fragments (Verbeek, 1990).

1.5.5 Land use

The study area contains a few settlements and one village namely Leshibitse, which is more populated and developed than the others. The primary economic activities in the area are livestock production and rain-fed crop farming. However, rain-fed crop farming is only limited to the rainy season which makes the livestock production the major economic activity in the study area (Masike, 2008). The area is predominantly used for free range grazing a phenomenon that can be attributed to the decline in rain-fed agricultural activities in the country due to recurrent and prolonged drought periods. In terms of spatial area, rain-fed crop farming accounts for approximately 5% whereas the rest of the study area is used for free range grazing (WSB, 2015). Crops grown in the area include sorghum, beans and melons which tend to cope with less fertile soil (WSB, 2015).

1.5.6 Vegetation

There are two vegetation groups found in Masama east well field: hardveld and transition hardveld-sandveld, with the latter occupying approximately 90% of the area. The hardveld forms a small portion in the extreme north east of the study area and it is associated with plant species such as Acacia Tortilis, Terminalia Sericea and Peltophorum Africanum. The transition hardveld-sandveld is associated with the Acacia Tortilis, Terminalia Sericea and Ziziphus Mucronata. Acacia Tortilis is known locally as *Mosu* and it forms a structure with the resemblance of an umbrella, hence the other name, the umbrella thorn. It is a drought resistant plant species that is common in regions with erratic rainfall and has the ability to cope with temperature as high as 50^{o}C (Verma, 2016).

Peltophorum Africanum (known locally as *Mosetlha*) is a deciduous tree that is common in warmer and dry parts of Southern Africa experiencing rainfall from 300 - 900 mm per annum. It grows well in deep sandy to sandy loam soil derived from sandstone or quartzite and has a growth rate between 1 and 1.5 m per annum. This tree is considered a botanical indicator of high concentrations of arsenic in the soil when it occurs in excess (Mongalo, 2013). Terminalia Sericea is a small tree (6 – 9 m tall) that survives in very poor soils which are regarded as non-conducive for farming activities. It is also a drought resistant species that is suitable for afforestation and land improvement purposes (Amri, 2010). Ziziphus Mucronata (buffalo thorn), known as *Mokgalo* by the locals normally takes the form of a shrub or medium tree reaching heights of up to 9m. It grows well in the company of other thorny plant species in dry, drought stricken regions and it is a botanical indicator of groundwater presence (Manyarara et al., 2016).

1.5.7 Population and water supply and demand

Majority of the high water demand centers are located in the eastern margin of Botswana where more than half of the country population reside. These centers depended on surface water extracted from dams, pans and rivers to meet their water demand. However, recurrent droughts, population distribution and erratic rainfall patterns in such areas lead to a decline in the quantity of surface water resources. The water demand rose and the attention turned to groundwater which now represents over 56% of all the water consumption in the eastern margin of the country (Masike, 2008). Future projections indicate that both groundwater and surface water will not be able to meet the high demand in these centers, including the study area (Masike, 2008). This may be attributed to high abstraction rates due to skyrocketing livestock numbers and low replenishment rates of both surface and groundwater resources (Masike, 2008). The greater Gaborone area requires 110, 000 m^3/day of water of which 20, 000 m^3/day is supplied by Masama east wellfield through the North South Carrier (WSB, 2015).

1.6 Structure of the Thesis

The structure of this thesis is outlined below.

Chapter 1

This chapter reflects on the background and importance of this study to Botswana and the scientific field in general. It also identifies and explains the problem in the study area as well as the expected outcome of the study. This section further provides an in-depth description of the study area and outlines the research questions and objectives of the study.

Chapter 2

The geological and hydrogeological characteristics of Masama well field are discussed in this section. All the rock sequences and geological structures within the well field are characterized and their role in groundwater flow as well as pollutant transportation is also discussed. Geologic maps and borehole logs are used to provide a clear picture of the geology of Masama east well field.

Chapter 3

Relevant research media, e.g. journal articles, books are examined in this section to demonstrate a good comprehension of the groundwater pollution vulnerability concept as well as the methods and requirements of evaluating groundwater vulnerability of a given area. Several definitions and methods are discussed in relation to the current study and the gap in literature that is to be filled. Case studies are also analyzed to determine the performance of various groundwater vulnerability methods and assess their suitability to this study. Potential pollutants identified in the well field are also reviewed to determine their implications on the environment with respect to health and water quality.

Chapter 4

This section outlines and describes all the techniques, equipment, software and data used in the execution of groundwater pollution vulnerability assessment of Masama east well field. The type

of data required and its sources as well as the steps taken in calibrating and validating the groundwater pollution vulnerability model are clearly stated in this section.

Chapter 5

In-depth interpretation and analysis of the results of this study is provided and the validity of the groundwater pollution vulnerability technique used is determined. The outcome of this study is presented in the form of tables and a set of overlay maps corresponding to the various physio-chemical properties of the well field. The implications of these result and model calibration are also fully discussed. Water quality data, e.g. nitrates concentrations and various drinking water standards are used to validate the outcome of the study either by visual inspection or application of statistical techniques.

Chapter 6

The findings obtained in the previous section are summarized and their implications on the area of interest are discussed with the main emphasis being on the gap in literature that is filled by this study. That is, the contribution made by this study to the scientific field is outlined in this section and recommendations on how to improve outcome of this study are also provided.

Chapter 7

This section provides a list of all publications/ documents cited in this study.

2. GEOLOGY AND HYDROGEOLOGY OF THE STUDY AREA

2.1 Geology

2.1.1 Lithostratigraphy of the study area

Kalahari Group

The study area is located on the eastern fringes of the Central Kalahari Karoo basin hence the dominance of the Karoo Supergroup Formations of the Mesozoic era within its boundaries (Modie, 2000). The basin covers approximately 70% of Botswana and it is characterized by a blanket cover in the form of the Kalahari Group of the Cenozoic age, including the study area (Figure 2.2). As a result the occurrence of rock outcrops is limited and the geology of the area was mainly deduced from borehole logs and geophysical data analysis (Bordy et al., 2010). The sand, calcretes and clay of Kalahari Beds Formation form the youngest sequence in the study area (Table 2.1). Borehole logs indicate that these beds vary in thickness throughout the study area, increasing from roughly 1 meter in ENE to over 40 meters in the WSW portion.

Post Karoo Dolerites

The post Karoo dolerite dykes and sills are located in the SSW portion of the well field and they bear the orientation, ESE-WNW. These igneous rocks intruded both the Karoo and Waterberg formations in the well field (Figure 2.1). Borehole logs indicate that the dolerites are weathered at shallower depth (<50 m.b.g.l) while they are fresher at greater depth (>70 m.b.g.l) in some parts of the study area.

Stormberg Basalt Group

The Stormberg Basalt Group forms the uppermost layer of the Karoo sequence and it is normally unconformably overlain by the Kalahari Group within the study area (Segwabe, 2008; Bordy et al., 2000). This group is characterized by crystalline and massive amygdaloidal basalts of the Ramoselwana Volcanic Formation. The flood basalt formation exhibits variable thickness ranging from a few meters to over 350 meters, more especially towards the south western portion of the study area where it is dominant. Segwabe (2008) also correlated the Stormberg Basalt Group with the Drakensberg Group of the main Karoo Basin in the Republic of South Africa.

Lebung Group

The Ntane Sandstone Formation of Lebung Group is unconformably overlain by the Stormberg Basalt Group and the Kalahari Group in the absence of the basaltic formation. It is composed of fine to medium grained and well-sorted Aeolian sandstone (Bordy et al., 2000). The formation occurs in purple and brown colors and it exhibits well rounded grains, implying extensive reworking and the possibility of an external source (Modie, 2000). The base of the Lebung Group, Mosolotsane Formation comprises of reddish siltstones and fine-grained sandstones (Masike, 2008). A study conducted by Bordy et al. (2010) revealed the deposition environment of Mosolotsane Formation to be a meandering river system in semi-arid climatic conditions. The Ntane Sandstone Formation is the only member of the Lebung Group that has outcrops in the study area in Leshibitse village. The Group covers part of the northern half and accounts for roughly 25% of the total well field area.

Beaufort Group

The non-carbonaceous mudstones and siltstones of Tlhabala Formation underlie the Mosolotsane Formation and forms part of the stratigraphy correlated with the Beaufort Group in the main Karoo basin. Tlhabala Formation is located along the eastern and northwestern margins within the study area. It is also found south west of the well field area in the Artesia and Mmamantswe region, beneath the cover of the Kalahari Beds Group and beyond the boundaries of the well field area (WSB, 2015).

Ecca Group

The coal bearing upper Ecca Group comprises the Letlhakeng, Korotlo and Dibete Formations. These formations are composed of coal, mudstones, siltstones and sandstones (Table 2.1). The Mmamabula Formation constitutes the middle part of the Ecca Group and it is composed of interceded sandstone, siltstone and carbonaceous mudstones. Field observations indicate that the sandstone is characterized by angular grains which reflect that they may have been transported over a relatively shorter distance (Modie, 2000). Mmaphashalala Formation is the base of the Ecca Group sequence and consists of post-glacial lacustrine mudstones and siltstones.

Dwyka Group

Dukwi Formation of the Dwyka Group represents the base of the Karoo sequence and it comprises of tillites and shales, varved siltstones and mudstones. Studies conducted by Smith (1984) and Williamson (1996) concluded that Karoo sequence was initially deposited in a marine environment which later transformed into a terrestrial environment as a result of invasion by flora and fauna (Segwabe, 2008). The presence of coal within the Ecca Group Formations justifies the above statement since the formation of coal deposits is associated with deltaic depositional environments (Modie, 2000).

Molopo Farm Complex

The upper part of the Molopo Farm Complex layered intrusive rocks are found in the northwest portion of the study area, but beyond its boundary. This igneous intrusion consists of norites which are attributed to a similar deposition time as the Bushveld Igneous Complex in the Republic of South Africa, i.e. 2044 Ma. (Wigley, 1995). Norites are mostly composed of orthopyroxene and plagioclase with chromite and phlogopite occurring as rare constituents (Reichhardt, 1994). Like most formations within the well field, the Molopo Farm Complex is also overlain by the sands, silcretes and calcretes of the Kalahari Group.

Waterberg Group

Apart from the Karoo Supergroup sequence, formations known as the Waterberg Group from the Proterozoic age are exposed beneath the Kalahari Group in the extreme south eastern portion of the study area. This sequence is made up of the Masama Sandstone, Lokgalo Siltstone, Twee Rivier Sandstone and Manyelanong Hill Formations (Figure 2.1). These formations consist mostly of reddish sandstones, siltstones, conglomerates and shales as illustrated in Table 2.1.

Archaean Basement

The granite gneiss and amphibolite of the Limpopo mobile belt form the Archaean basement in the study area. The basement is overlain by both the Waterberg and Karoo Supergroup Formations with no occurrence of outcrops throughout the study area.

2.1.2 Geologic structures of the study area

Masama east well field is also located within the southern belt of the Central Kalahari Sub-Basin, a portion of the Central Kalahari Karoo Basin bordered to the south by pre-Karoo sequences and the Zoetfontein Fault in the north (Modie, 2000). The Central Kalahari Basin, itself is considered to represent a synform plunging in the northwest orientation (Pretorius, 1978 cited in Segwabe, 2008). Although the Karoo Formations in Botswana including the study area have undergone intense faulting, they can still be correlated with each other (Segwabe, 2008). Findings from geophysical surveys attributed the Central Kalahari Karoo basin to a rift basin characterized by the dominance of WNW-ESE trending faults forming horst and graben structures within the study area (Modie, 2007 cited in Segwabe, 2008; Lindhe et al., 2014). Some of these faults are associated with the Zoetfontein Fault system and coincide with the boundaries of the Karoo sequnce in the study area, signifying a potential influence from the Pre-Karoo geologic structures that had undergone reactivation during the Waterberg Supergroup era (Segwabe, 2008).

Boleleme, Masama, Pitsetshweu, Makhujwane, Quarantine, Seswane and Khurutshe faults are some of the faults that lead to block faulting in the study area resulting in compartmentalized geologic formations. Another major geologic structure located in the study area is the regional mid-Karoo unconformity that separated the lower Karoo sequence deposited during an era termed as a period of regional sag and the upper Karoo sequence associated with a period of regional uplift (Segwabe, 2008). The Stormberg Basalt and Lebung Groups form the upper Karoo sequence whereas the Beaufort, Ecca and Dwyka Formations correspond with the lower Karoo sequence.

Table 2.1. Geology of Masama east well field (Adopted from Smith, 1984).

Age	Stratigraphic Unit			Lithology
	Supergroup	Group	Formation	
Cenozoic		Kalahari	Kalahari Beds	Sand, calcrete and clay
			Post Karoo Dolerites	Dolerite dykes & sills, diorites, granodiorites and syenites
Mesozoic	Karoo	Stormberg Basalt	Ramoselwana Volcanics	Crystalline, massive, amygdaloidal basalt
		Lebung	Ntane Sandstone	Aeolian sandstone. Medium to fine-grained with minor mudstone intercalations. Partially fluvial towards the base
			Mosolotsane	Fluvial red beds. Siltstone and fine- grained sandstone
		Beaufort	Tlhabala	Non-carbonaceous mudstones and siltstones with minor sandstones
		Ecca	Letlhakeng	Siltstones and carbonaceous mudstones with coal
			Korotlo	Coals and coaly mudstones and sandstone
			Dibete	Coals and carbonaceous mudstones
			Mmamabula, (upper, middle, and lower)	Interceded sandstone, siltstone and carbonaceous mudstones
			Mmaphashalala	Post-glacial lacustrine mudstones and siltstones marking the base of the Ecca Group
		Dwyka	Dukwi	Base of Karoo sequence, tillites and shales, varved siltstones and mudstones
			Upper Molopo Farm Complex	Norites
Proterozoic	Waterberg		Twee Rivier Sandstone	Sandstone
			Masama	Red arkosic sandstone, quartzites, siltstones, shale & greywacke
			Lokgalo	Reddish siltstone, mudstone and shales
			Manyelanong Hill	Reddish sandstone and conglomerate
Archaean	Basement	Limpopo Mobile Belt		Granite gneiss and amphibolite

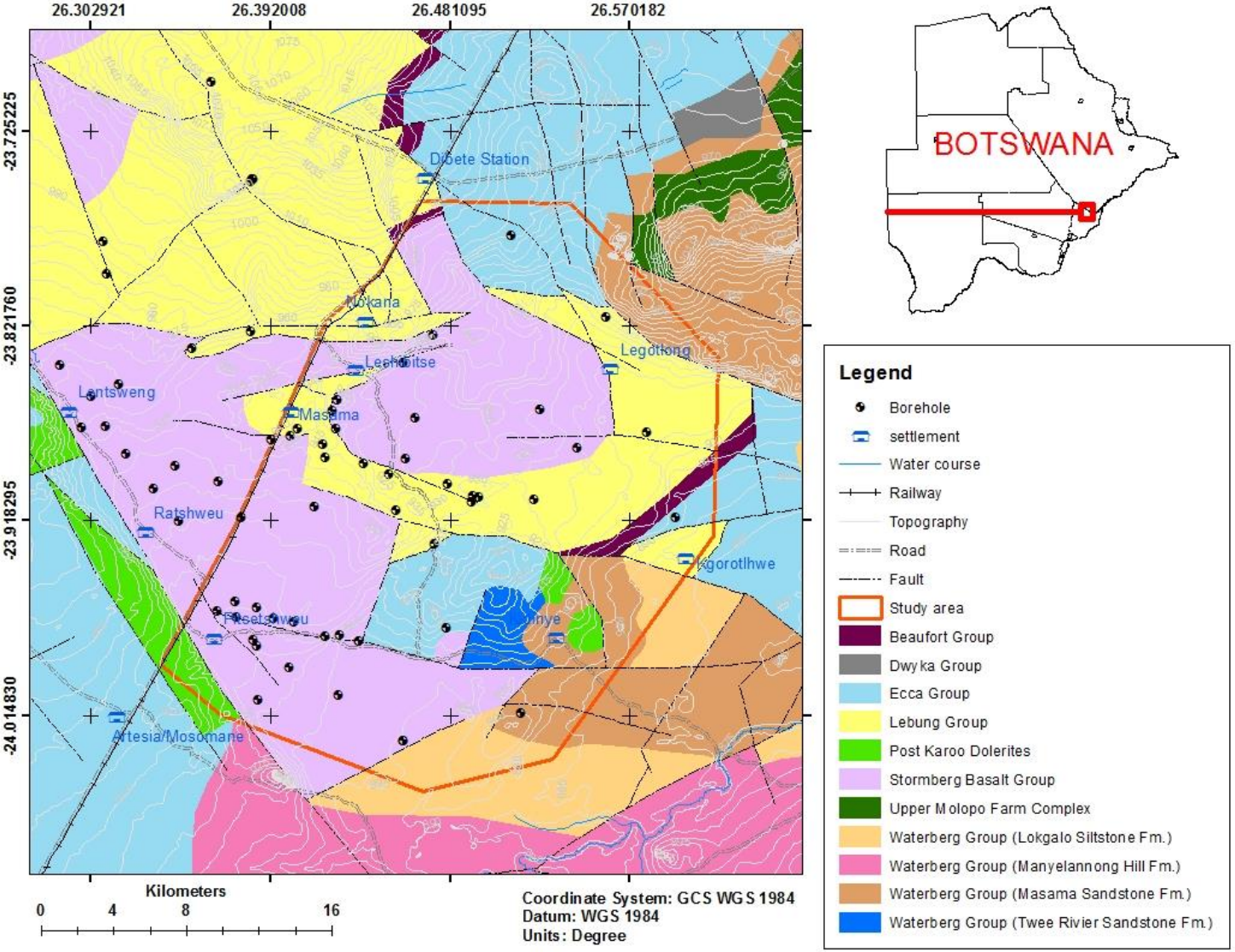

Figure 2.1. Geologic map of the study area (Source: DGS, 2009).

Figure 2.2. Distributions of the Karoo Basins in Southern Africa (after Bordy et al., 2010).

2.2 Hydrogeology

Groundwater is mostly found within the Karoo Formations, particularly the Ntane sandstone which is considered to be the main aquifer in the area although the Mmamabula sandstone also bears significant amounts of groundwater. These two feldspathic sandstones are classified as fractured porous aquifers, i.e. they exhibit dual porosity since water flows through both their pore spaces within the rock matrix and the fractures as well (Masike, 2008). Although the Ntane sandstone aquifer is a dual porosity medium, majority of the groundwater is found along portions that have undergone intense fracturing. This was proven by the occurrence of high yield boreholes along

fractured zones compared to other zones (Masike, 2008). These fractured zones resulted from a series of SSE-NNW and ENE-WSW trending faults that intersect each other (Figure 2.1).

Ntane sandstone aquifer is confined in portions of the well field overlain by the Stormberg Basalt Group, i.e. in the southwestern and central portions (Figure 2.3). It is also unconfined across the northern half of the well field area, particularly the portions whereby the Lebung Group is exposed beneath the Kalahari Beds Formations (Figure 2.1). The average thickness of the Ntane sandstone aquifer was estimated at 120m within the study area. Both the transmissivity and storativity vary throughout the aquifer ranging from 3 - 1500 m^2/day and 0.00003 - 0.009, respectively (WSB, 2015). A 200m thick aquiclude made up of the Mosolotsane, Tlhabala, Letlhakeng and Korotlo Formations divides the Ntane sandstone and Mmamabula sandstone aquifers by forming an impermeable horizontal layer between them (WSB, 2015; Masike, 2008). The aquiclude occurs mostly beneath zones delineated in the geologic map as the Stormberg Basalt and Lebung Groups (Figure 2.1).

Ntane sandstone aquifer has proven to be a high transmissivity zone even though groundwater is encountered at great depths thus resulting in drilling of deep boreholes (Masike, 2008). There are 79 boreholes drilled within the study area with depth ranging from 30.00 – 471.00 m.b.g.l, having an average depth of 210.70 m.b.g.l. Majority of these boreholes tap into the Karoo aquifers, particularly the Ntane Sandstone Formation and they are located along or near fault zones. A total of 74 boreholes terminate within the Ntane Sandstone Formation and their estimated groundwater yield ranges from 34.00 – 100.00 m^3/h. The static water level recorded in these boreholes ranged from 33.02 – 130.85 m.b.g.l. Three boreholes terminate within the Ecca Group and two of them were dry during the groundwater level monitoring exercise. The static water level and the estimated groundwater yield in the non-dry borehole were 51.50 m.b.g.l. and 80.00 m^3/h, respectively. The two remaining boreholes all terminate within the Waterberg Group and they were both dry during the groundwater level monitoring exercise hence the lack of information regarding their static water level and estimated groundwater yield.

The distance between these boreholes varies from 10m to over 1km. Borehole logs obtained from the study area indicate that boreholes drilled within the Ntane Sandstone Formation either terminate within the sandstone or the underlying Mosolotsane Formation (Figure 2.4). As a result,

the impact of the regional mid-Karoo unconformity on groundwater movement in the well field could not be established since the boreholes terminate tens of meters above it.

The Karoo aquifers constitute more than 80% of the study area whereas the remaining portion is covered by the Waterberg fractured aquifers. Aquifers from the Waterberg Supergroup are associated with faulting and dolerite intrusions whereby groundwater flow occurs along fracture zones only, and they have lower yields of groundwater compared to the Karoo Supergroup aquifers (Masike, 2008). Perched aquifers also exist in the well field with depth ranging from 10 - 40 m.b.g.l as indicated by borehole records. Hund-dug wells are used locally to retrieve groundwater from these aquifers and it is used for domestic consumption and to support small scale livestock production (Masike, 2008).

Ashton et al. (2001) justified the occurrence of groundwater and active recharge within the Ntane sandstone in Botswana basing on results from drilling activities. Recharge values vary in the study area depending on the method of estimation. Values of 1.6 mm/year and 9 - 18 mm/year were obtained from soil moisture balance method and chloride mass balance method, respectively (Masike, 2008). Previous studies also revealed that recharge tends to be higher under unconfined conditions and around Masama fault zone whereby the Stormberg basalt is thinner (Masike, 2008). Faults occurring throughout the study area lead to block faulting and compartmentalized geologic formations. These compartments are only hydraulically continuous in the presence of faults positioned side by side, otherwise they form barriers of groundwater flow (Masike, 2008; WSB, 2015).

Field observations revealed the existence of improperly constructed pit latrines in Leshibitse and poor waste management or disposal, constituting some of the factors that have been known to lead to a decline in water quality in the Limpopo River Basin (Petrie et al., 2015). However, the quality of groundwater in the study area remains within acceptable limits for human consumption with respect to both the WHO and BOS 32:2009 Class I drinking water specifications. Borehole records indicate that the total dissolved solids range from 90 - 515.6 mg/l, with an average of 297.81 mg/l within the study area which means groundwater from the well field can be classified under the freshwater category.

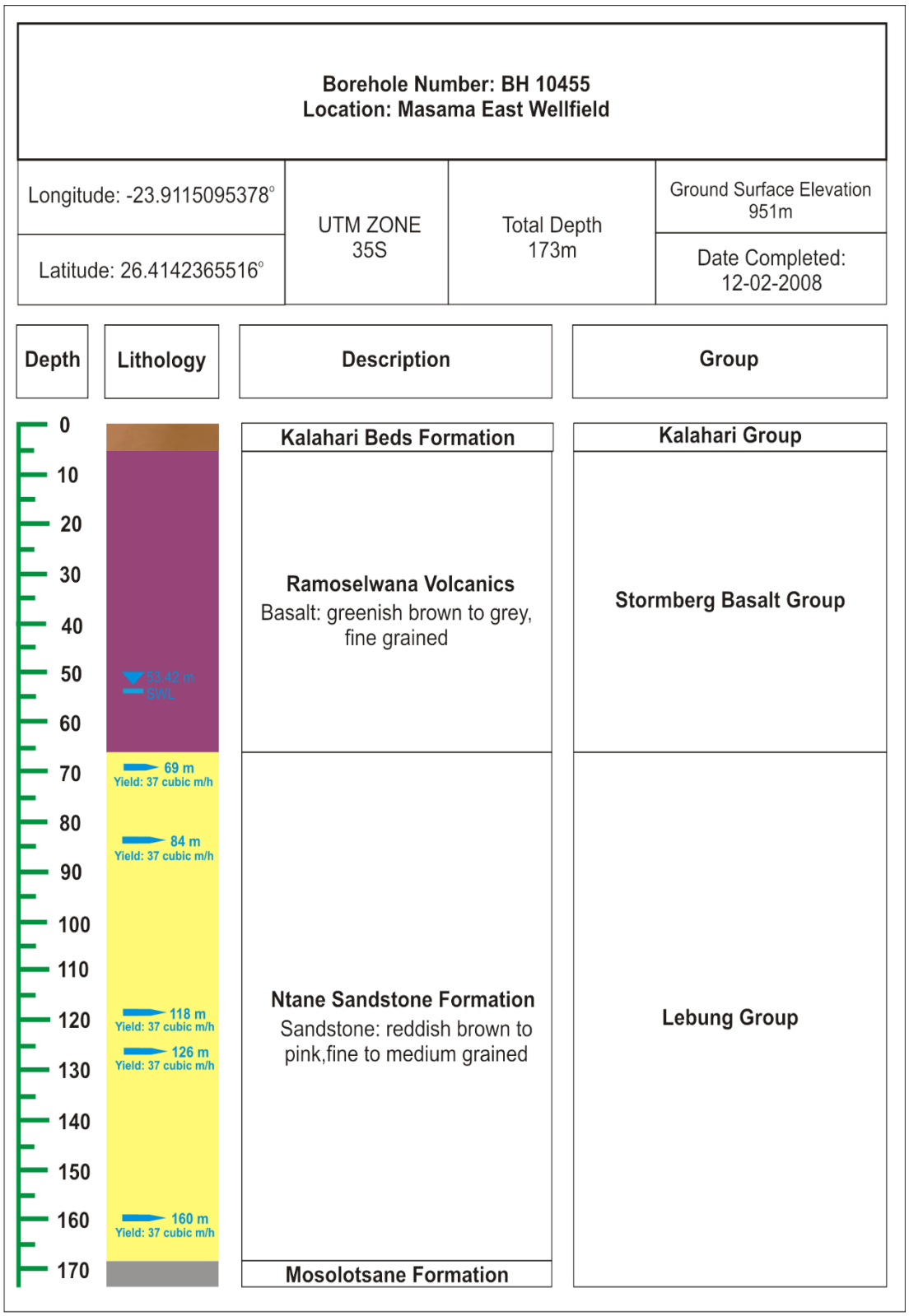

Figure 2.3. Borehole log from the confined portion of Ntane Sandstone Aquifer.

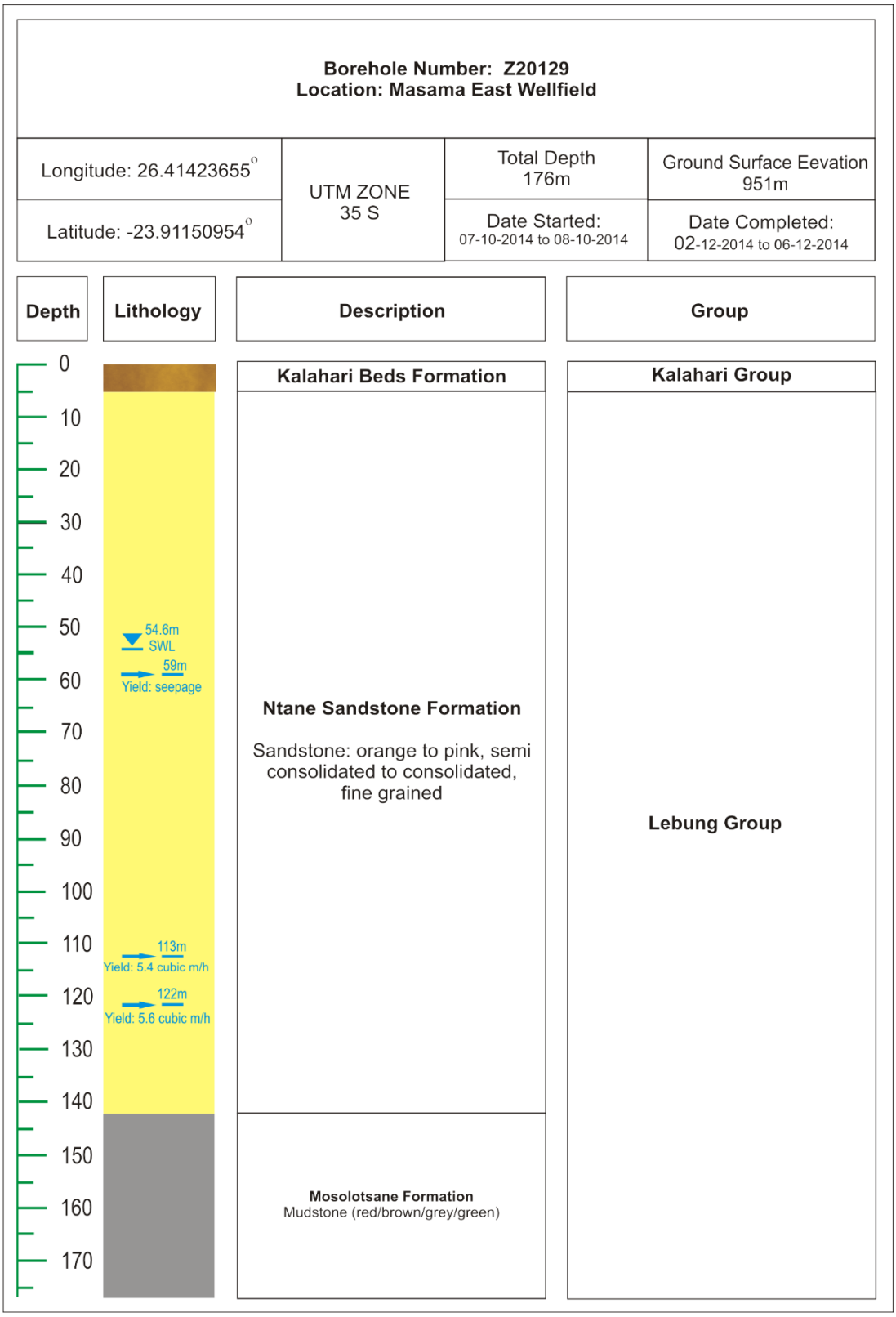

Figure 2.4. Borehole log from an unconfined portion of the Ntane Sandstone Aquifer.

3. LITERATURE REVIEW

3.1 Definition of groundwater vulnerability

Groundwater vulnerability studies date back to the late sixties when methods such as Hydrogeological Complex and Setting (HCS) method were applied for the first time (Oke, 2015). Ever since then, numerous studies have been conducted on the subject matter and received a wide coverage in literature. Despite being in existence for over 50 years, the term groundwater vulnerability still has no single definition agreed upon by the scientific community (Daly et al., 2002; Soricheta, 2010). The definition of groundwater vulnerability has been refined over time and some of the definitions proposed in the past are documented below.

Albinet and Margat (1970) defined groundwater pollution vulnerability as "the penetrating and spreading abilities of the pollutants in aquifers according to the nature of the surface layers and the hydrogeological conditions" (cited in Soricheta, 2010).

Bachmat and Collin (1987) stated that, "groundwater vulnerability is the sensitivity of groundwater quality to anthropogenic activities which may prove detrimental to the present and/or intended usage-value of the resources" (cited in Vrba and Zoporozec, 1994).

NRC (1993) referred to groundwater vulnerability to contamination as "the tendency or likelihood for contaminants to reach a specified position in the groundwater system after introduction at some location above the uppermost aquifer" (cited in Focazio et al., 2002).

3.2 Basic concepts of groundwater vulnerability

Groundwater pollution vulnerability is dependent on the natural characteristics of the hydrogeological setting, i.e. how it interacts with the variety of materials entering it and also on the physio-chemical characteristics of the specific contaminants (Robins et al., 2007; Vrba & Zoporozec, 1994; Focazio et al., 2002; Jovanovic et al., 2006). Therefore, there is the need to study such characteristics for any given area before determining its groundwater vulnerability state. Although groundwater vulnerability is not a measurable property, it is dependent on the fact that some portions exhibit a higher groundwater pollution vulnerability in relation to the others, for any hydrogeological setting (Vrba & Zoporozec, 1994).

Oke (2015) mentioned two kinds of groundwater vulnerability namely, intrinsic and specific groundwater vulnerability. Intrinsic vulnerability of groundwater is induced by human activities and considers the geo-hydrological properties of an area, although it does not depend on the contaminant type and source, whereas specific vulnerability of groundwater considers the characteristic of a certain contaminant or set of contaminants and relates them to the different aspects of the intrinsic vulnerability (Daly et al., 2002; Goldscheider et al., 2000; Gogu & Dassargues, 2000).

Furthermore, groundwater vulnerability methods can be classified as resource protection and source protection vulnerability methods. This is purely based on the target of the groundwater vulnerability assessment. Goldscheider et al. (2000) states that the groundwater surface is the target for the resource protection vulnerability and the route to it consist of vertical movement via the overlying formations whereas water in the borehole is the target for the source protection vulnerability and the route to it is a horizontal pathway in the aquifer.

3.3 Groundwater vulnerability assessment methods

3.3.1 *Subjective methods*

Subjective methods make use of the different properties (e.g. geology) of an area and the assignment of scores or indices to each property. They are divided into three more sub-groups: hydrogeological complex setting method, parametric system method and subjective hybrid method.

Hydrogeological Complex Setting Method

The HCS assumes that the groundwater vulnerability of two regions are similar provided their hydrogeological properties are also similar (Vrba and Zoporozec, 1994). It is mostly used to evaluate groundwater vulnerability of any given area on a medium to broad scale (Soricheta, 2010).

Parametric System Method

According to (Soricheta, 2010) parametric system methods make use of parameters and ratings to evaluate groundwater vulnerability of any given area, e.g. Matrix system, rating system and Parametric count system methods. Matrix system method uses a combination of fixed parameters

and rating to assess groundwater vulnerability of any site at a local scale whereas the rating system method uses a combination of a dynamic set of parameters and ratings to assess groundwater vulnerability of any site. Parametric count system method is similar to both matrix system and rating system methods except for the application of weights in order to illustrate how vital the parameters are in evaluating groundwater vulnerability. Some of the most widely applied parametric system methods including the method of choice for this study, DRASTIC index model are discussed below.

DRASTIC index model

This is a parametric count system method applied throughout the world on both local and regional scales (Soricheta, 2010). It was developed by the United States Environmental Protection Agency (US EPA) for application in groundwater contamination at a specific location with respect to its hydrogeological parameters (Aller et al., 1987; Knox et al., 1993). The term DRASTIC stands for the parameters depth to groundwater, net recharge, aquifer media, soil media, topography, impact of vadose zone and hydraulic conductivity of the aquifer. These parameters play an important role in the groundwater flow system and they are normally described at any given site with the aid of ranges, ratings and weights obtained from look-up tables provided (Piscopo, 2001). The rated and weighted parameters are normally interpolated to produce map elements that illustrate the variation of such parameters in a given area.

The magnitude of groundwater vulnerability at the given sites is computed in the form of DRASTIC index (DI). This is a dimensionless value obtained from the summation of the product of the rating and weight of each parameter. Higher DI values indicate areas of high-risk to groundwater pollution (Knox et al., 1993; Piscopo, 2001). The map elements are normally overlaid to form the standard DRASTIC index map of the given area using the equation below.

$$\mathbf{DI} = \mathbf{D_r D_w} + \mathbf{R_r R_w} + \mathbf{A_r A_w} + \mathbf{S_r S_w} + \mathbf{T_r T_w} + \mathbf{I_r I_w} + \mathbf{C_r C_w} \qquad (3\text{-}1)$$

Where;

- r is the rating for the site under evaluation, which normally ranges from 1 - 10; and
- w is the weight which normally ranges from 1 - 5 depending on the importance of the given parameter.

This model is based on the following assumptions:

- The potential contaminants enter the groundwater system via the ground surface;
- Precipitation is the principal transporting agent of the potential contaminants into the groundwater system;
- The potential contaminants move at the same rate as the water; and
- The study area is equal to or greater than 100 acres.

The DRASTIC index model is considered to be an effective tool for provision of relative evaluation of groundwater pollution vulnerability as opposed to absolute solutions. However, this method also requires the availability of different types of data which in turn leads to complexity in terms of computational power and analysis (Piscopo, 2001; Al-Adamat et al., 2003). Ignorance of vital hydrogeological properties (e.g. multi-layered vadose zone and preferential flow) and specific properties of contaminants (e.g. sorption and decay) have been the major source of criticism of this model (Jovanovic et al., 2006). Aller et al. (1987) states that this methodology is applicable to both confined and unconfined aquifer systems. The shared opinion among different authors is that the outcome of the DRASTIC model is merely a general guide to the degree of groundwater vulnerability of an area. For anyone interested in the better comprehension of the groundwater processes and movement of potential contaminants in that area, a detailed assessment is a requirement.

GOD Method

GOD is a rating system method that was developed by Foster (1987) to investigate the potential vulnerability of a given area with the aid of groundwater occurrence, overall lithology of aquifer and depth to groundwater table. This method works well in most types of aquifers but the karst aquifers. It is also simple to use even though it tends to produce vulnerability maps that have limited resolution (Fraga et al., 2013). Five vulnerability classes exist in this method (Table 3.1) and the vulnerability of a given area is computed using the equation shown below.

$$\mathbf{I = G.O.D} \qquad (3\text{-}2)$$

Where I is the final index which ranges from 0 (insignificant vulnerability) to 1.0 (extreme vulnerability).

Table 3.1. GOD method vulnerability classes

GOD	Vulnerability Class
0-0.1	Insignificant
0.1-0.3	Low
0.3-0.5	Moderate
0.5-0.7	High
0.7-1.0	Extreme

Aquifer Vulnerability Index (AVI) Method

Aquifer Vulnerability Index Method was developed by Van Stempvoort et al. (1993) and unlike the above mentioned methods, it does not apply weights and ratings to evaluate the groundwater vulnerability of a given area (Vias et al., 2004). The emphasis of the method lies solely on characterizing the vadose zone, it uses a ratio of the thickness of each sedimentary layer overlying the aquifer (d) and the estimated hydraulic conductivity (k) of each of the above mentioned layers (Vias et al., 2004). The equation below is used to compute the groundwater vulnerability of a given area using the AVI method.

$$\mathbf{AVI} = \sum_{\mathbf{i=1}}^{\mathbf{N}} \frac{\mathbf{d_i}}{\mathbf{k_i}} \qquad (3\text{-}3)$$

Where N is the total number of sedimentary layers above the aquifer.

Subjective hybrid methods

Soricheta (2010) describes this method as the use of various parts of the subjective and objective methods in combination. The author also states that the outcome of such method is subjective and usually applicable to a specific study.

3.3.2 *Objective Methods (data-driven models)*

These methods include physical process-based methods and statistical methods of groundwater vulnerability assessment.

Process-based simulation method

Process-based simulation methods enable the assessment of groundwater vulnerability with the aid of mathematical equations in an attempt to represent the physical and chemical processes that

control the movement of water and contaminants in the groundwater system of interest (Oke, 2015). They are dependent on the determination of travel time and/or concentration of contaminants in the groundwater system (Lindström, 2005). Soricheta (2010) attributes such method to the analysis of isotopes and environmental tracers used to monitor the movement and evolution of groundwater to process-based simulation methods. The same author states that the methods are highly recommended for delineating well protection zones and are best suited to local rather than regional scales. Pollutant transport models, e.g. advective-dispersive-reactive (ADR) model are process-based simulation methods that offer an alternative path of predicting and mapping groundwater pollution vulnerability of a given area. They are used to predict the spatial and temporal variation in concentration of a potential pollutant in groundwater as it migrates vertically from the soil surface into the aquifer (Tombul et al., 2005). However, application of these models require good comprehension of groundwater flow equations and mechanics since they govern the movement of pollutants within the subsurface via molecular diffusion and dispersion (Mirbagheri, 2004). The process-based simulation methods can be easily verified but may also prove to be expensive with regard to the amount of data required and cost associated with the application of techniques such as isotopic analysis. They are seldom used and more applicable to specific groundwater vulnerability assessment (Oke, 2015). These methods require large amounts of data and their performance in data scarce regions may introduce errors in their outcome (Lindström, 2005).

Statistical Methods

Statistical methods employ the probability function to predict the extent and magnitude of contamination with the aid of the aquifer properties and the origin of the contaminant (Focazio et al., 2001). Statistical methods are not commonly applied in groundwater vulnerability evaluation throughout the world hence the lowest coverage in terms of publications, compared to process-based simulation methods and subjective methods (Lindström, 2005). Soricheta (2010) reckons that the Logistic Regression analysis is the most preferred statistical method in groundwater vulnerability evaluation, provided there is sufficient water quality data. Statistical models are not easy to create and they tend to be inflexible, i.e. they are only applicable in regions that have common environmental qualities as the one from which they originate (Oke, 2015; Lindström, 2005). Groundwater vulnerability maps produced using statistical methods are not normally ready

for use by the relevant stakeholders (i.e. land-use regulators), therefore they require further explanation owing to their excessive number of classes (Soricheta, 2010).

3.4 Validation of groundwater vulnerability maps

Ghazavi and Ebrahimi (2015) define validation of groundwater vulnerability map as the use of an independent technique in the verification of the groundwater vulnerability assessment. It is done to determine how reliable the groundwater vulnerability map is with regard to the geographic area in question. This is normally achieved by using various techniques that determine the quality and the overall performance of the model in use. Soricheta (2010) argues that a better way to assess the performance and quality of a groundwater vulnerability map is by comparing it with the measurements obtained in the study area (e.g. concentration of contaminant).

Previous studies established that groundwater vulnerability exhibits a close relationship with water quality in the vicinity of an anthropogenic source of pollution (Hao et al., 2017). Groundwater does not normally contain excessive nitrate content under its natural conditions, it is often leached from the Earth surface (Javadi et al., 2011). Porcel et al. (2014) states that nitrate has the ability to be transported long distances away from its source due to its limited capability to stick to soil particles and high solubility. For these reasons, nitrate is one of the most appropriate and commonly applied media to verify the groundwater vulnerability map for many authors.

3.5 Review of case studies

Davidson et al. (2002) described a groundwater vulnerability mapping exercise conducted in order to aid in provincial planning through production of maps that delineated high-risk areas in terms of groundwater contamination. The exercise utilized three methods which included the DRASTIC model, Ontario Ministry of the Environment and Energy Aquifer Vulnerability Index and the Grand River Conservation Authority. The DRASTIC model was discarded owing to its large data requirements while the other methods were considered to be more conservative and applied in the final groundwater vulnerability map. The authors pointed out that groundwater vulnerability has no means of being verified scientifically and the error was bound to be present in the end product owing to the different kinds and amounts of data used. It is also stated in the article that the final vulnerability maps must be revised with any further well development and hydrogeological studies.

Muhammad et al. (2015) evaluated the groundwater vulnerability of Lahore, Pakistan with the aid of the DRASTIC method and used GIS to produce the resultant groundwater vulnerability map. According to the authors, DRASTIC method has the ability to map areas of different levels of vulnerability and various lithological units at a regional scale. They also endorse the use of overlay and index methods e.g. DRASTIC method to conduct intrinsic aquifer vulnerability, which is the main objective of this study. The conclusion of the study was that low vulnerability result from dense human settlements and low water levels while high vulnerability were attributed to pasture type lands and agricultural areas.

The study conducted by Al-Adamat et al. (2003) describes a groundwater vulnerability and risk mapping exercise in the basaltic aquifers of the Azraq basin in Jordan. DRASTIC index method, remote sensing and GIS were used to complete the exercise. Only six of the DRASTIC parameters were used in this area because the required data for estimating hydraulic conductivity was unavailable. The vulnerability map produced was combined with the land use map in the DRASTIC model for assessment of potential risk of groundwater contamination in the area. The majority of the Azraq basin area at 84% was confirmed to be at moderate risk whereas the remaining portion was low-risk in terms of groundwater pollution. It was concluded that the above mentioned methodology is more appropriate on a regional scale, therefore it is applicable to the study area. The article also mentions the possible but rare use of the DRASTIC method in arid and semi-arid regions such as the current study area, Masama East well field, Khurutshe area, Botswana. For instance, Fritch et al. (2000) successfully conducted groundwater vulnerability assessment on Paluxy aquifer in the arid North-central Texas, USA with the aid of a modified DRASTIC equation and GIS.

Anornu et al. (2012) also conducted an assessment of potential groundwater pollution in the Densu River Basin in Ghana. The GIS component enabled the authors to incorporate different satellite and cartographic maps and pumping test data into the DRASTIC methodology. This is promising for the current study since it also deals with pumping test data analysis along the way. Findings from this assessment indicated that 47% of the basin has high-risk, 43% has medium-risk and the remaining 10% has low-risk in terms of groundwater pollution. The need for careful urban planning of settlements, siting of irrigation schemes and sanitation facilities was therefore recommended for high-risk areas. Soricheta (2010) used a statistical method, particularly the

Weights of Evidence (WofE) modelling technique was used to evaluate groundwater vulnerability in two separate aquifers located in the Po Plain area, Italy. One of the objectives of the experiment was to determine the limitations associated with statistical methods. The author succeeded in evaluating groundwater vulnerability as different vulnerability classes were determined and the validation tests support the findings.

Locally, Alemaw et al. (2004) evaluated the vulnerability of Kanye well field to groundwater to pollution with the help of soil types, mapped geology, borehole information, GIS system and Thiessen polygons method. The results revealed that 58% of the well field has high-risk, 34% has moderate-risk and 8% has low-risk with regard to groundwater pollution. However, the authors used only two hydrogeological parameters ignoring the recharge component which is considered by several researchers in the field to be vital in the vertical transportation of contaminants from the surface to the water table (Aller et al., 1987 and Muhammed et al., 2014 are in agreement with this concept). The recharge value could have possibly changed the outcome of the assessment if it was incorporated.

3.6 Potential pollutants in the study area

Daly et al. (2002) associates intrinsic vulnerability with groundwater pollution caused by human beings or activities related to them. Land uses such as rain-fed crop production, livestock production and the existence of residential land within the study area constitute the anthropogenic sources of groundwater pollution. Field observations indicate that the residential land comprises of pit latrines (some are not properly constructed) while the agricultural land comprises of kraals, ploughing fields and livestock watering points. These areas are bound to exhibit poor sewerage system, improper waste disposal and spreading of manure which introduce pollutants to the ground surface, and eventually the groundwater system in the area. Potential pollutants that are likely to be introduced by such anthropogenic sources within the study area are discussed below.

Microbial Pathogens (bacteria, virus and protozoa)

Human and animal faecal waste account for majority of microbial pathogens found in groundwater which often lead to water-borne diseases and conditions such as diarrhea when ingested. Certain pathogenic micro-organisms originate in the digestive system of both humans and animals, and

their existence in an aquifer signifies groundwater contamination from anthropogenic sources, particularly faecal waste (Lin et al., 2012; cited in Jonker, 2016). These pathogens are normally introduced into the groundwater system by poorly constructed pit latrines, kraals, ploughing fields, livestock feeding lots and watering points which are well known faecal waste disposal sites. Interaction by human beings with such pathogens leads to the deterioration of their health and sometimes increases mortality rates (WHO, 2006). Deep groundwater source such as in the study area is considered safe to some extent by the scientific community in terms of contamination by microbial pathogens, owing to attenuation in both the soil and vadose zone (WHO, 2006; Jonker, 2016). Presence of clayey soil and confining layer also hinder the migration of pathogens from the surface into the aquifer via a process known as straining (WHO, 2006).

Nitrates

Nitrate occurs naturally in groundwater resources but excessive concentrations are normally a result of interaction of the groundwater resources with residential and agricultural land (WHO, 2006). Spreading of manure in ploughing fields, leaking sewerage systems or improperly constructed pit latrines, poorly constructed waste disposal sites constitute some of the ways in which nitrate migration into the groundwater system is enhanced. Nitrates typically range from 0 - 18 mg/l in groundwater and its health implications include methaemoglobinaemia (blue baby syndrome), a condition that leads to shortness of breath and death in infants by hindering proper transportation of oxygen in the blood stream (WHO, 2006).

Other potential pollutants exist within the study area and their occurrence in the groundwater system is natural and independent of human beings. Intrinsic groundwater vulnerability assessment does not cover such pollutants since they do not originate from anthropogenic sources in the study area (Table 3.2).

Table 3.2. Potential pollutants in the study area (adopted from WHO, 2006).

Potential pollutant	Source	Examples	Health implications
Arsenic	Occurs naturally	Rocks and soils (common regions of active volcanism)	Causes Arsenicosis and a variety of cancer conditions
Nitrates & Nitrites	Chemicals from agricultural activities and human settlements	Application of manure, fertilizer and pesticides; leaching from human and animal feces	Causes Blue baby syndrome (Methaemoglobinaemia)
Ammonia			
Pesticides			
Microbial pathogens (virus, bacteria, protozoa)	Human and animal faecal waste	Leaking septic tanks and pit latrines, manure, livestock feeding lots and watering points	Diarrhea ,Giardia, etc.
Fluoride	Occurs naturally	Acid volcanic rocks	Dental and skeletal fluorosis
Radon gas	Occurs naturally	Granitic rocks and pegmatites	Lung cancer
Uranium	Occurs naturally	Granitic rocks, pegmatites and sandstones	Kidney related diseases
Metals e.g. cadmium (Cd), lead (Pb), nickel (Ni), chromium (Cr) and copper (Cu)	Both natural and anthropogenic	Weathering of rocks, mining and manufacturing industries, combustion of fossil fuels, acid rain	Nausea, liver cirrhosis, allergies

3.7 Conclusion

The evaluation of groundwater pollution vulnerability relies on good understanding of the properties of a given hydrogeological setting hence the need to study them beforehand. It is also vital to take the nature and scale of the assessment into consideration since different methods of groundwater pollution vulnerability assessment exist with different data requirements. There are two kinds of methods namely, subjective methods and objective methods that can be employed to evaluate groundwater pollution vulnerability of a given area. Objective methods can be further split into process-based simulation methods and statistical methods. Process-based simulation methods are best suited to specific groundwater vulnerability evaluations and their application in data scarce regions are most likely to yield inaccurate results. Statistical models cannot be easily created and are unlikely to fit any other hydrogeological setting apart from the one where it was created. Subjective methods, particularly the DRASTIC index model are more applicable to intrinsic groundwater vulnerability assessment and therefore best suited to carry out this study. The model makes use of readily available data and can be used in combination with other methods.

4. METHODOLOGY

4.1 Overview of the methodology

The main objective of this study is to evaluate the intrinsic groundwater vulnerability of Masama well field. The well field covers a significant portion of Khurutshe area and it can be characterized as a data scarce region hence the selected technique should take that into consideration. Process-based simulation and statistical were discarded due to their data requirements, the high cost and inflexibility associated with their application. Subjective methods are more applicable to the nature of the groundwater pollution vulnerability evaluation in question as well as the study area. However, only the DRASTIC index model was selected for the study since it can be applied in both confined and unconfined aquifer systems. The techniques, tools and procedures followed to complete this study are discussed in detail in the subsequent sections.

4.2 Brief description of model used

DRASTIC Index model is used to assess the groundwater pollution vulnerability in Masama east well field. The model was selected because it takes the net recharge into consideration, among other reasons. Alwathaf and El Mansouri (2011) reckon that recharge is a major contributing factor in leaching of pollutants from the ground surface into the groundwater system. The model can make use of readily available secondary data to produce a relative evaluation of the groundwater pollution potential of an area (Al-Adamat et al., 2003). It is also flexible in the sense that one can apply it in combination with other information such as land use and potential source of contamination (Jovanovic et al., 2006; Oke, 2015).

4.3 Flow chart of the model

The figure shown below represents the steps undertaken to evaluate the groundwater pollution vulnerability of the study area.

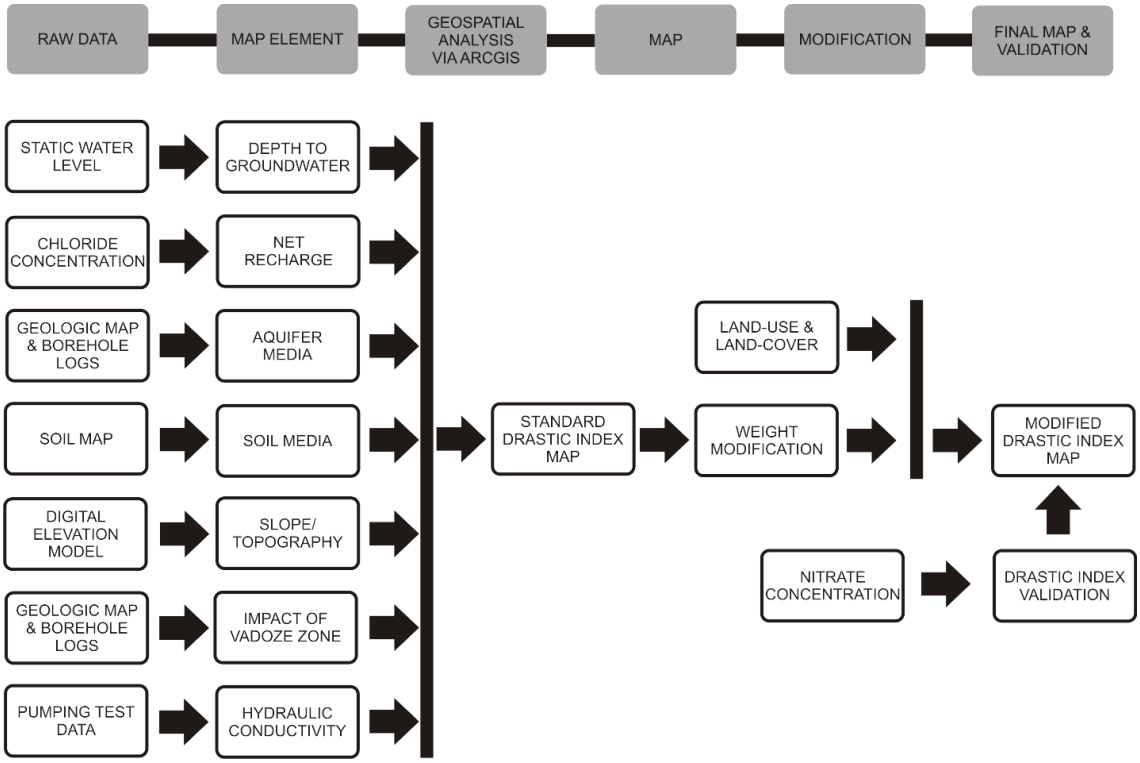

Figure 4.1. Flow chart of model used to evaluate groundwater vulnerability.

4.4 Required data and its sources

The DRASTIC index model required transformation of raw data into the final groundwater vulnerability map of the given area via a series of geospatial analysis techniques. Table 4.1 shows the data used to prepare the groundwater pollution vulnerability map of Masama east well field. It also shows the sources and the information to be derived from such data.

Table 4.1 Required data, sources and information to be derived

Map Element	Information Required	Required Data	Source of Data	Citation
Depth to groundwater	Depth to saturated zone (static water level)	Geological logs	Department of Water Affairs and Water Surveys Botswana	Aller et al. (1987), Piscopo (2001)
Recharge	Net recharge	Chloride concentration (dry and wet deposition), annual rainfall	Department of Water Affairs, Department of Meteorological Services and Water Surveys Botswana	Cook (2003), Sophocleus (2007)
Aquifer media	Aquifer type and thickness	Geological logs, geological reports and maps	Botswana Geoscience Institute, Department of Water Affairs and Water Surveys Botswana	Aller et al. (1987)
Soil media	Soil texture	Geological logs, geological reports and soil maps	Botswana Geoscience Institute, Ministry of Agriculture, Department of Water Affairs and Water Surveys Botswana	Aller et al. (1987), Piscopo (2001)
Topography	Slope	Digital Elevation Models	online from the Shuttle Radar Topographic Mission (SRTM) website	Aller et al. (1987), Colins et al. (2016)
Impact of vadose zone	Constituents of the unsaturated zone	Geological logs, reports and maps	Botswana Geoscience Institute, Department of Water Affairs and Water Surveys Botswana	Alwathaf and Mansouri (2011)
Hydraulic Conductivity	Transmissivity and hydraulic conductivity	Pumping test data	Department of Water Affairs and Water Surveys Botswana	Gupta (2014)
Land-use	Types of land use and land cover	Land use and land cover maps, field observations	Ministry of Agriculture and Water Surveys Botswana	Porcel et al. (2014)

4.5 Software

The groundwater pollution vulnerability of Masama east well field was evaluated in a geographic information system (GIS) environment. ArcMap 10.2.2 was used as a platform for performing all tasks related to data capturing, processing and analysis. Aquifer test 2016.1 was also used to compute the transmissivity and hydraulic conductivity from the pumping test data obtained from boreholes within the study area. This software package was developed by Schlumberger Water Services (SWS). Pumping test data from the confined aquifer was analyzed using the Theis method (1935), and data from the unconfined aquifer was analyzed using the Neumann method.

4.6 Preparation of the map elements for the standard DRASTIC index model

4.6.1 *Depth to Groundwater (D-Map)*

Depth to groundwater (D) refers to the vertical distance within the unsaturated zone between the ground surface and the static water level (SWL). This zone may be occupied by unconsolidated sediments and weathered rocks which act as a limitation to the movement of potential contaminants from the surface into the aquifer (Piscopo, 2001; Aller et al., 1987). Generally, deep groundwater levels are associated with increased filtering and disintegration of contaminants by micro bacterial activities within the unsaturated zone, a process known as attenuation. On the other hand, the existence of shallow groundwater levels reduces the attenuation capacity of the unsaturated zone overlying the aquifer thus increasing the probability of groundwater contamination (Piscopo, 2001).

Static water level (SWL) readings from 61 boreholes including both the production and monitoring wells within the study area were interpolated using the Inverse Distance Weighting (IDW) technique with the aid of the spatial analyst tool in ArcMap 10.2 (see Appendix IV). These readings were obtained during groundwater level monitoring exercises conducted by Water Surveys Botswana in 2016 which is a short period of time for record keeping. Attempts to acquire more groundwater level records proved to be fruitless as they were not available at the time of this study. As a result the deductions on the groundwater level trend may be less informative since they were deduced from insufficient amount of data. The groundwater level trend in the study area revealed that change in depth to groundwater was minimal and almost negligible throughout the year 2016

(Figure 4.2). For this reason, the author opted to combine static water levels from both the production (prior to pumping test) and monitoring boreholes in the construction of the D-Map element. The D-Map element was then rated, weighted and reclassified based on Table 4.2 to produce the depth to groundwater index map (D_rD_w). Inverse distance weighted interpolation is a technique that deduces the value of unknown or missing points basing on the distance and magnitude of the neighboring known values (Setianto and Triandini, 2013). This technique is easy to implement and interpret. It is calculated using the Equation (4-1) below.

$$Z_0 = \frac{\sum_{i=1}^{n} Z_i . d_i^{-n}}{\sum_{i=1}^{n} d_i^{-n}} \qquad (4\text{-}1)$$

Where:

- Z_0 is the value of the unknown point,
- Zi is the value of the known point,
- d is the distance to known point, and
- n is the number of sample points.

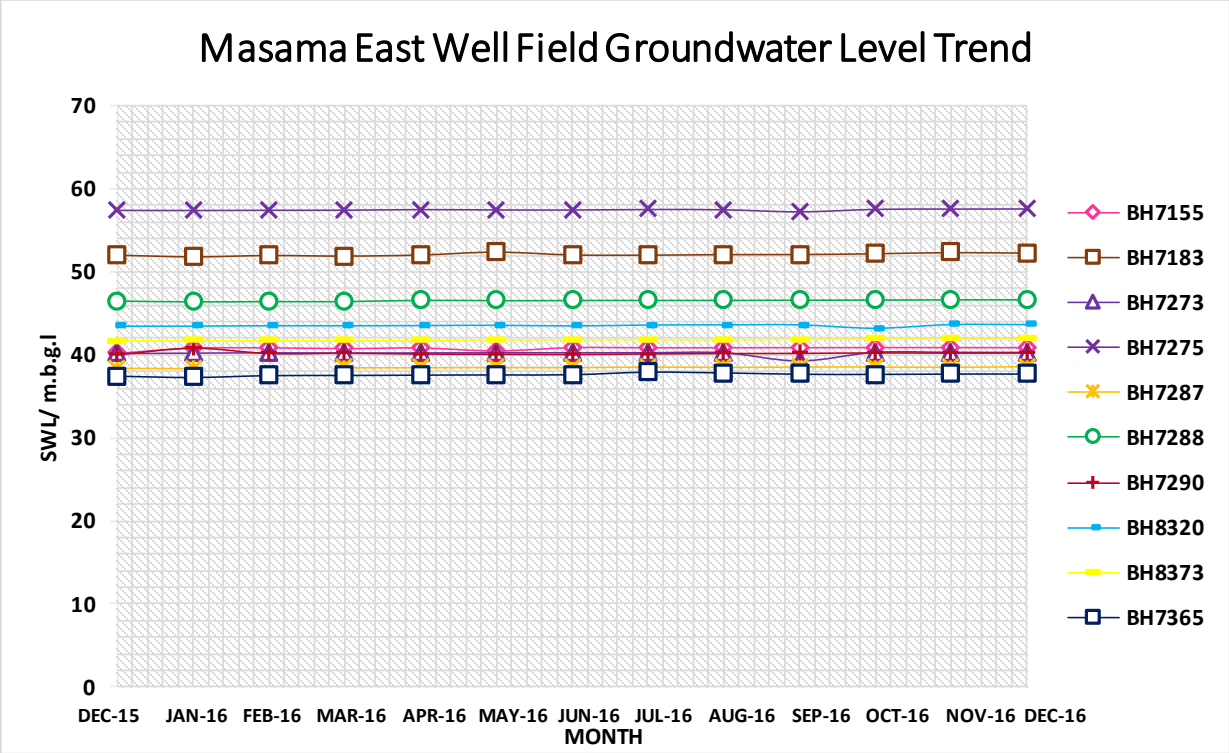

Figure 4.2. Groundwater level trend of the study area in 2016.

4.6.2 *Net Recharge (R-Map)*

Alwathaf and El Mansouri (2011) defines recharge as the amount of water in mm per unit area that percolates from the ground surface into the groundwater system per annum. The author also refers to recharge as the main component that is responsible for the movement of contaminants from the surface to the groundwater system. Net recharge was estimated in the study area using the Chloride Mass-Balance (CMB) method developed by Eriksson and Khunakasem (1969). It is an environmental tracer technique widely applied in the arid and semi-arid Southern Africa to carry out groundwater recharge estimation (Seeyan and Merkel, 2015). This method is based on the comparison of the total chloride concentration at the surface with the chloride concentration in the groundwater measured in boreholes (de Vries et al., 2000). Authors such as Cook (2003) and Sophocleous (2007) reckon that the CMB technique is mostly preferred due to its simplicity and cost effectiveness, in comparison to other tracer techniques.

Precipitation is considered to be the main source of groundwater recharge in many regions especially the arid and semi-arid ones. As a result various techniques used for estimating recharge including CMB incorporate a value for precipitation in their computations. The equation below was used to estimate the net recharge value at each sampling location;

$$\mathbf{R_T} = \frac{\mathbf{P} * \mathbf{Cl_P}}{\mathbf{Cl_{gw}}} = \frac{\mathbf{TD}}{\mathbf{Cl_{gw}}} \qquad (4\text{-}2)$$

Where;

- R_T is the net recharge in mm/year;
- Cl_{gw} is the constant chloride concentration of the groundwater;
- Cl_P is the chloride concentration at the surface (wet and dry deposition);
- P is the effective precipitation at the study area in mm; and
- TD is the total atmospheric chloride deposition from precipitation and dry fall out.

Chloride concentration in groundwater (Cl_{gw}) was measured from groundwater samples collected by Water Surveys Botswana from 32 boreholes within the study area. Groundwater sampling locations covered a sufficient portion of the study area even though the sampling process was dependent on the geographic locations of existing boreholes, instead of following a predefined

sampling technique. The total atmospheric chloride deposition values, TD used to compute the net recharge in the study area were 400, 525 and 750 mg/m^2/annum. These values were estimated basing on data collected over two decades ago during the Groundwater Recharge Estimation Studies (Phase I and II) (Selaolo, 1998). A mean of the net recharge computed using the three TD values was calculated for each sampling site and the resulting average recharge values were interpolated using IDW in a GIS environment (see Appendix II). The interpolated values were then rated, weighted and reclassified basing on Table 4.2 to produce the net recharge index map (R_rR_w).

4.6.3 *Aquifer Media (A-Map)*

Aller et al. (1987) defines aquifer media as the consolidated and/or unconsolidated rock or sediments which have the capability of transmitting a significant amount of water. Basically, it is the medium from which the aquifer is made. The A-map was prepared basing on the interpretation and analysis of both the geologic map and 79 borehole records of the study area obtained from the Botswana Geoscience Institute (formerly Department of Geological Survey) and the Department of Water Affairs, respectively. It was constructed using IDW interpolation in the spatial analysis tool (ArcMap 10.2). The resultant map was then rated, weighted and reclassified according to Table 4.2 in order to produce the aquifer media index map (A_rA_w).

4.6.4 *Soil Media (S-Map)*

Aller et al. (1897) and Piscopo (2001) reckon that the soil at any given location has an influence on the vertical movement of water and contaminants from the surface to the underlying vadose zone. They also state that the occurrence of silts and clays within the soil hamper the movement of contaminants into the aquifer by reducing its permeability. Clay materials tend to form an impervious crust within the soil that lengthens the residence time of contaminants and favors the attenuation of such contaminants. Clay and silt content of any given soil is proportional to the soil permeability and it can therefore be used as an indicator of pollution potential of a given area. High clay and silt content in the soil implies that it has low permeability which results in low pollution potential and vice versa (Piscopo, 2001).

A soil map showing different soil types and textures within the study area was constructed basing on 79 borehole records and the soil map of Botswana. The Ministry of Agriculture provided the soil map whereas the borehole records were provided by the Department of Water Affairs. The

soil types identified from the above sources were, rated, weighted and reclassified basing on Table 4.2 in order to produce the soil media index map (S_rS_w).

4.6.5 *Topography (T-Map)*

Colins et al. (2016) defines topography as the slope or variation in elevation of any given area. It is expressed as the percentage of slope values, whereby low slope percent represents flat areas and high slope percent values are normally hilly areas. Flat areas exhibit minimum run off which results in the occurrence of stagnant water whereas hilly areas are characterized by high occurrence of run off. Stagnant water present greater risk of groundwater pollution in an area as pollutants are afforded enough time to be leached into the aquifer whereas high run off washes away pollutants reducing migration of pollutants from the surface into the aquifer. The topography map was constructed using the slope (expressed in percentages) calculated from the Shuttle Radar Topographic Mission Digital Elevation Model (SRTM DEM) of the study area (pixel size of 30m). This Map was then rated, weighted and reclassified basing on Table 4.2 as recommended by Aller et al. (1987) and Colins et al. (2016) in order to produce the topography index map (T_rT_w).

4.6.6 *Impact of Vadose Zone (I-Map)*

The vadose zone is the unsaturated layer located between the ground surface and the aquifer itself. Alwathaf and El Mansouri (2011**)** states that the texture of material that makes up the vadose zone influences the period of time it takes the pollutants to reach the water table. Areas with fine grained material e.g. clay, have lower risk of groundwater pollution due to low permeability and vice versa. The impact of vadose zone map was also prepared with the aid of the geologic map and 79 borehole records from the study area. The resulting raster map was rated, weighted and reclassified based on as illustrated in Table 4.2 to produce the impact of vadose zone index map (I_rI_w).

4.6.7 *Hydraulic Conductivity (C-Map)*

Hydraulic conductivity refers to the aquifer's capability to transmit water, which controls the rate and movement of pollutants within the aquifer (Gupta, 2014). High conductivity values indicate higher risk of groundwater pollution while low conductivity values indicate lower risk of groundwater pollution in a given area. Pumping tests were conducted on 18 pumping wells and 23 observation between June 2014 and January 2015 in the study area. Residual drawdown and drawdown data obtained during the recovery period and the constant rate test were analyzed using

the Aquifer Test 2016.1 software to derive the hydraulic conductivity values (Appendix I and III). These hydraulic conductivity values were interpolated using the IDW method in the spatial analyst tool in ArcMap 10.2. to produce the C-map. The C-map was further rated, weighted and reclassified in order to produce the hydraulic conductivity index map (C_rC_w) based on Table 4.2 .

Table 4.2 Ratings and weights assigned to the DRASTIC parameters

Depth to Groundwater		Net Recharge		Aquifer Media		Soil Media	
Range (m)	Rating	Range (mm/year)	Rating	Range	Rating	Range	Rating
0-1.5	10	0-50	1	Karst limestone	10	Thin or absent/ Gravel	10
1.5-4.5	9	50-100	3	Basalt	9	Sand	9
4.5-7.5	8	100-175	6	Sand & gravel	8	Peat	8
7.5-10	7	175-250	8	Massive sandstone/ limestone	6	Shrinking clay	7
10-12.5	6	>250	9	Bedded sandstone/ limestone/ shale	6	Sandy loam	6
12.5-15	5			Glacial till	5	Loam	5
15-19	4			weathered metamorphic/ igneous	4	Silty loam	4
19-23	3			metamorphic/ igneous	3	Clay loam	3
23-30	2			Massive shale	2	Muck	2
>30	1					Non shrinking clay	1
DRASTIC Weight=5		DRASTIC Weight=4		DRASTIC Weight=3		DRASTIC Weight=2	
Topography		Impact of Vadose Zone		Hydraulic Conductivity			
Range (%)	Rating	Range	Rating	Range (m/day)	Rating		
0-2	10	Karst limestone	10	<4	1		
2-6.	9	Basalt	9	4.-12	2		
6.-12	5	Sand & gravel	8	12.-30	4		
12.-18	3	Sand & gravel with silt	6	30-40	6		
>18	1	Bedded sandstone/ limestone	6	40-80	8		
		limestone/ shale/silty clay	3	>80	10		
		Confining layer	1				
DRASTIC Weight=1		DRASTIC Weight=5		DRASTIC Weight=3			

4.7 Production of the standard DRASTIC index map

A standard DRASTIC index map of the well field was constructed by addition of the map elements. This map was meant to illustrate the variation in groundwater vulnerability to pollution of Masama east wellfield as recommended by Aller et al. (1987) and it was further divided into different vulnerability classes ranging from very low to high groundwater vulnerability basing on the DI of the given area. These vulnerability classes were colour coded in order to increase their visibility on the map. The expected outcome was that higher DI values would indicate areas exhibiting a higher risk of groundwater pollution whereas areas with lower DI values would still be susceptible to groundwater pollution but with lower risk (Knox et al., 1993; Piscopo, 2001).

4.8 Calibration of the standard DRASTIC index map

4.8.1 *Sensitivity Analysis*

The DRASTIC index model uses seven parameters to evaluate the groundwater vulnerability with the aim of obtaining a true representation of any given site, thus increasing the accuracy of the model. However, Babiker et al. (2005) reckon that one can evaluate the groundwater vulnerability of any site using fewer parameters and obtain results with higher accuracy and low cost. Napolitano and Fabbri (1996) consider the model to be subjective as a result of using seven parameters, ratings and weights in groundwater vulnerability evaluation. The standard DRASTIC index model also employs fixed ratings and weights to evaluate groundwater vulnerability even though they are reliant on the properties of the given site. Barbiker et al. (2005) states that these ratings and weights vary from one place to another which introduces the need for calibrating the model to fit the given site.

Sensitivity analysis were performed in order to check the necessity of using all seven DRASTIC parameters in evaluating the groundwater pollution vulnerability of the study area and to reduce the subjectivity associated with the model. Two kinds of sensitivity analysis namely, map removal sensitivity analysis (MRSA) and single parameter sensitivity analysis (SPSA) were performed on the groundwater vulnerability map of Masama east well field obtained using the standard DRASTIC index model.

Map Removal Sensitivity Analysis (MRSA)

This technique was developed by Lodwick et al. (1990) and its primary role is to determine whether there is a need to use all seven DRASTIC parameters in groundwater vulnerability assessment in a given site. Basically, it measures the variation of the groundwater vulnerability map due to removal of one or more DRASTIC parameters (Saidi et al., 2011). The MRSA technique was applied in two forms to the Masama east well field groundwater vulnerability map with the aid of Eq. 4-3. First, the variation in groundwater vulnerability map due to removal of one parameter at a time was computed and then computation of the variation as result of the removal of one or more parameters followed.

$$\mathbf{S} = \left(\left|\frac{\mathbf{V}}{\mathbf{N}} - \frac{\mathbf{V_{xi}}}{\mathbf{n}}\right|\right)\mathbf{x}\frac{\mathbf{100}}{\mathbf{V}} \qquad (4\text{-}3)$$

Where,

- S is the sensitivity index of the given parameter;
- V is the overall intrinsic vulnerability index;
- V_{xi} is the intrinsic vulnerability index obtained after removal of one or more parameters;
- N is the number of parameters used to compute V; and
- n is the number of parameters used to compute V_{xi}.

Single Parameter Sensitivity Analysis (SPSA)

SPSA was developed by Napolitano and Fabbri (1996) with the aim of evaluating the effect of each DRASTIC parameter in the computation of the DRASTIC index. This was achieved by comparison of the effective weight computed by Eq. 4-4 with the theoretical weight assigned by Aller et al. (1987) for each parameter (Napolitano and Fabbri, 1996). Saidi et al. (2011) states that the use of effective weight in place of the theoretical weight in each DRASTIC parameter has the potential to increase the accuracy of the groundwater vulnerability map of any given site.

$$\mathbf{W} = \frac{\mathbf{P_r P_w}}{\mathbf{V}} * \mathbf{100} \qquad (4\text{-}4)$$

Where,

- W is the effective weight of the given parameter;
- P_r and P_w are the rating value and the weight for the given parameter, respectively; and
- V is the overall vulnerability index.

The effective weights calculated for each DRASTIC parameter in the single parameter sensitivity analysis were used in place of the theoretical weights assigned by Aller et al. (1987) in order to produce a more realistic groundwater vulnerability map that serves as better representation of the potential groundwater pollution vulnerability in Masama east well field.

4.8.2 *Integration of the Land-Use map element (L-Map) into the DRASTIC index model*

Porcel et al. (2014) states that land use can be used as a direct measurement of the impact of human activities on the environment. The author also attributes urbanization and agricultural activities to the introduction of contaminants into the soil and the underlying groundwater systems in some areas around the globe which eventually lead to groundwater quality deterioration. Porcel et al. (2014) identified agricultural activities as the basic source of groundwater pollution in many areas and justifies the use of land use as an additional parameter in the evaluation of groundwater pollution vulnerability for any site. A land use map of the study area was rated, weighted and reclassified basing on Table 4.3 adopted from Secunda et al. (1998). The outcome was a land use index map that was incorporated into the groundwater pollution vulnerability map using the equation below.

$$\mathbf{MDI_{LU} = DI_{SPSA} + L_r L_w} \qquad (4\text{-}5)$$

Where,

- MDI_{LU} is the modified DRASTIC Index;
- DI_{SPSA} is the DRASTIC index after weight modification via SPSA; and
- L_r and L_w are the values for rating and weight of land-use parameter, respectively.

Table 4.3 Ratings and weight of land-use (Secunda et al., 1998)

Land-use	Rating
Vegetation and Barren Land	5
Water and wet area	7
Residential and agriculture land	8
Weight = 5	

4.9 Groundwater Quality

Groundwater samples obtained from 32 boreholes within the study area by WSB were analyzed at the Botswana Geoscience Institute and Water Utilities Corporation laboratories in order to determine the quality of groundwater in the aquifer. Groundwater was sampled at the end of borehole development and constant rate test, i.e. during drilling and pumping test, respectively. The groundwater sampling exercise took place between May 2014 and January 2015, the sampling sites are illustrated in Figure 4.3 below.

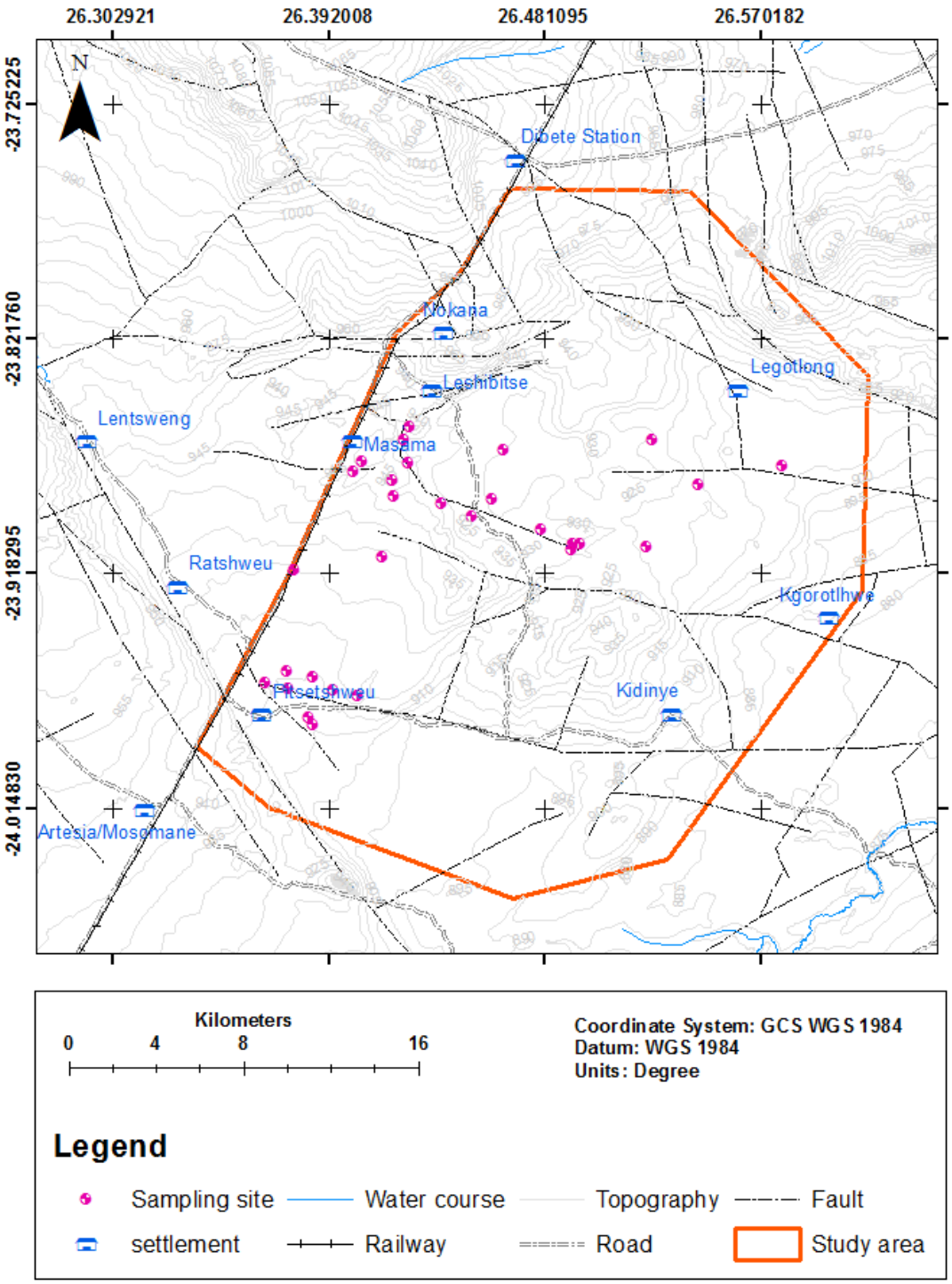

Figure 4.3. Groundwater sampling sites in Masama east well field during the period of time between May 2014 and January 2015.

4.10 Validation of the groundwater vulnerability map

Various validation techniques for groundwater vulnerability assessment exist but only one approach was adopted in this study. The approach involved the comparison of nitrate distribution in the study area with the land-use map. Nitrate concentration values were obtained from groundwater samples from boreholes within the well field. These values were interpolated using IDW in ArcMap spatial analyst tool to produce a nitrate distribution map. The nitrate distribution map was compared to the land-use map of the study area to establish the relationship between nitrate concentration values and the overlying land-use. This comparison may also serve a means of justifying the integration of land use parameter into the final groundwater pollution vulnerability map. That depends on whether the two parameter have a strong correlation or not. The Spearman rank correlation coefficient, r_s discovered by Spearman (1904) was used to determine the degree to which the land use map and nitrate concentration values of Masama east well field are related. The r_s is considered as a special case of the Pearson's product-moment coefficient and it is used to determine the correlation of two variables when the outcome of the Pearson correlation coefficient is misleading (Hauke and Kossowski, 2011). It has the form;

$$\mathbf{r_s = 1 - \frac{6\sum_{i=1}^{N} d_i^2}{N(N^2-1)}} \qquad (4\text{-}6)$$

Where,

- r_s is the Spearman rho correlation coefficient;
- d_i is the difference in rankings of characteristics pollutants and ranking of risk of pollution index; and
- N is the sample size.

5. RESULTS AND DISCUSSIONS

5.1 Evaluation of the standard DRASTIC map

5.1.1 *Depth to groundwater map element (D-map)*

Depth to groundwater values ranged between 33.6 and 70.0 meters below ground level (m.b.g.l) throughout the study area (Figure 5.1). These are relatively deep water levels which favor increased attenuation of contaminants. Generally, the unclassified D-map indicates that depth to groundwater tends to increase from the east towards the western margin of the well field with the deepest point located near Masama settlement. Due to depth to groundwater exceeding 30 m.b.g.l throughout the study area, the D-map was assigned a rating of 1 and each cell in the polygon was multiplied by 5 (its weight) in order to produce the depth to groundwater index map, D_rD_w (Figure 5.2). Contaminants may still be able to reach the groundwater but the chances are minimal since attenuation capacity and residence time of those contaminants are increased.

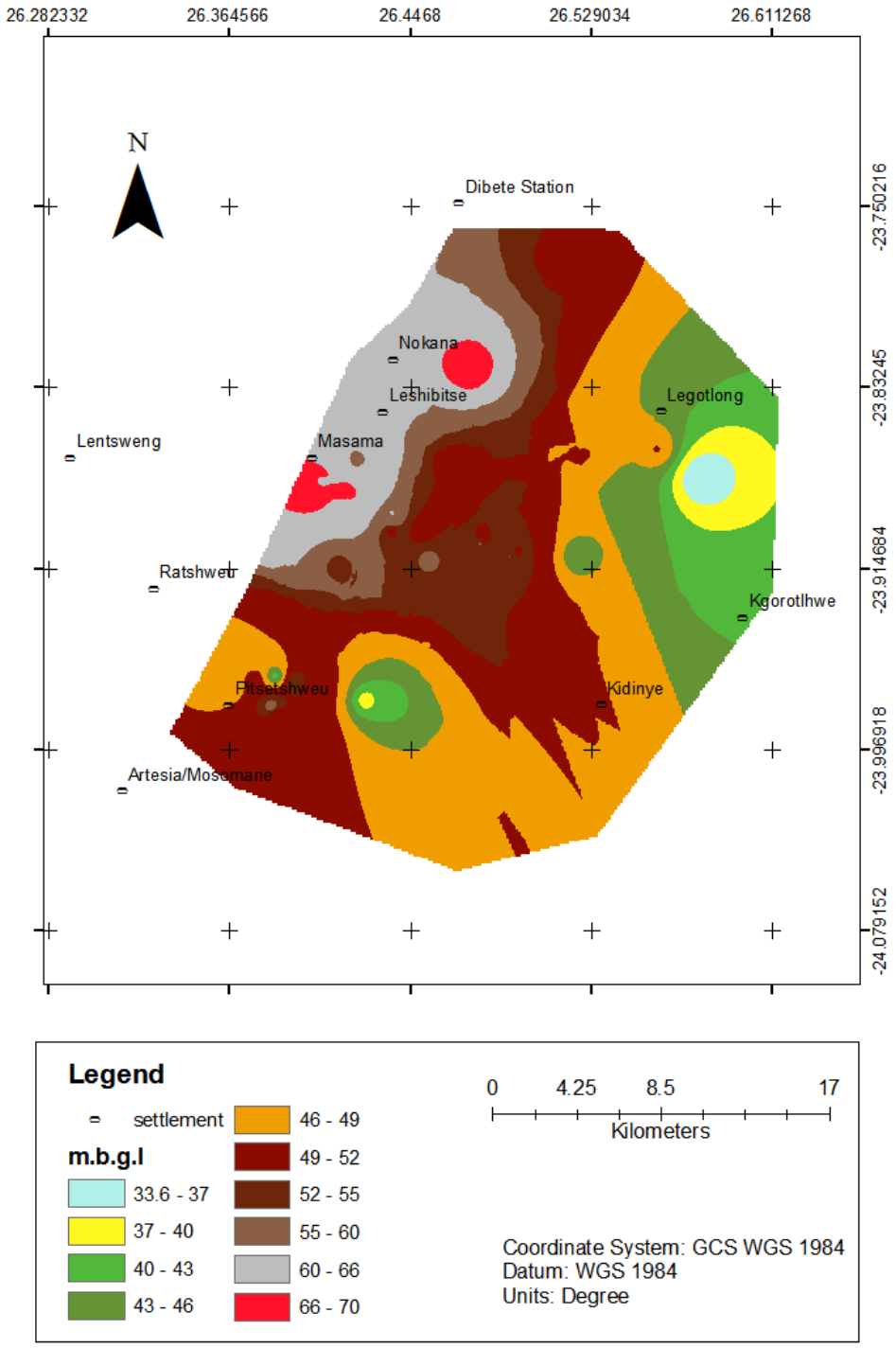

Figure 5.1. Depth to groundwater map (D-map) of the study area.

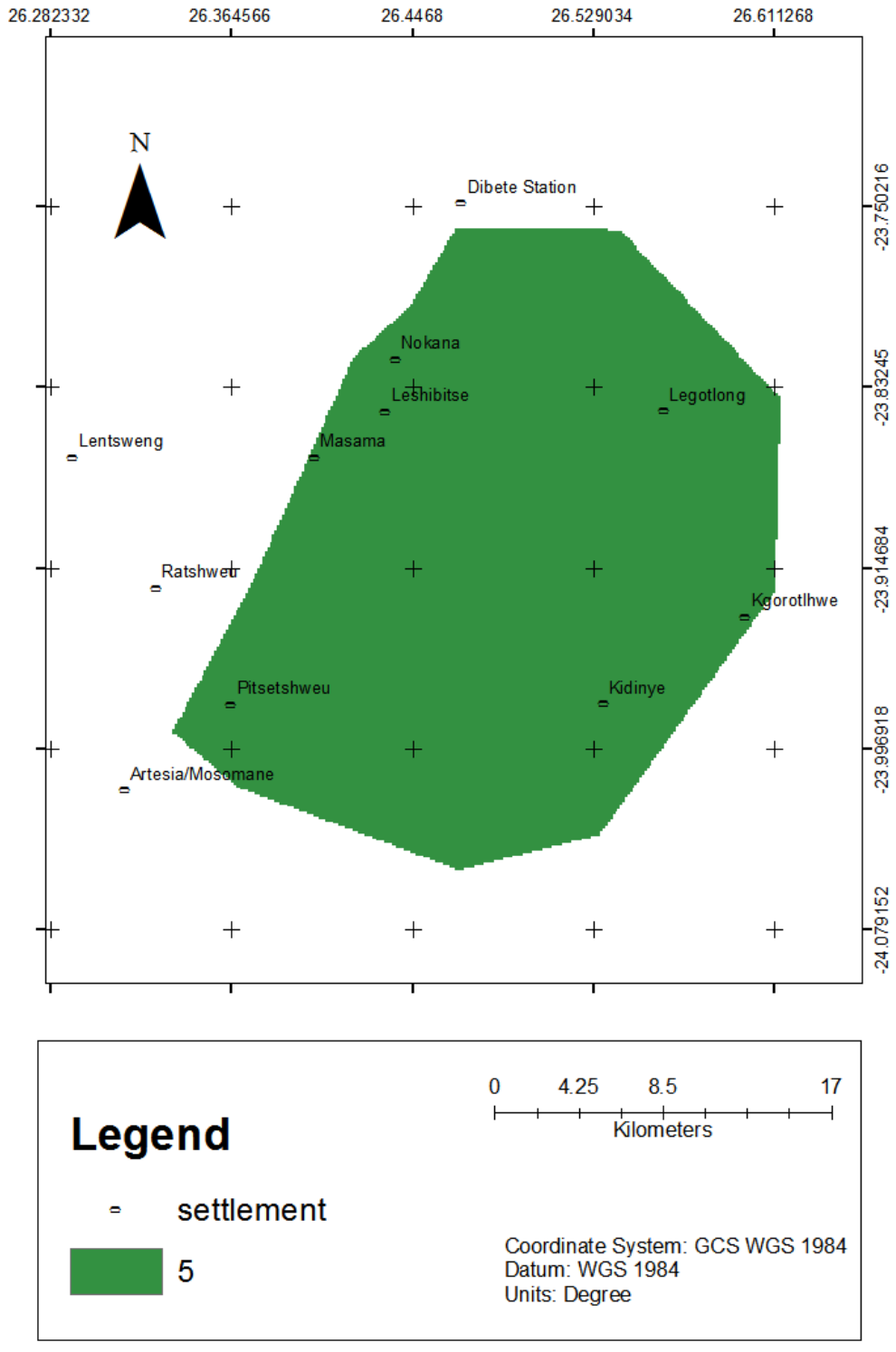

Figure 5.2. Depth to Groundwater index map (D_rD_w) of the study area.

5.1.2 *Net recharge map element (R-map)*

Net recharge values obtained in the study area are generally very low and they range from 4 to 46 mm per annum (Figure 5.3). This is a common phenomenon in semi-arid environments like Masama east well field (Seeyan and Merkel, 2015) and it also means that potential contaminants have a limited likelihood of entering the groundwater system through recharge. Groundwater recharge is considered to be an agent through which potential contaminants migrate from the ground surface into the groundwater system. The more the amount of net recharge, the more chances of groundwater contamination occurrence. The highest values for net recharge were recorded within the unconfined Ntane Sandstone Formation around Masama fault zone and this observation is consistent with findings from previous studies (Masike, 2008). This is the same portion of the well field where deeper water levels were recorded which implies that the Masama fault zone might be a preferential pathway for groundwater recharge. A homogeneous rating of 1 was assigned to the whole study area since all the net recharge values were less than 50 mm per annum. Each cell within the study area polygon was then multiplied by a weight of net recharge (4) to produce the net recharge index map (R_rR_w) as depicted in Figure 5.4.

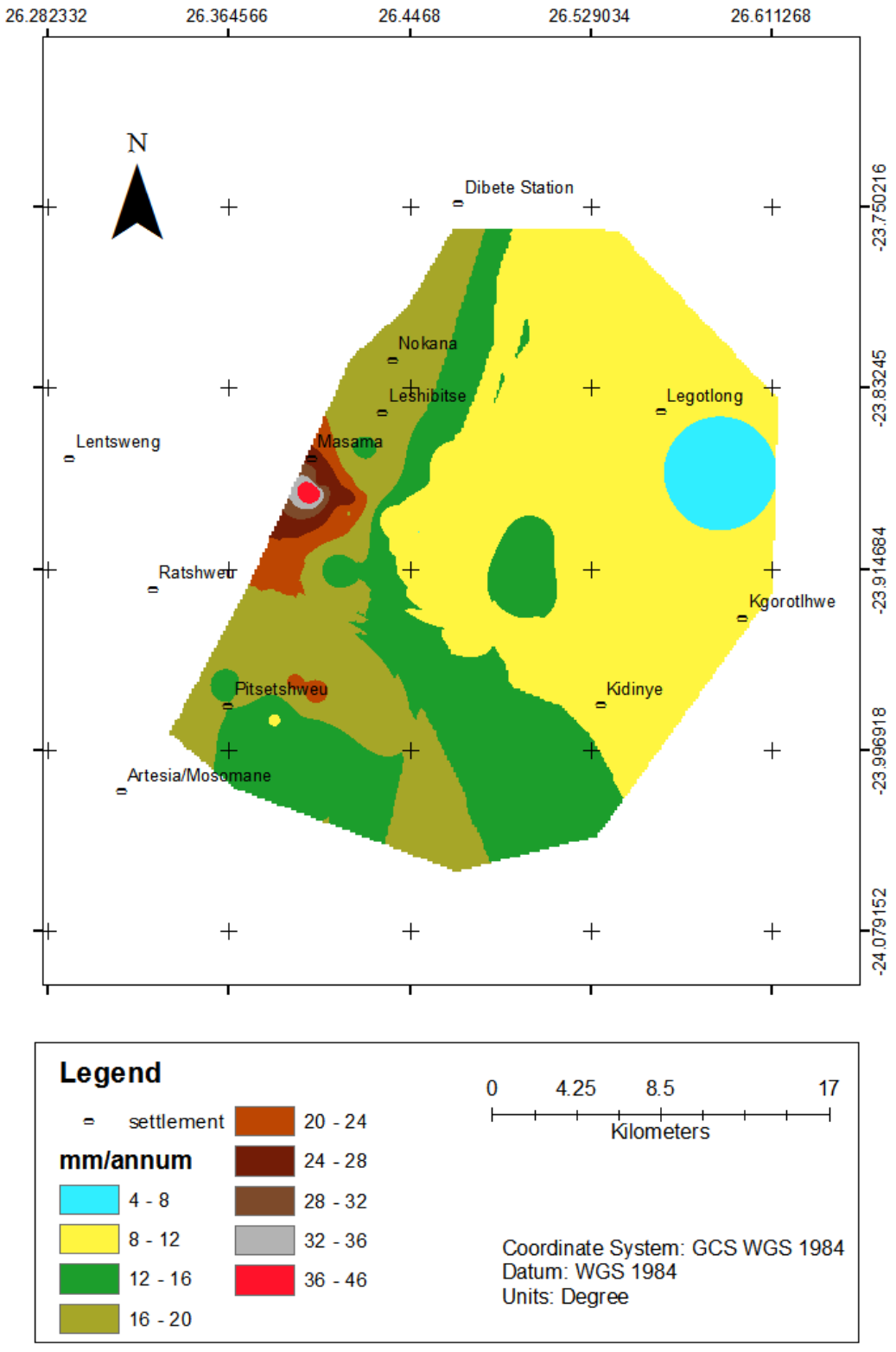

Figure 5.3. Net recharge map (R-map) of the study area.

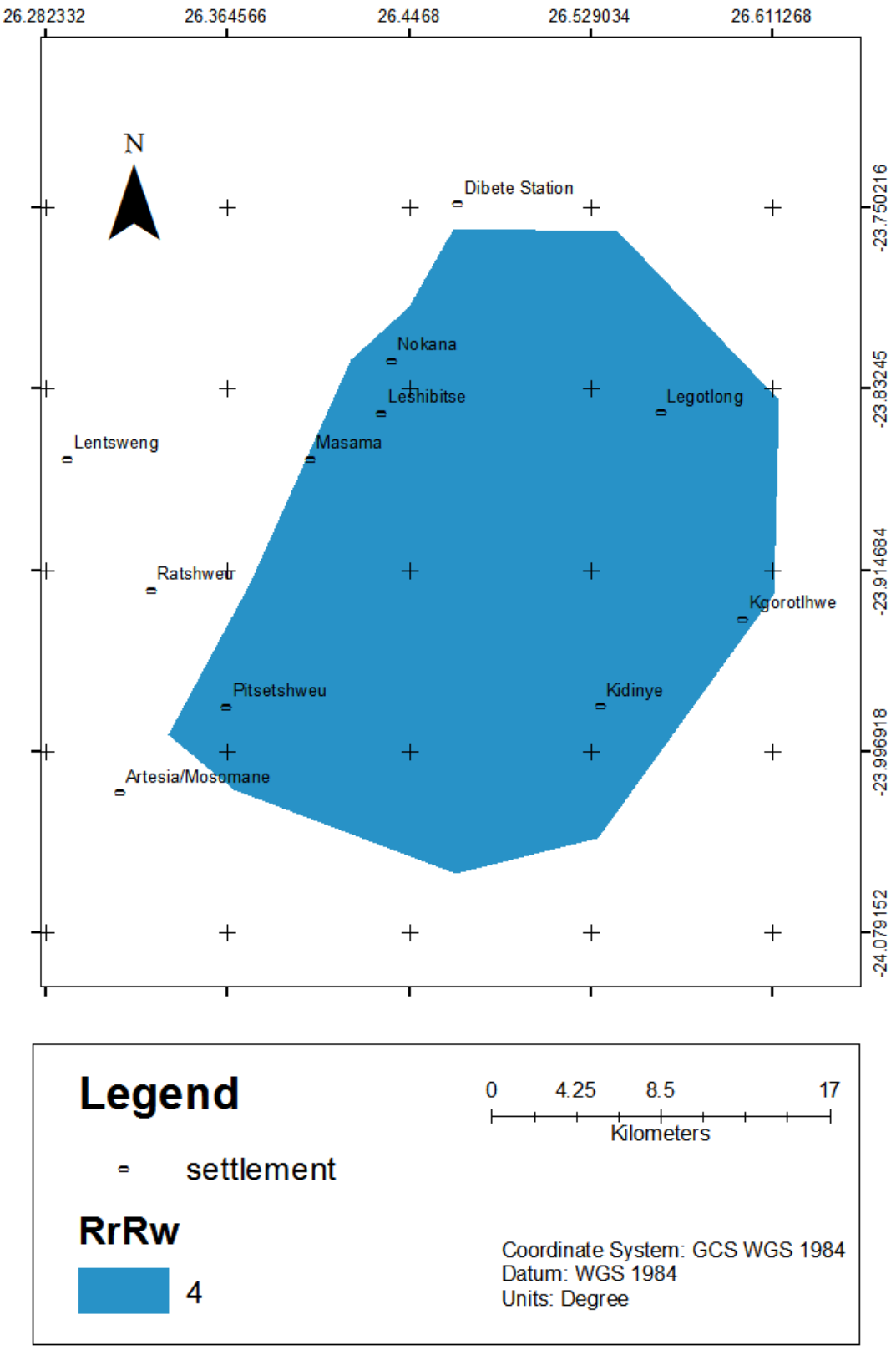

Figure 5.4. Net recharge index map (R_rR_w) of the study area.

5.1.3 *Aquifer media map element (A-map)*

The A-map was constructed basing on the interpretation of the geologic map and borehole records of Masama east well field. The Ntane Sandstone Formation (Lebung Group), Mmamabula Sandstone Formation (Ecca Group), Waterberg Group Sandstone Formations (i.e. Masama, Manyelanong Hill and Twee Rivier) and the Post Karoo Dolerites were delineated as aquifers found within the study area (Figure 5.5). The geologic map and borehole logs indicate that majority of the groundwater strikes were encountered within these rock units, more especially the Ntane Sandstone Formation which is considered as the main aquifer in terms of transmissivity by WSB (2015) and Masike (2008).

The Post Karoo dolerites were assigned a rating of 3 whereas the remaining sandstone formations of Ecca, Lebung and Waterberg Group were assigned a rating of 6 as proposed by Aller et al. (1987). Contaminant migration is expected to be low within the Post Karoo Dolerites owing to their low porosity hence the low rating. The sandstone formations in the well field naturally have higher porosity and were also subjected to intense fracturing which justifies their higher rating of 6. The A-map polygon was then multiplied by 3 to produce the aquifer media index map (A_rA_w) that assumed the form illustrated in Figure 5.6.

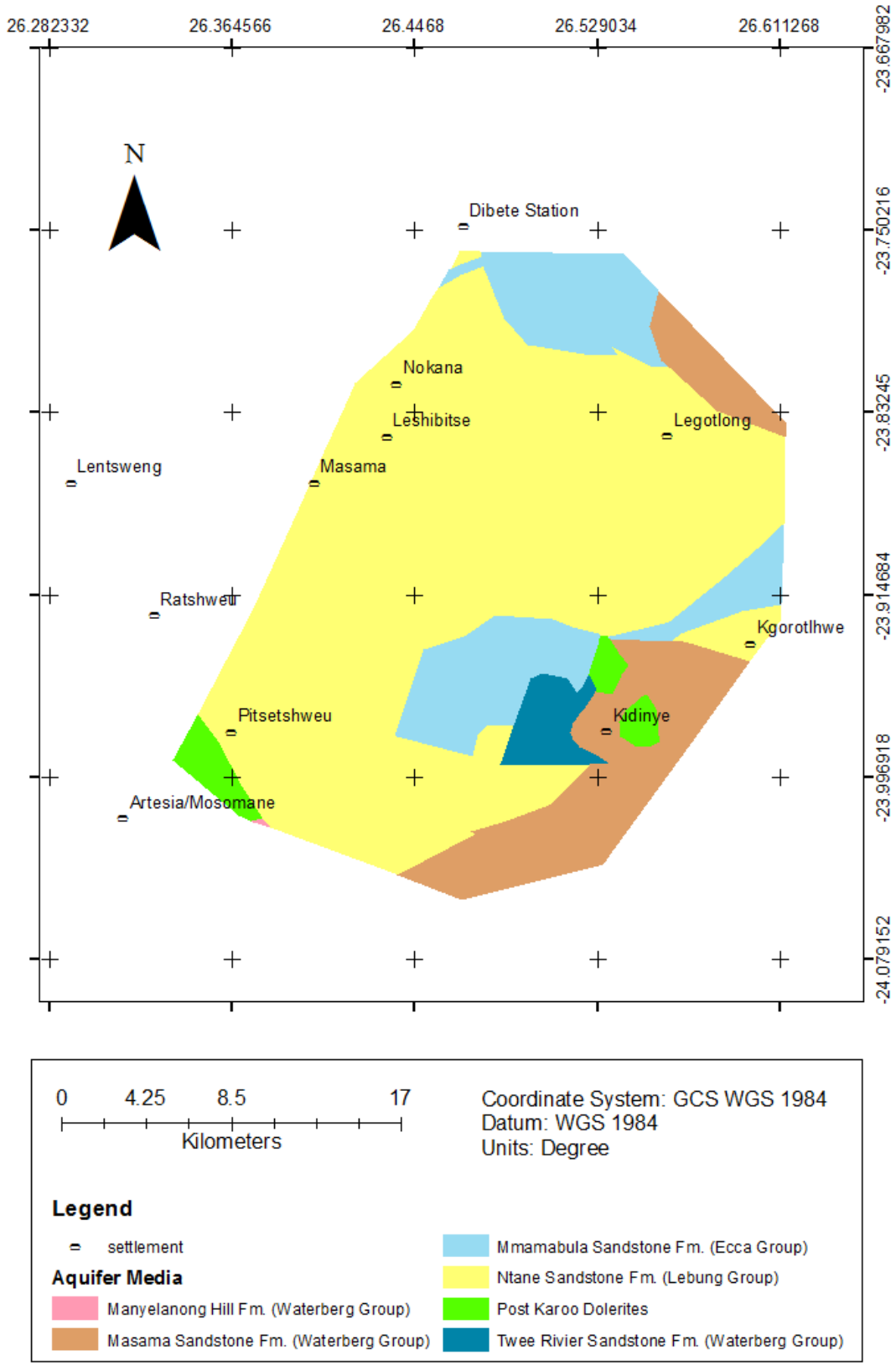

Figure 5.5. Aquifer media map (A-map) of the study area.

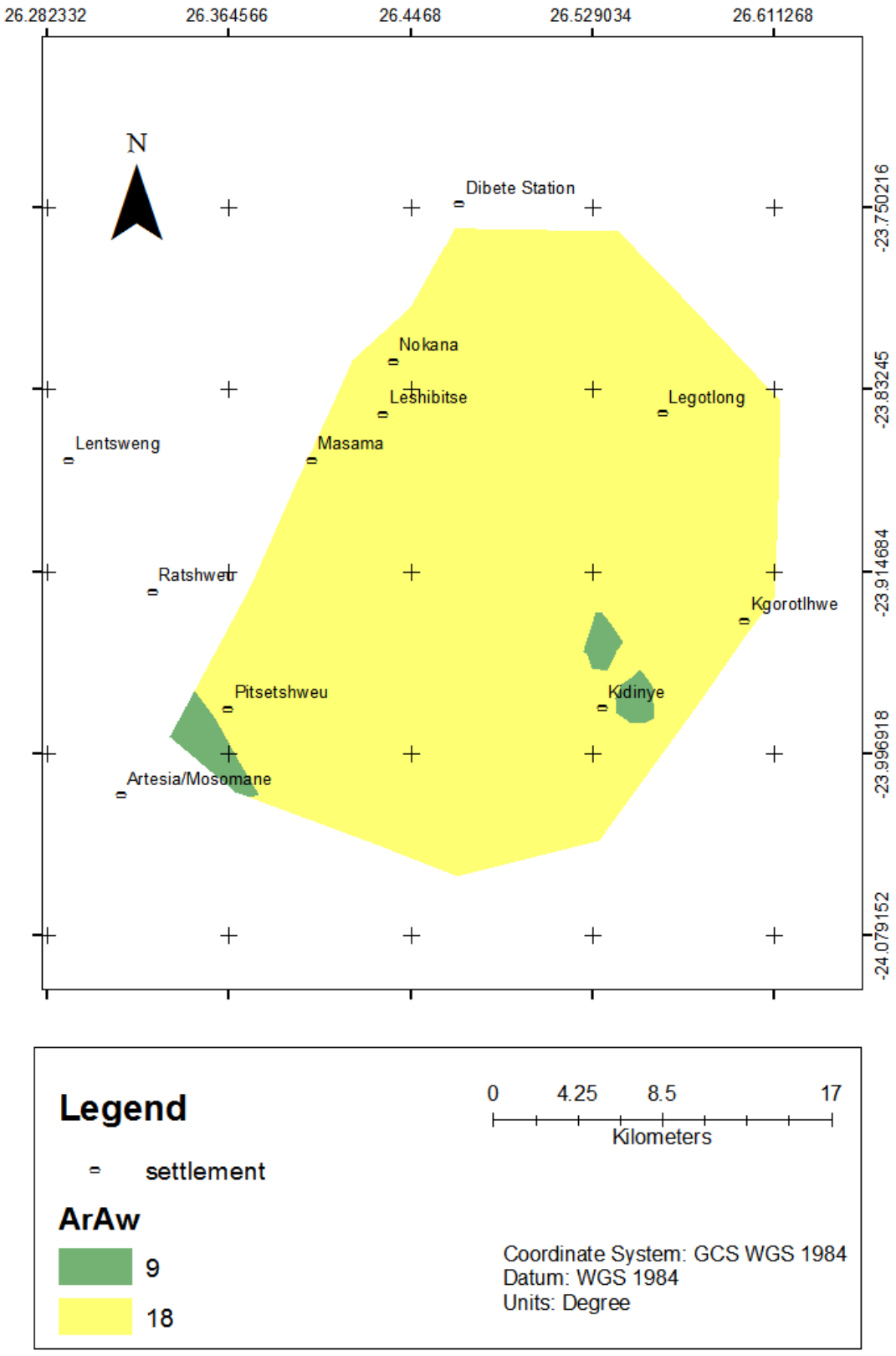

Figure 5.6. Aquifer media index map (A_rA_w) of the study area.

5.1.4 *Soil media map element (S-map)*

Composition and texture of soil tend to have an impact on the amount of water migrating from the ground surface to the groundwater system hence the groundwater vulnerability to pollution (Aller et al., 1987). Four (4) different soil types namely, calcaric luvisols (loamy), luvic arenosols (sandy loam), ferralic arenosols (sand) and petric calcisol (gravel) were identified within the study area (Figure 5.7). These soil types were assigned the ratings of 5, 6, 9 and 10, respectively. Gravel and sand are coarse-grained soils which are mostly likely to allow more water from the surface to reach the groundwater system whereas loamy and sandy loam soils contain a bit of clay which in many cases act as a limitation to the movement of water from the surface into the groundwater system (Aller et al., 1987). Each cell within the S-map was multiplied by the weight of 2 to produce the soil media index map (S_rS_w) as shown in Figure 5.8.

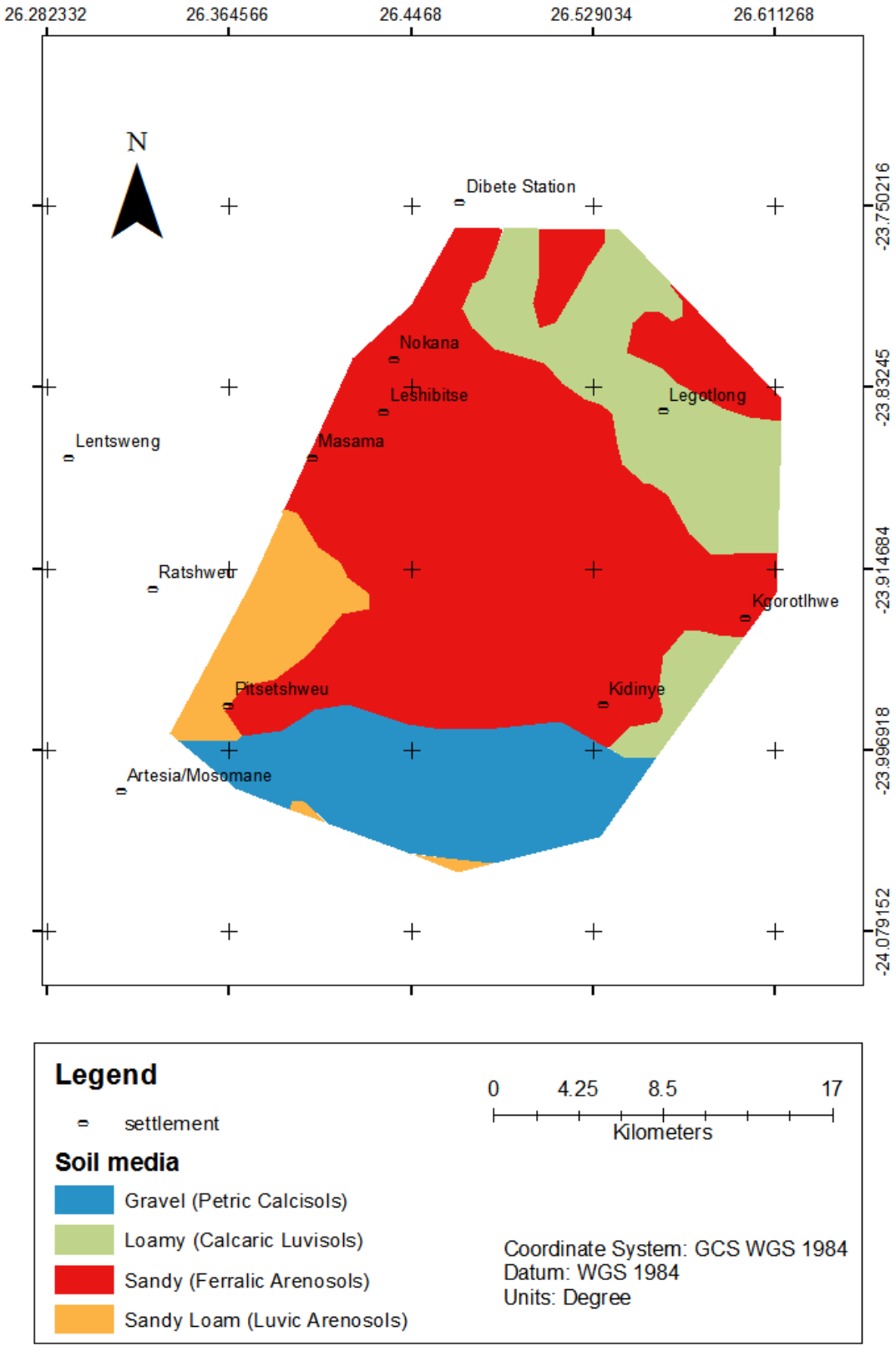

Figure 5.7. Soil media map (S-map) of the study area.

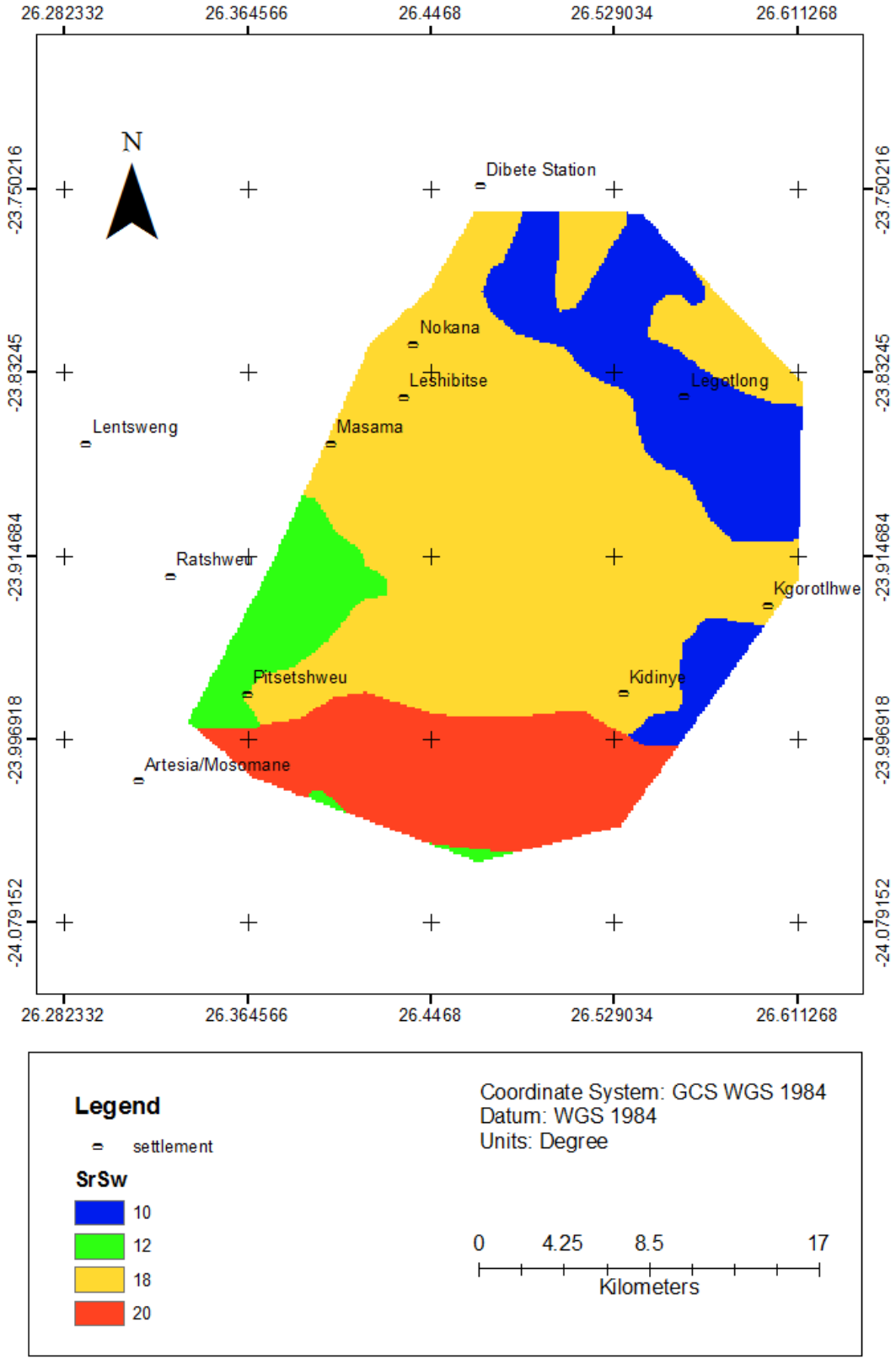

Figure 5.8. Soil media index map (S_rS_w) of the study area.

5.1.5 *Topography map element (T-map)*

Majority of the study area has a slope value that is greater than 18%, meaning that potential pollutants will most likely be washed off by runoff. However, a few localized slope values of 0-2% exist in the study area where potential pollutants are most likely to infiltrate the soil and eventually reach the groundwater system owing to ponding (Figure 5.9). The portion of the study area with slope value exceeding 18% was assigned rating of 1 whereas the one with slope value ranging between 0 and 2% was assigned the rating of 10. Figure 5.10 shows the Topography index map (T_rT_w) of the study area.

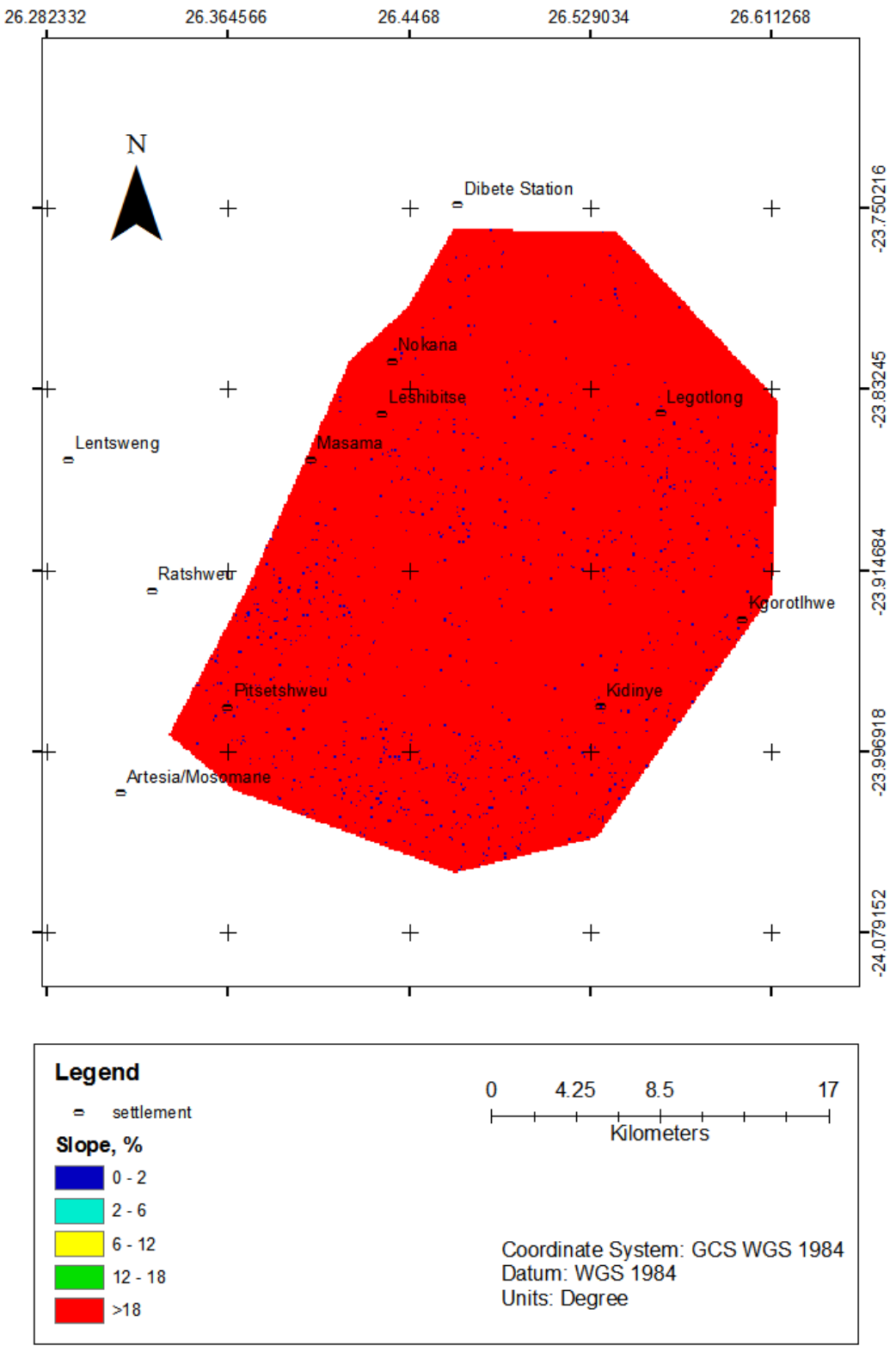

Figure 5.9. Topography (slope) map (T-map) of the study area.

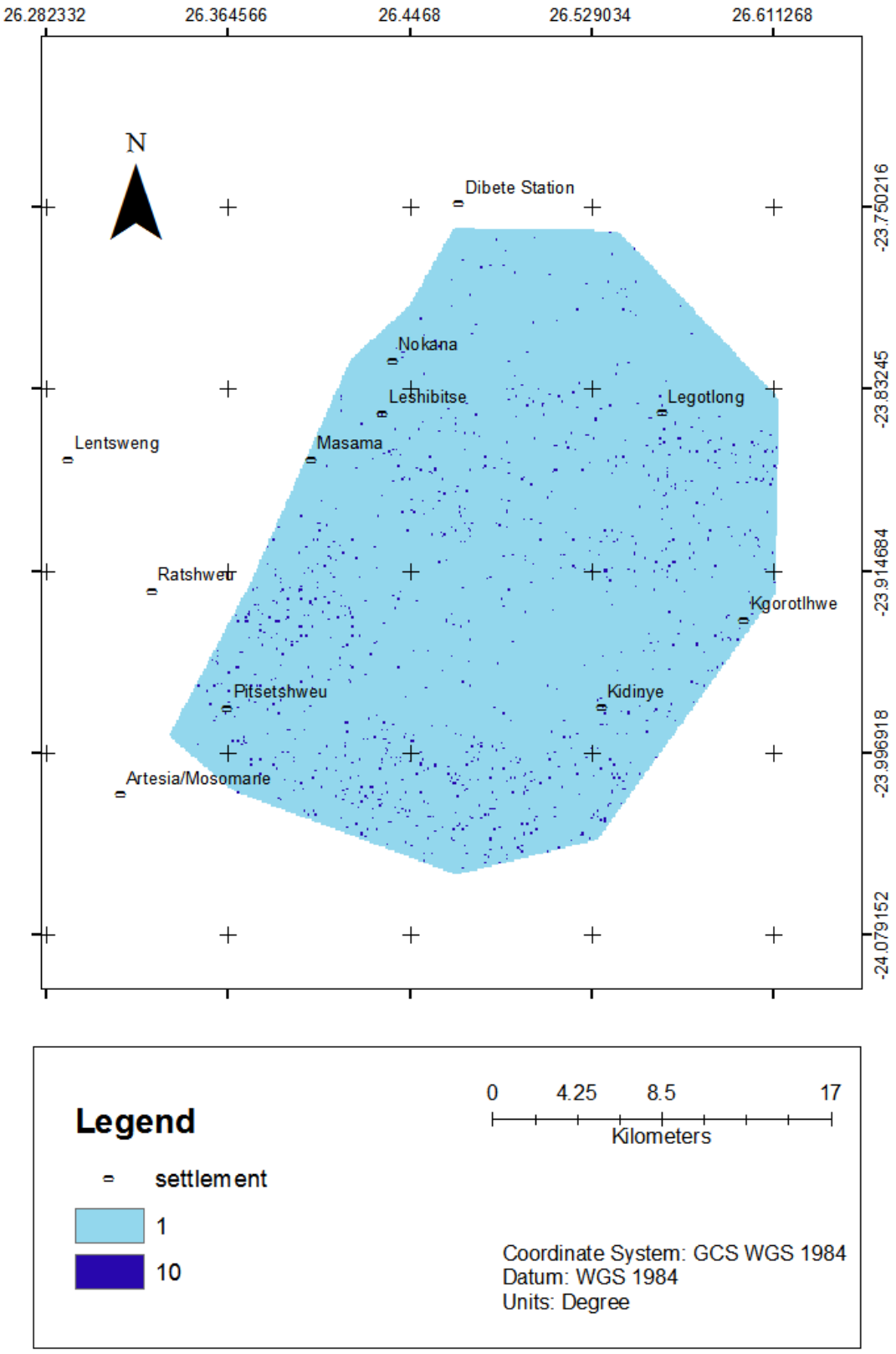

Figure 5.10. Topography index map (T_rT_w) of the study area.

5.1.6 *Impact of vadose zone map element (I-map)*

The flood basalts of the Ramoselwana Volcanic Formation (Stormberg Basalt Group) were identified in this study as the component of the vadose zone along the western margin of the well field. These rocks overlie the Ntane sandstone aquifer and form a confining layer occupying approximately 40% of the total well field area. The sand, clay and calcrete of the Kalahari Beds Formation (Kalahari Group) form the vadose zone in areas where it directly overlies the Ntane Sandstone aquifer, the Post Karoo dolerites and the Waterberg Group sandstone aquifers. This occurs mostly in the northern and eastern portions of the well field covering approximately 40% of its total area (Figure 5.11).

The mudstones and siltstones of Tlhabala Formation (Beaufort Group), Lokgalo Siltstone Formation (Waterberg Group) and Korotlo/ Dibete Formation (Ecca Group) form the component of the vadose zone for the remaining portion of the well field since they overlie the Mmamabula and Manyelanong Hill Formation aquifers of the Ecca and Waterberg Groups, respectively (Figure 5.11). The basalts, sand, clay and calcrete, mudstones or siltstones were then assigned rating of 1, 3 and 8, respectively as proposed by Aller et al. (1987). The impact of vadose zone index map was produced by multiplying each cell within the I-map polygon with the weight of 5 (Figure 5.12).

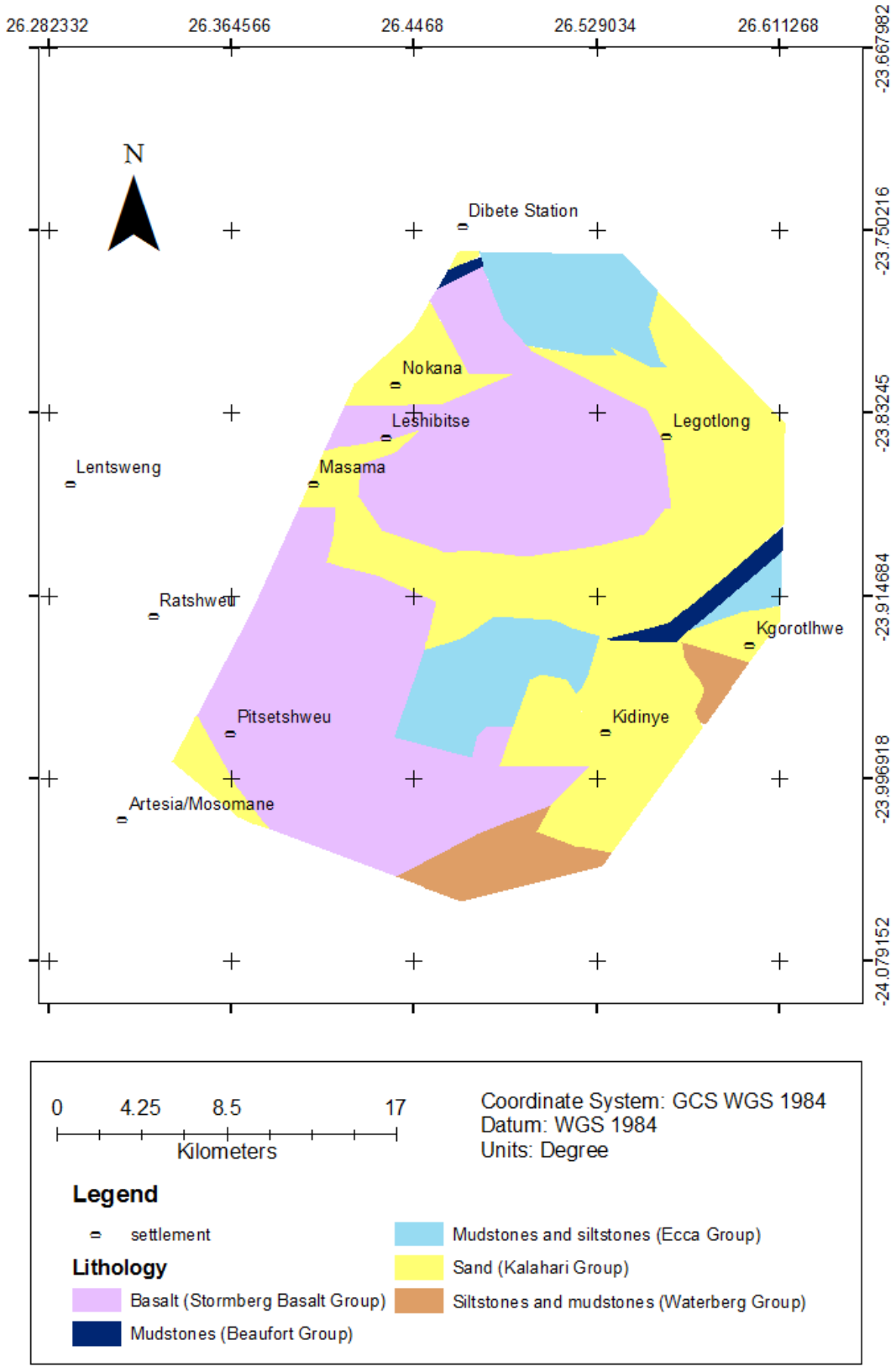

Figure 5.11. Impact of vadose zone map (I-map) of the study area.

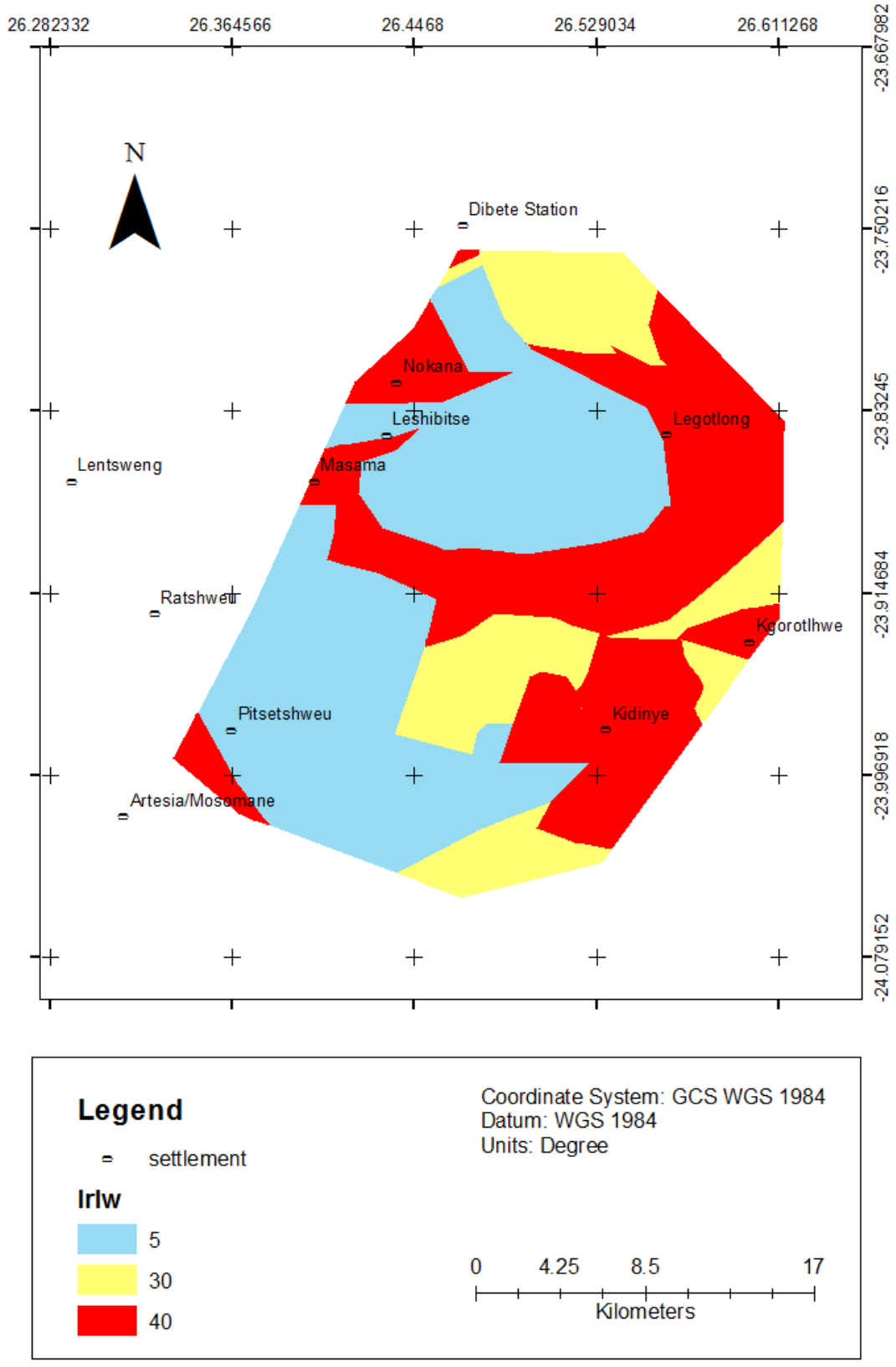

Figure 5.12. Impact of vadose zone index map (I_rI_w) of the study area.

5.1.7 *Hydraulic conductivity map element (C-map)*

Hydraulic conductivity dictates how easy or difficult it is for groundwater to flow through any given aquifer and the higher the conductivity value the higher the risk of groundwater contamination (Aller et al., 1987). Conductivity values in the study area ranged from 0 - 80 m/day (Figure 5.13). The hydraulic conductivity of the study area is mostly low to moderate except for a few localized areas where its values are high. Approximately 70% of the total well field area is a low hydraulic conductivity zone. This portion is characterized by hydraulic conductivity ranging from 0 – 12 m/day and it covers the northern, southern and western parts of the study area.

The moderate hydraulic conductivity zone is located in the central and southeastern parts of the study area with values ranging from 12 – 30 m/day. This portion accounts for just over 29% of the total well field area. The remaining portion with values ranging from 30 – 80 m/day is a high conductivity zone and it is located along the Masama fault zone. This proves that indeed a hydraulic connection exists along the Masama fault zone as indicated by WSB (2015) and Masike (2008). The C-map was reclassified and assigned five rating classes namely, 1, 2, 4, 6 and 8 which were then multiplied by a weight of 3 to produce the hydraulic conductivity index map (Figure 5.14).

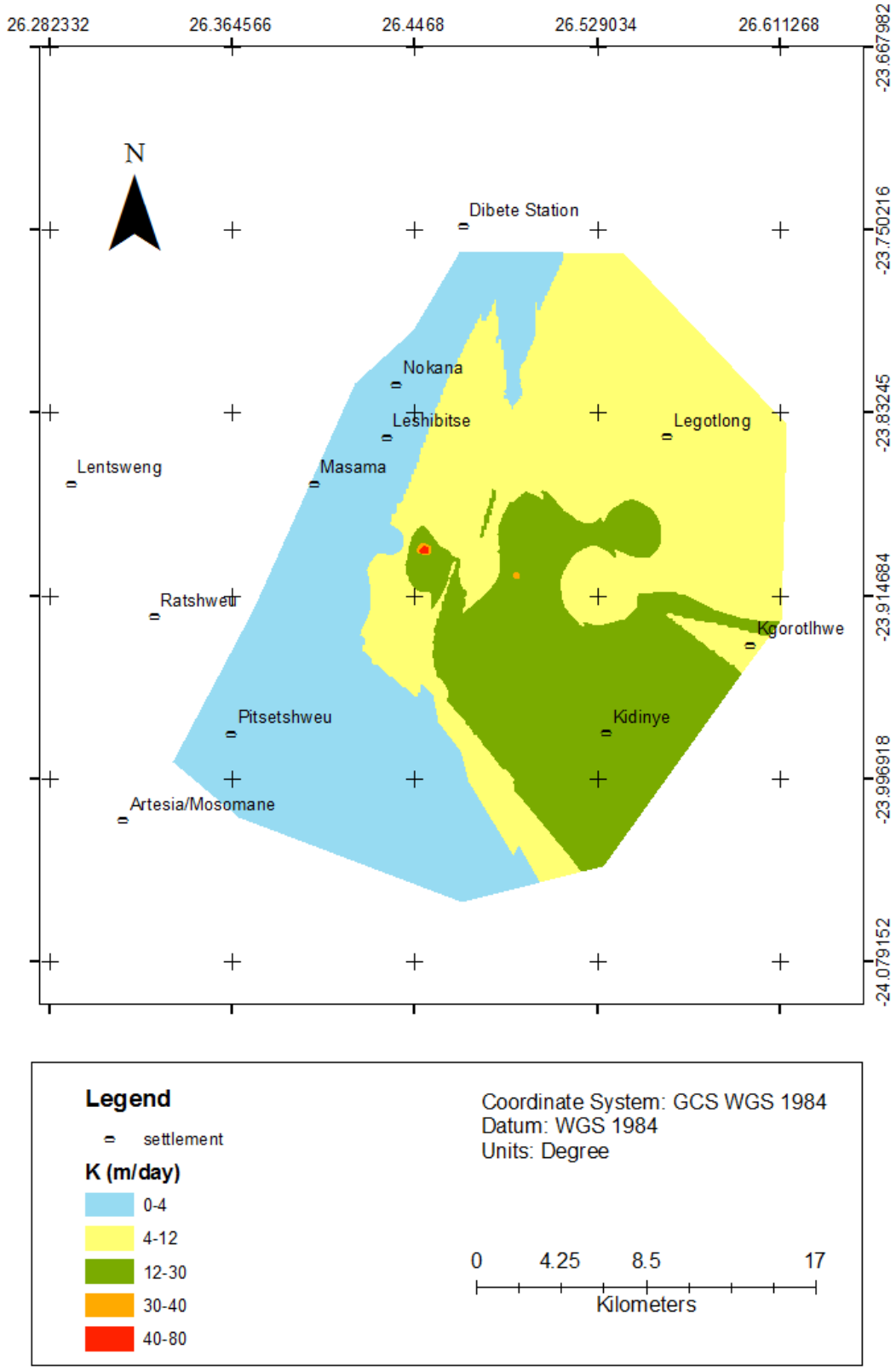

Figure 5.13. Hydraulic conductivity map (C-map) of the study area.

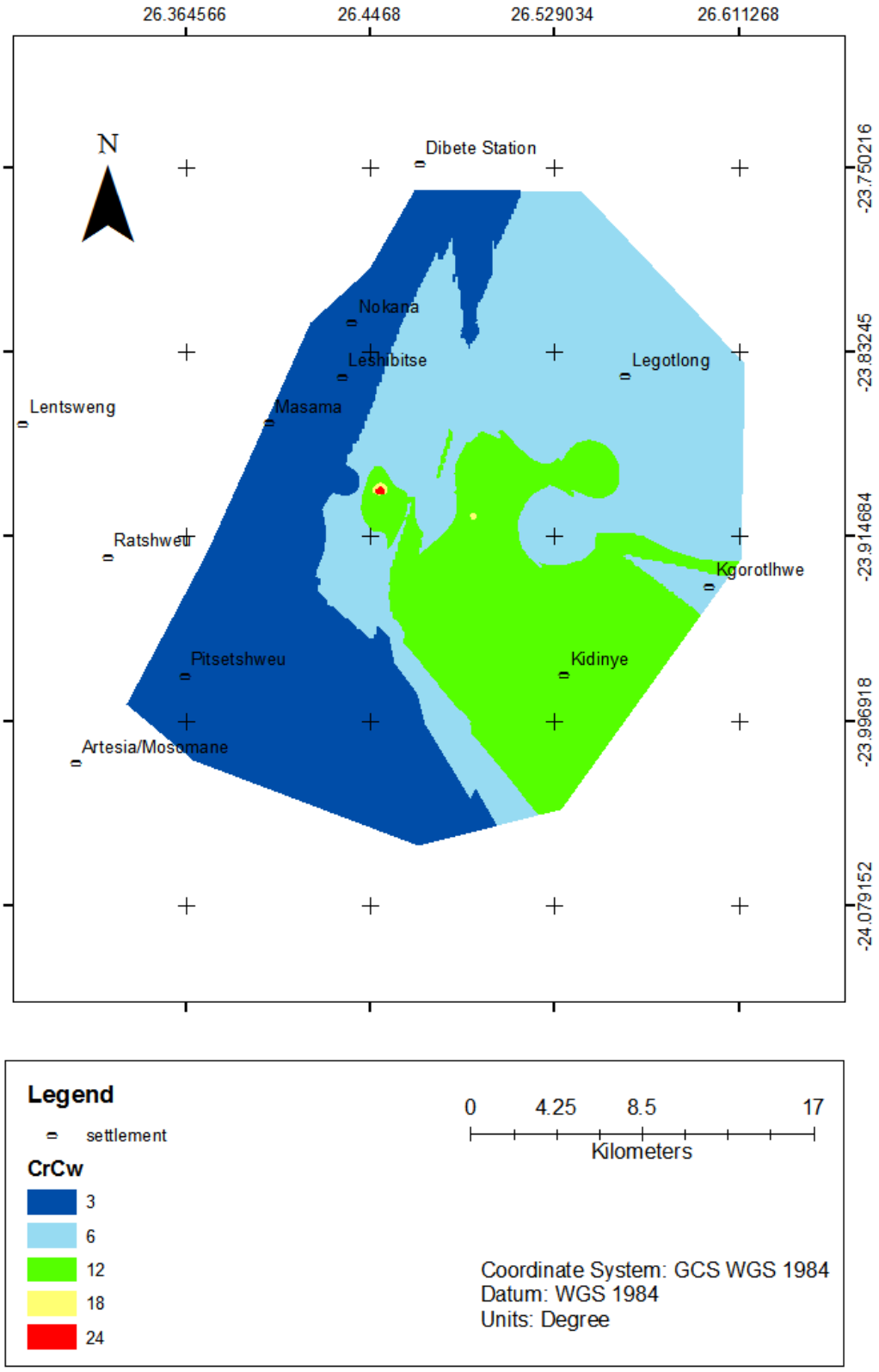

Figure 5.14. Hydraulic conductivity index map (C_rC_w) of the study area.

5.2 Classification of the standard DRASTIC index map

The standard DRASTIC map was produced by overlaying the seven (7) map elements discussed above. The map was then divided into four colour coded groundwater vulnerability zones namely;

- Very low groundwater vulnerability zone (dark blue),
- Low groundwater vulnerability zone (light blue),
- Moderate groundwater vulnerability zone (yellow), and
- High groundwater vulnerability zone (red).

5.2.1 *Very Low Groundwater Vulnerability zones*

Very low groundwater vulnerability zones covered the south western and northern parts of the study area (Figure 5.15). They constituted a spatial area of 329.7 km^2 which was about 45.2% of the total study area hence most of the Masama east well field is less likely to be affected by groundwater pollution occurrences. The following geological and hydrogeological factors justify classification of this zone as a very low groundwater vulnerability area;

- A thick amygdaloidal basalt of the Stormberg Basalt Group forms a confining layer over the aquifer in this zone. This formation is massive and exhibits low primary porosity due to limited weathering at depth which is normally associated with low to negligible groundwater vulnerability;
- Some of the deepest piezometric surfaces observed in the study area were located within this zone more especially near Leshibitse, Nokana and Masama settlements. Potential pollutants were less likely to reach the groundwater system due to increased attenuation capacity and residence time of contaminants in this zone;
- The study area generally slopes gently towards the south easterly direction and the highest elevation points were also found within this zone meaning it is more likely that runoff will occur and wash away potential pollutants before infiltration takes place; and,
- Low net recharge and hydraulic conductivity values in the study area indicated that potential pollutants were less likely to reach the groundwater system from the ground surface.

5.2.2 *Low Groundwater Vulnerability zones*

Majority of the low groundwater vulnerability zones were located in the NNE and SSW parts of the well field. These zones covered 20.1% of the total well field area which amounted to 146.6 km^2 (Figure 5.15). Factors that may have contributed towards the increase in the groundwater vulnerability in these zones are but not limited to;

- The absence of a confining layer and the existence of more permeable sand and mudstone formations in the vadose zone which means that potential pollutants are more likely to migrate to the groundwater system;
- Majority of these zones were characterized by relatively shallower depth to groundwater meaning that attenuation capacity and residence time of contaminants would be slightly less than those in the very low groundwater vulnerability zones;
- The existence of sandy loam and loamy soil in such zones, more especially the NNE parts limits movement of potential pollutants from the surface into the groundwater system as these soils contain clayey layer which in many cases acts as an impermeable layer; and,
- Pumping test data analysis indicates generally low hydraulic conductivity within these zones which is also likely to limit the amount of potential pollutants reaching the aquifer.

5.2.3 *Moderate Groundwater Vulnerability zones*

These zones were located in the eastern margin towards the center of the study area and they covered a spatial area of 234.1 km^2 (Figure 5.15). They were the second most abundant groundwater vulnerability class at 32.1% of the total study area which is nearly a third of the wellfield. Factors influencing their classification are as follows;

- The aquifer media within these zones consist of the more permeable sandstone formations from the Karoo Supergroup and Waterberg Group;
- Sand and gravel are found within these zones and they tend to be more permeable thus allowing potential pollutants to migrate from the surface into the groundwater system; and,
- The vadose zone comprises of mostly sand which created the expectation that the groundwater vulnerability in such zones would be greater than in the very low and low groundwater vulnerability zones.

5.2.4 *High Groundwater Vulnerability zones*

High Groundwater Vulnerability zones were the least abundant in the study area and majority of them were located in the extreme south eastern portion (Figure 5.15). They covered a spatial area of 19.0 km^2 constituting about 2.6% of the total study area. These zones were generally found in localized flat areas (slope of 0-2%) and mostly within Petric Calcisols (gravel). High groundwater vulnerability zones are underlain by a vadose zone comprising of sand, clay and calcrete of the Kalahari Group. The highest hydraulic conductivity values recorded within the study area were observed in such zones along the Masama fault zone. Under this conditions potential pollutants are most likely to migrate from the surface into the groundwater system with very limited resistance by the local hydrogeological settings hence high groundwater vulnerability to pollution is expected.

Moderate to high groundwater vulnerability zones are more likely to allow movement of pollutants from the surface into the aquifer due to limited attenuation capacity and reduced residence time of contaminants in local geological formations. Very low to low groundwater vulnerability zones are less likely to allow the movement of pollutants from the surface into the aquifer due to increased attenuation capacity and residence time of contaminants. Only the most persistent pollutants stand a slim chance of infiltrating the groundwater system under very low to low groundwater vulnerability zones.

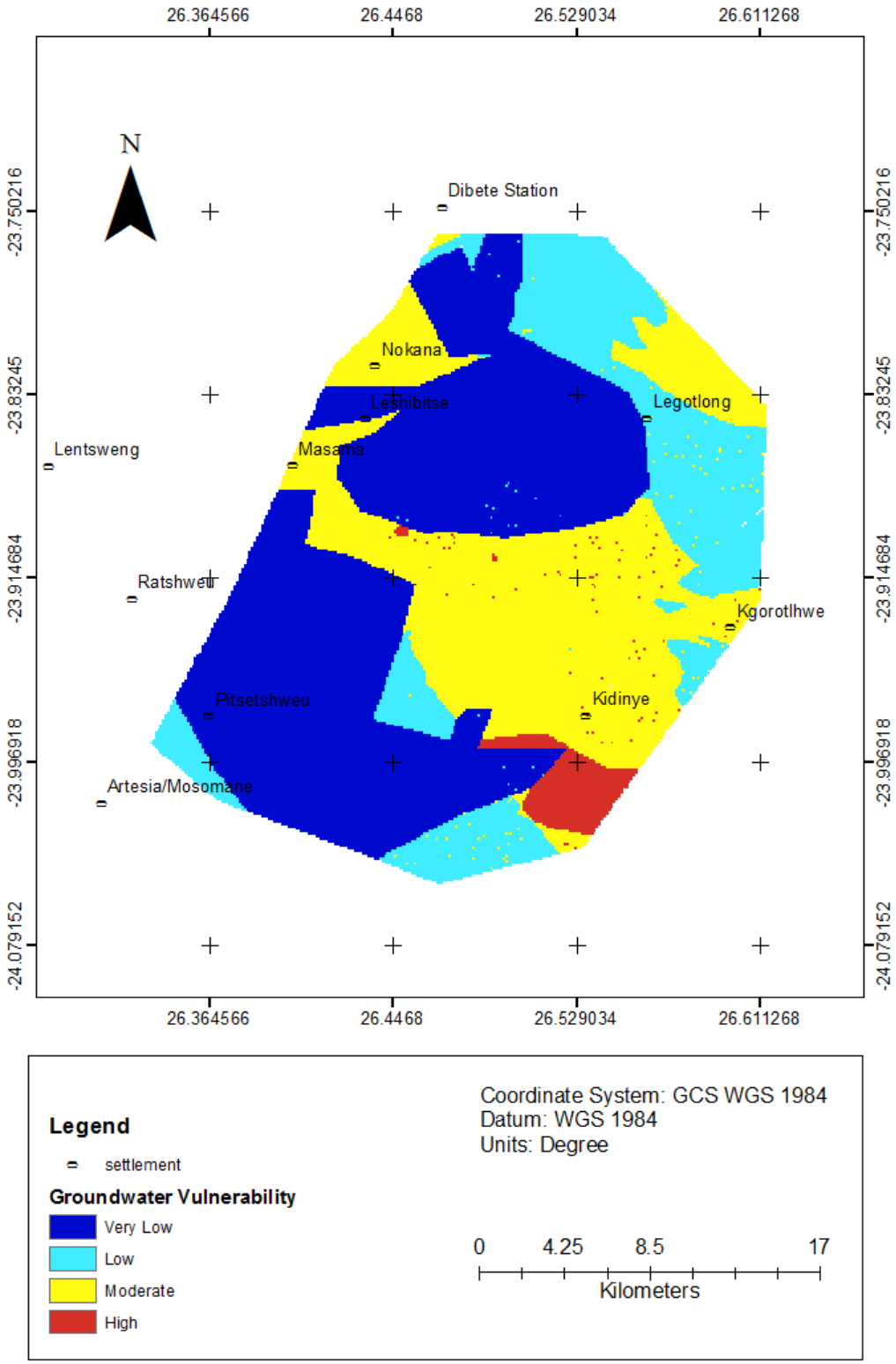

Figure 5.15. Groundwater pollution vulnerability map of the study area computed using the standard DRASTIC index model.

5.3 Sensitivity analysis

The DRASTIC method is considered to be a subjective method owing to its use of seven (7) parameters, ratings and weights. Barbiker et al. (2005) disagree with the use of all seven parameters in evaluating groundwater vulnerability. The authors believe that it's possible to use fewer parameters and obtain highly accurate results at low cost. Barbiker et al. (2005) reckons that the ratings and weights used in the DRASTIC index method vary from one place to another hence the need for calibrating the standard DRASTIC index map. Sensitivity analysis was used to check the necessity of using all seven DRASTIC parameters in evaluating groundwater vulnerability of Masama east well field as well as to reduce the subjectivity associated with the method.

5.3.1 *Map Removal Sensitivity Analysis*

This kind of analysis was applied in two forms, first variation in groundwater vulnerability due to removal of one parameter at a time was computed and then variation in groundwater vulnerability as result of the removal of one or more parameters at a time was computed. The outcome of removal of one parameter at time indicated that there was variation in the groundwater pollution vulnerability map of the study with the removal of each parameter (Table 5.1). The impact of vadose zone was the parameter with the greatest mean variation index of 9.35% followed by soil media and topography at 2.69% and 2.00%, respectively. The parameter with the least mean variation index was the hydraulic conductivity with 1.01%. Removal of one or more parameter at time was based on Table 5.2, the parameters with the least variation index were removed first. Hydraulic conductivity was removed first and soil media was removed last leading to a mean variation index of 18.72% (Table 5.2). The mean variation tends to increase with the removal of one or more parameters. Barbiker et al. (2005) attributed this increase in the mean variation index to the inability of these parameters to properly illustrate the actual hydrogeological conditions of any given area.

Table 5.1 Map removal sensitivity analysis-removal of one parameter at a time

Parameter removed	Variation Index (%)			
	Minimum	Mean	Maximum	Standard Deviation
D	0.65	1.20	1.55	0.31
R	0.99	1.43	1.71	0.25
A	0.62	1.87	3.87	1.13
S	0.60	2.69	5.44	1.47
T	0.40	2.00	2.21	0.47
I	6.35	9.35	15.31	2.67
C	0.11	1.01	1.82	0.57

Table 5.2 Map removal sensitivity analysis-removal of one or more parameters at a time

Parameter used	Variation Index (%)			
	Minimum	Mean	Maximum	Standard Deviation
DRASTI	2.71	4.07	5.04	0.68
ASTI	3.06	5.46	7.34	1.12
I	3.87	18.72	33.33	11.12

5.3.2 *Single Parameter Sensitivity Analysis*

This technique was used to evaluate the effect of each DRASTIC parameter in the computation of the DRASTIC index and it was achieved by comparing the effective weight with the theoretical weight assigned by Aller et al. (1987) for each parameter (Napolitano and Fabbri, 1996). The most effective parameters were aquifer media, soil media and impact of vadose zone with effective weights of 24.77%, 23.34% and 29.46%, respectively (Table 5.3). They were also the only parameters whose effective weights were greater in comparison to their theoretical weights. All the other parameters had effective weights that were less than their theoretical weights and topography with 2.74% was the least effective parameter in the evaluation of Masama east well field groundwater vulnerability to pollution.

Table 5.3 Single parameter sensitivity analysis

Parameter	Theoretical Weight	Theoretical Weight (%)	Effective Weight (%)				Effective Weight
			Mean	Minimum	Maximum	Standard Deviation	
D	5	21.74	7.13	5.00	10.42	1.87	1.6
R	4	17.39	5.68	4.00	8.33	1.50	1.3
A	3	13.04	24.77	10.11	37.50	7.26	5.6
S	2	8.70	23.34	11.9	36.73	7.42	5.3
T	1	4.35	2.74	1.00	18.52	4.40	0.6
I	5	21.74	29.46	8.47	47.62	15.73	6.7
C	3	13.04	8.29	3.37	15.00	3.49	1.9

5.4 Weight Modification of the groundwater pollution vulnerability Map

Saidi et al. (2011) and Napolitano and Fabbri (1996) both justify the use of effective weight in place of the theoretical weight in each DRASTIC parameter siting the reason for that as potentially increased accuracy of the groundwater vulnerability map. The theoretical weights initially assigned by Aller et al. (1987) were replaced with the effective weights computed from the single parameter sensitivity analysis technique. These weights were then used to compute the modified DRASTIC index for each cell within the Masama east well field polygon and the result was a modified groundwater pollution vulnerability map (Figure 5.16).

The areas initially classified as very low groundwater vulnerability zone were reduced to 320.9 km^2 (44.0% of the total study area) whereas the low groundwater vulnerability zone also decreased to 94.8 km^2 (13.0% of the total study area). The very low groundwater vulnerability zones still coincide with the confining layer and the low groundwater vulnerability zones are located within the sandy loam and loamy soil. The high groundwater vulnerability zone increased in area to 158.3 km^2 (21.7% of the total study area) while the moderate groundwater vulnerability zone decreased in area to 155.4 km^2 (21.3% of the total study area). The high groundwater vulnerability zones are restricted to the sandstone formations which are considered to be the aquifer media within the study area.

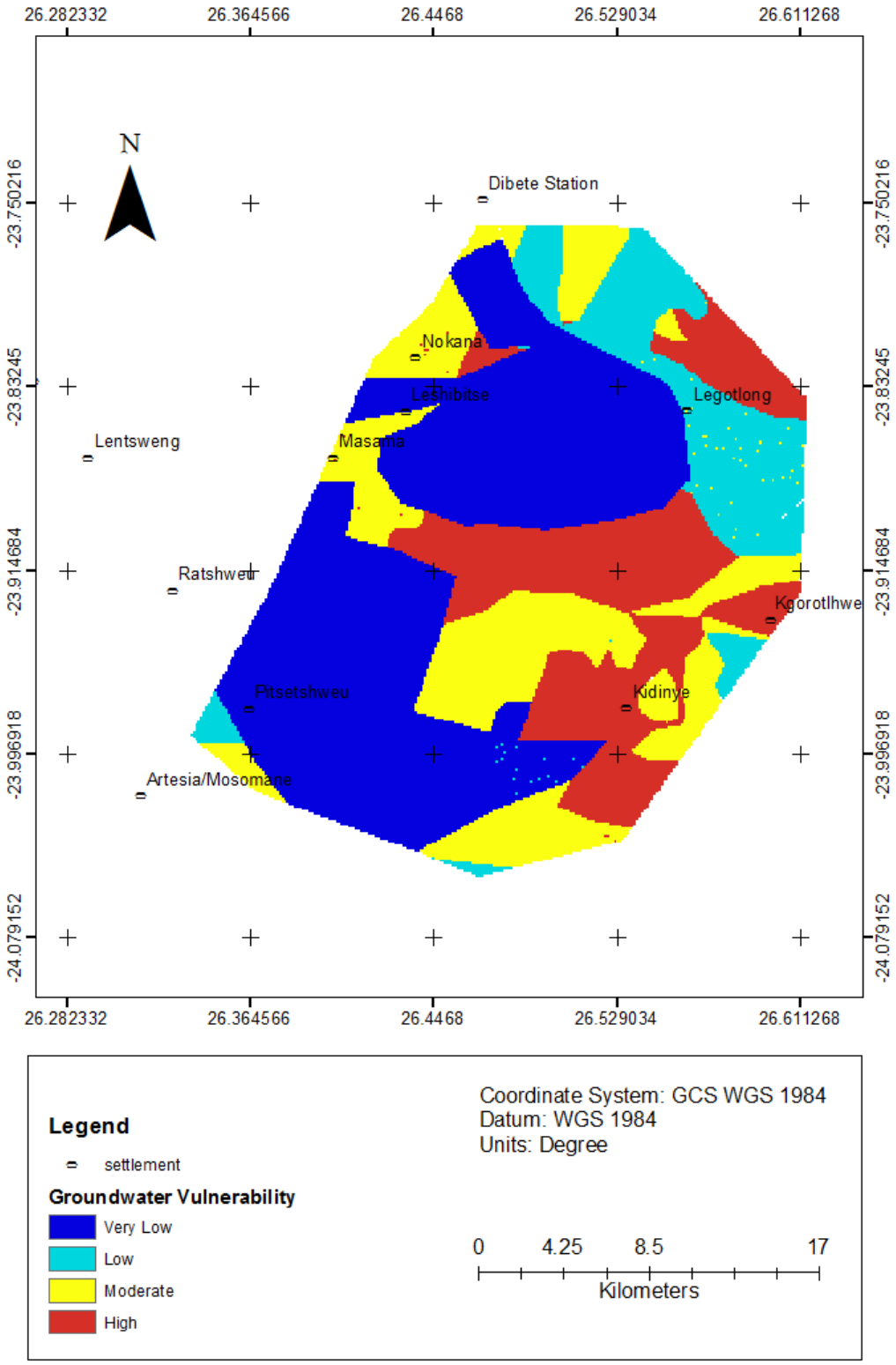

Figure 5.16. Groundwater pollution vulnerability map of the study area after weight modification.

5.5 Integration of Land Use parameter into the Modified DRASTIC map

The land use map was divided into three classes labeled, residential and agricultural land, vegetation and barren land, water and wet area which were assigned the rating 8, 7 and 5, respectively as proposed by Secunda et al. (1998). The residential and agricultural land is confined to the north western portion whereas patches of water and wet areas are found in the SSE portion of the study area. The dominant land use class is the vegetation and barren land followed by residential and agricultural land and water and wet area, respectively (Figure 5.17). Each cell in the land use distribution map was multiplied by a weight of 5 to produce the Land use index map as indicated in Table 4.3 (Figure 5.18).

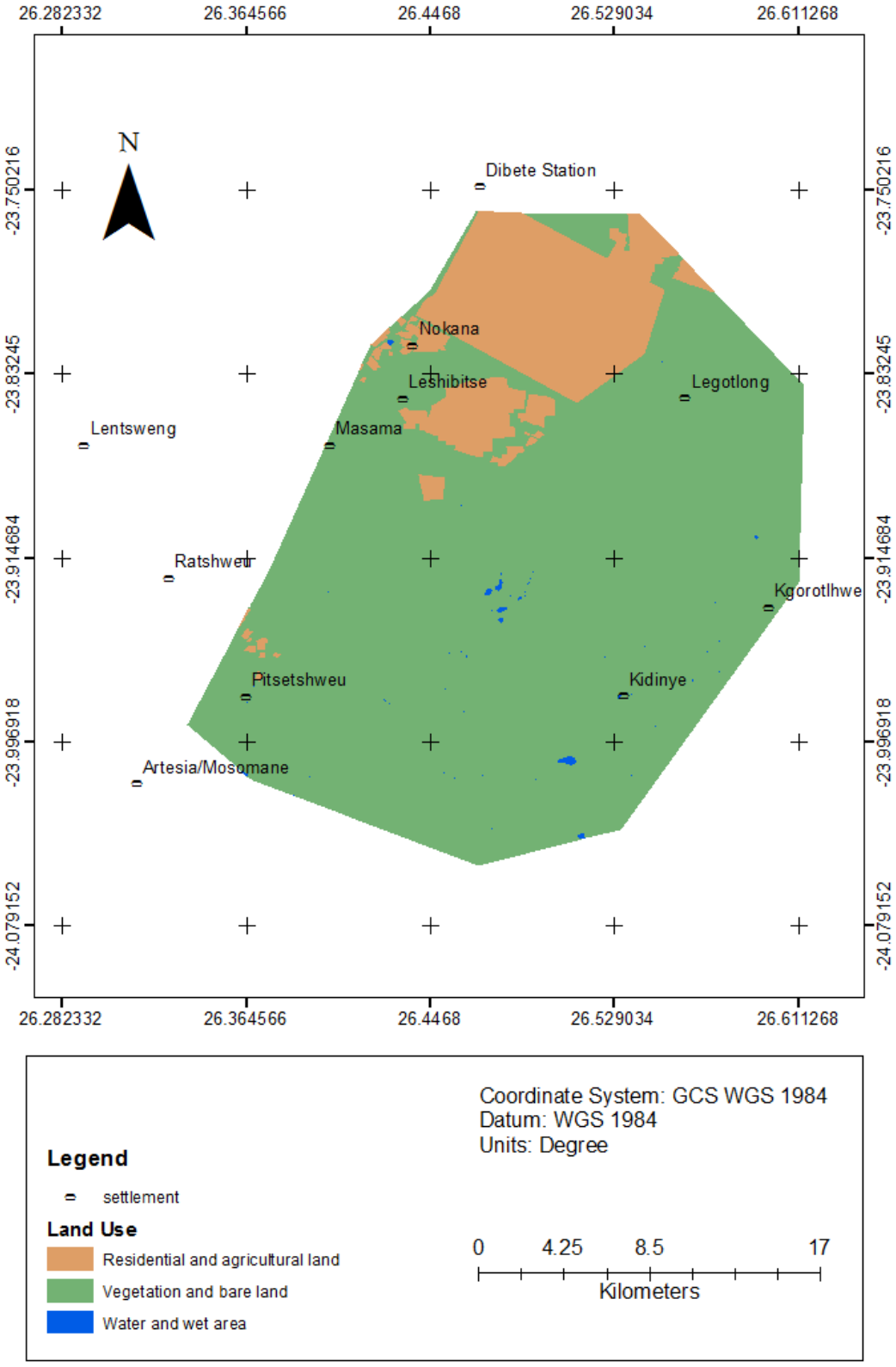

Figure 5.17. Land use map of the study area.

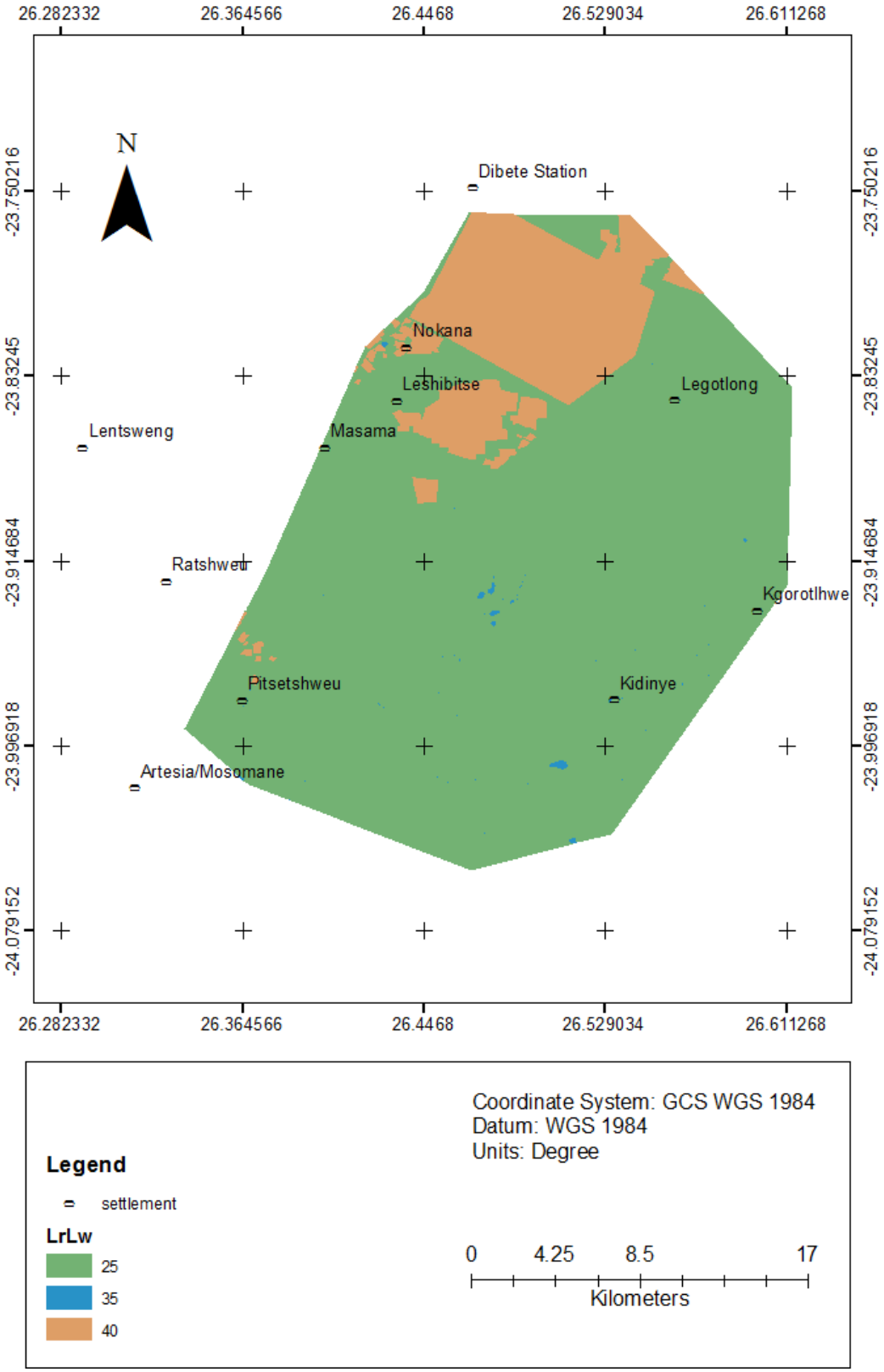

Figure 5.18. Land use index map (L_rL_w) of the study area.

The land use index was integrated into the groundwater vulnerability evaluation to produce the final groundwater pollution vulnerability of Masama east well field. The areal extent of the very low groundwater vulnerability zone was further reduced to 284.5 km^2 (39.0% of the total study area) whereas the low groundwater vulnerability zone increased to 145.2 km^2 (19.9% of the total study area). Existence of residential and agricultural land is the reason for these variations since they are known to be primary sources of groundwater pollution and eventually lead to an increase in groundwater vulnerability (Porcel et al., 2014). The high groundwater vulnerability zone covered an area of 99.2 km^2 (13.6% of the total study area) whereas the moderate groundwater vulnerability zone increased in area to 200.6 km^2 (27.5% of the total study area).

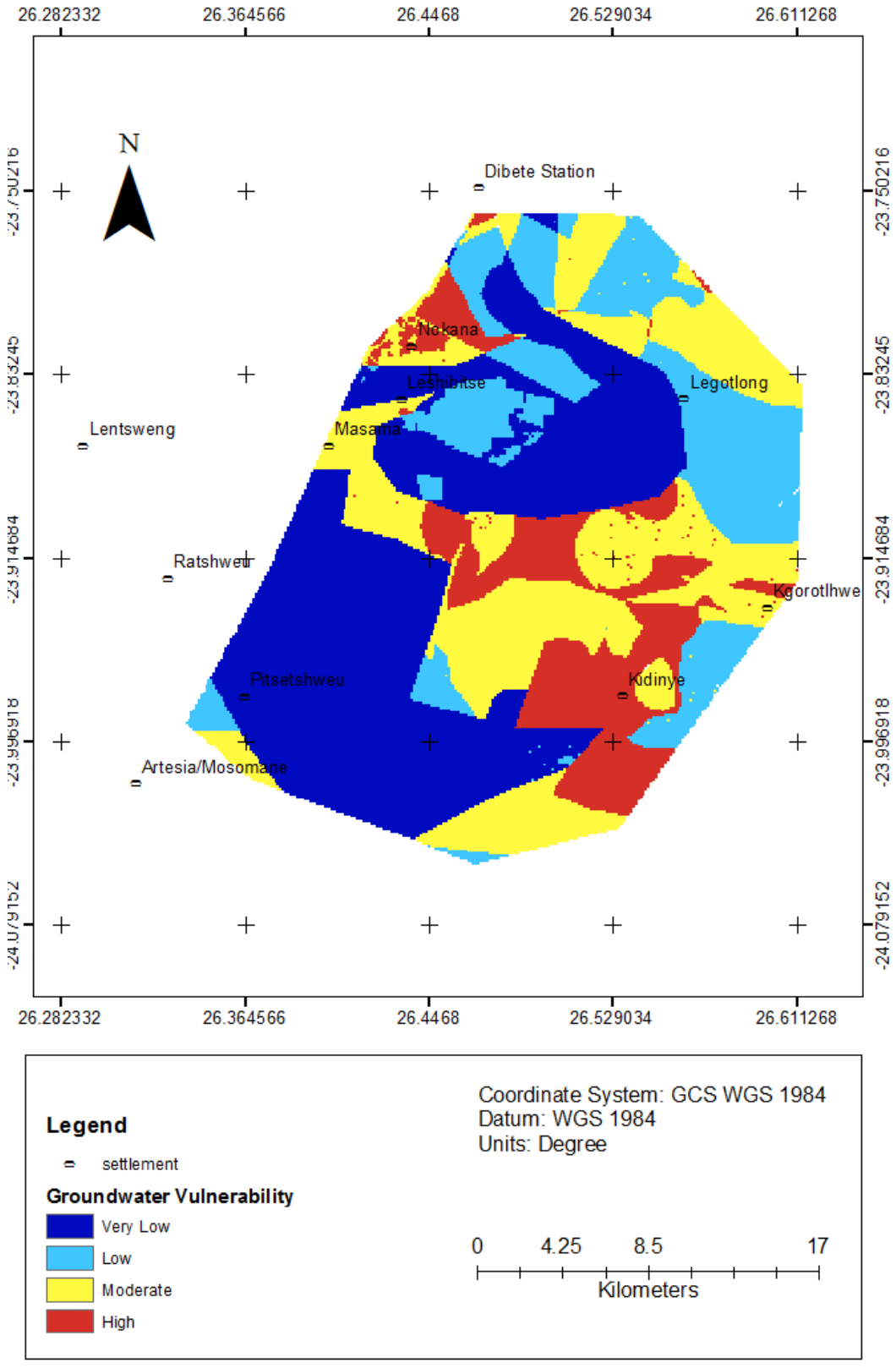

Figure 5.19. Final groundwater pollution vulnerability map of Masama east well field.

5.6 Groundwater quality

5.6.1 General groundwater quality

Water quality data obtained from boreholes within the study area were analyzed and compared to both the WHO and BOS 32:2009 drinking water specifications in order to determine whether the groundwater from such boreholes is suitable for human and livestock consumption. The total dissolved solids content of the groundwater meets the standards of both the WHO and BOS 32:2009 class I drinking water specifications with values ranging from 90.00 - 515.60 mg/l and an average value of 297.81 mg/l (Table 5.4). The groundwater in the study area can therefore be classified as freshwater (TDS<1000 mg/l).

The pH of the groundwater samples obtained within the well field ranged from 6.03 - 9.43 mg/l, an average value of 7.99 mg/l. These values fall within the BOS 32: 2009 Class I drinking water specifications (5.5 – 9.5) even though several groundwater samples recorded pH values in excess of the 8.5 limit set by the WHO. The electrical conductivity (EC) of groundwater in the study area varies between 133.32 and 830.00 µS/cm, with an average of 458.98 µS/cm. BOS 32:2009 Class I drinking water specifications are fully satisfied by groundwater within the study area whereas several boreholes produced groundwater with EC above the WHO drinking water specifications limit of 750 µS/cm.

5.6.2 Major Cations

Analysis of the groundwater samples obtained from the study area indicated that majority of the major cations concentration (i.e. Ca^{2+}, Na^{+}, K^{+} and Mg^{2+}) fall within the limits of WHO and BOS 32:2009 Class I drinking water specifications, except for the samples from boreholes Z20128, Z20130 and Z20147 (Table 5.4). Groundwater obtained from Z20128 and Z20130 exhibited Mg^{2+} ion concentration in excess of 30 mg/l whereas Z20147 recorded Ca^{2+} ion concentration greater than 75 mg/l. The 30 mg/l and 75 mg/l stated above represent the upper limits of concentration for magnesium and calcium ions in groundwater as suggested by the World Health Organization (WHO, 2006). Groundwater obtained from the study area recorded Ca^{2+}, Mg^{2+}, Na^{+} and K^{+} ion concentrations ranging from 12.50 – 127.40, 3.35 – 33.08, 16.43 – 66.47 and 1.68 – 13.57 mg/l, respectively. The average concentration values were 48.07, 18.12, 34.78 and 6.15 mg/l for Ca^{2+}, Mg^{2+}, Na^{+} and K^{+} ions, respectively.

5.6.3 Major Anions

Cl^-, HCO_3^-, SO_4^{2-} and NO_3^- ions form the major cations in the groundwater within the well field and they were satisfactory in terms of the WHO and BOS 32:2009 class I drinking water specifications with concentrations ranging from 10.95 – 116.00, 0 – 268.40, 0.69 – 20.30 and 0.05 – 25.86 mg/l, respectively. The average concentrations values were 47.55, 0.001, 6.91 and 6.42 mg/l. Consumption of the water with that amount of nitrates would not result in any health complications. However, the existence of nitrate concentration exceeding 10 mg/l in the groundwater is indicative of human impact since natural nitrates content of groundwater is normally lower than 10 mg/l (WHO, 2006).

5.6.4 Trace Elements

The F^-, Fe^{2+} and Mn^{2+} ions form the trace elements in the groundwater within the study area with concentration ranging from 0 – 1.18, 0 – 2.21 and 0 – 0.56 mg/l, respectively. The content of these trace elements in the groundwater meet the BOS 32:2009 class I drinking water specifications except for two boreholes namely, Z20131 and Z20132. They have F^- ion concentration in excess of 1.00 mg/l and as a result they only satisfy the BOS 32:2009 class II drinking water specifications. Groundwater within the well field promotes good dental health and bone development since both dental and skeletal fluorosis are not likely to result from consuming such water.

WHO (2006) reckons that presence of clays and silts in the top soil leads to attenuation of bacteria, viruses and other pathogens. The same author also states that the above mentioned pathogenic micro-organisms are not likely to reach groundwater at depths greater than five (5) m.b.g.l. Generally, groundwater in the Ntane sandstone aquifer (main aquifer in the study area) is accessible by drilling of deep boreholes (over 100 m.b.g.l) and it is overlain by a confining layer and clayey soils (Masike, 2008). This means that the chances of pathogenic micro-organism reaching groundwater from the ground surface in the well field are very low, if not negligible.

Table 5.4. Hydrochemical parameters of groundwater in Masama east well field.

BH No	PH	EC (µS/cm)	Alkalinity $CaCO_3$ (mg/l)	HCO_3 (mg/l)	Cl (mg/l)	SO_4 (mg/l)	NO_3 (mg/l)	F (mg/l)	Na (mg/l)	K (mg/l)	Ca (mg/l)	Mg (mg/l)	Fe (mg/l)	Mn (mg/l)	TDS (mg/l)
Z 19484	8.07	420	14.4	136.64	43.97	2.9	12	0.11	22.4	3.9	38	15.3	0.19	0.01	260.8
Z 19485	8.32	455	14.4	156.16	49.08	3.3	7.5	0.11	25.6	6.72	42	15.4	1.57	0.12	345.7
Z 19486	7.56	830	14.4	268.4	116	6.63	11.46	0.13	61.9	10.2	59.33	25.75	0	0.01	515.6
Z 19487	8.39	328	0	112.24	28.37	2.73	4.1	0.14	36.68	1.93	22.52	5.07	0.55	0.02	363.9
Z 19488	8.68	405	14.4	141.52	31.49	8.33	2.97	0.27	38.26	2.54	28.88	10.92	0	0.01	242.6
Z 19489	8.18	468	14.4	156.16	41.13	10.5	1.84	0.21	37.32	2.69	36.71	13.74	1.89	0.05	309.3
Z 19490	8.51	497	19.2	194.22	32.06	2.77	25.86	0.1	41.15	5.66	33.79	16.6	0.03	0	303.3
Z19493	8.48	521	9.6	170.8	50.5	19	0.77	0.58	39.8	6.6	47.5	11.3	0	0	357.8
Z19491	8.63	400	14.4	146.4	28.37	11.2	0.72	0.72	36.5	2.07	28.5	10.8	0	0	285.1
Z20014	8.84	410	14.4	0	26.7	11	1.85	0.25	36	2.35	22	8.05	0	0	248.7
Z20128	7.71	547	223	0.00091	28.19	6.49	8.05	0.12	48.71	6.18	53.43	31.67	0.95	0	356
Z20129	6.57	433	0	0	39.7	4.21	2.99	0.16	26.6	2.53	44.4	13.4	0	0	272
Z20130	7.17	579	263	0.00107	24.61	6.17	8.92	0.14	56.19	5.31	52.63	33.08	0.25	0	376
Z20131	6.03	496	0	0	28.36	2.16	4.25	1.07	34.69	6.09	39	17	0	0	312
Z20132	7.7	429	179	0.00073	11.8	0.82	3.04	0.08	41.98	2.94	35.29	17.69	0.06	0	279
Z20133	7.29	463	0	0	41.13	2.12	4	0.13	37.1	5.78	35.8	16.4	0	0	291
Z20134	8.26	512	230	0.00093	10.95	0.69	4.58	0.11	66.47	4.23	44.63	20.72	0.03	0.07	333
Z20135	7.39	590	0	0	66.95	2.71	1.7	0	34.1	4	53.4	26.2	0	0	371
Z20136	6.67	373	169	0.00069	63.28	3.09	14.04	0.1	49.87	7.92	40.45	19.32	0.05	0	242
Z20137	8.88	577.56	171	0.00069	65.2	2.81	3.76	0.08	31.67	9.25	63.78	23.17	0	0	350
Z20138	7.78	310	74	0.0003	71.7	4.16	17.5	0.08	37.75	7.23	57.81	19.71	0	0	187.86
Z20768	8.1	480	199	0.00081	53.5	3.9	16.8	0.06	35.94	4.69	49.69	22.94	0.17	0.03	290.88
Z20140	8.42	412.54	219	0.00089	71	5.07	0.05	0.11	42.75	10.71	56.71	24.88	0.35	0	250
Z20141	8.07	412.54	137	0.00056	49.1	2.8	1.95	0.09	27.83	4.36	39.27	18.93	0.15	0	250
Z20142	6.61	430	135	0.00055	34.02	5.17	14.85	0.11	24.6	5.11	37.79	20.15	0.15	0	320
Z 20143	8.07	0	265	0.00108	50.2	3.97	1.54	0.12	46.15	13.57	60.8	28.29	1.91	0.08	360

BH No	PH	EC (µS/cm)	Alkalinity $CaCO_3$ (mg/l)	HCO_3 (mg/l)	Cl (mg/l)	SO_4 (mg/l)	NO_3 (mg/l)	F (mg/l)	Na (mg/l)	K (mg/l)	Ca (mg/l)	Mg (mg/l)	Fe (mg/l)	Mn (mg/l)	TDS (mg/l)
Z 20144	7.98	390	125	0.00051	43.6	2.52	2.65	0.05	24.04	5.23	39.31	16.75	0.07		236.34
Z20145	9.43	640	234	0.00095	60	3.9	0.63	0.11	39.71	8.4	59.31	23.03	0.89	0	387.84
Z 20146	8.19	400	138	0.00056	28.6	9.02	0.14	0.18	41.83	3.5	31.49	11.14	0.02		242.4
Z20147	8.2	363.04	157	0.00064	39.5	15		0.24	40.82	3.14	127.4	12.33	2.03	0.01	220
Z20148	7.26	148.51	49	0.0002	23.1	6.1	8.1	0.1	18.47	5.72	12.5	3.35	0.32	0	90
Z 20149	8.15	0	146	0.00059	50.37	20.3	0.33	0.17	37.36	3.72	43.71	16.68	0.19	0.03	260

5.7 Validation of the groundwater pollution vulnerability map

5.7.1 *Comparison of the Nitrate distribution map and the land-use map*

The approach to verifying the groundwater vulnerability evaluation involved the comparison of the nitrate distribution map with the land use map of the study area in order to establish the relationship between them. The two maps were placed side by side and visually inspected to determine their relationship. Generally, the nitrate content of groundwater in the study area is low with an average value of 6.42 mg/l. These values all fall below the 50.00 mg/l limit of BOS 32:2009 Class I drinking water specifications which means the groundwater is not yet polluted and it is safe for both human and animal consumption. Majority of the vegetation and barren land coincides with low nitrate concentrations as well as the water and wet area (Figure 5.20).

However, there are patches in the nitrate distribution map in excess of 10.00 mg/l, particularly the areas south of the farms near Leshibitse and east of the Masama Livestock Improvement Center (beyond the boundaries of the well field). These patches indicate the impact of human activities on the groundwater as they are associated with anthropogenic sources of pollution, e.g. improperly constructed waste disposal systems, livestock and crop production (Alwathaf and El Mansouri, 2011). As a result nitrates concentration values greater than

10.0 mg/l were expected to coincide with the residential and agricultural land as such land use is associated with increased occurrence of groundwater pollution by authors like Javadi et al. (2011). It was not the case in this study as the nitrates concentration in excess of 10.0 mg/l fell within the vegetation and bare land and the unconfined Ntane Sandstone aquifer. The general groundwater flow direction, geology and topography in the well field could be the reason for such discrepancies. The following scenarios were used as the possible explanation for the above mentioned discrepancies;

The first scenario involves the deposition of nitrates in the form of fecal waste and fertilizer application in the farms located SE of Leshibitse. Their infiltration does not occur directly beneath them during storm events since they overlie a confining layer comprising of the thick amygdaloidal basalt of the Stormberg Basalt Group. Instead, storm runoff washes the nitrates in the SSE direction following the drainage of the study area. The storm runoff containing the nitrates then infiltrated the soil and the underlying unconfined Ntane Sandstone aquifer, at a particular point along the Masama fault zone that recorded the highest hydraulic conductivity (Figure 5.13). The nitrates dispersed radially form this point within the aquifer and resulted in the red patch located south east of Leshibitse village in Figure 5.20 b which represent a zone of high nitrate content in groundwater.

The second scenario encompasses the infiltration and spreading of nitrates from the Masama Livestock Improvement Centre, a 43km^2 ranch capable of hosting 600 cattle (WSB, 2015). This center is located west of the A1 main road and beyond the boundaries of the study area. It also overlies the unconfined Ntane Sandstone aquifer and a couple of fault zones including Masama fault zone. The storm runoff containing the nitrates infiltrated the unconfined Ntane Sandstone aquifer probably along an extension of the Masama fault zone located west of Masama settlement. Masike (2008) also attributed the occurrence of groundwater recharge in the study area to the thin basalt layer within this fault zone and that was justified by the highest recharge value observed near Masama settlement (Figure 5.3). Following the general groundwater flow and drainage of the study area, the nitrates spread in the SE direction within the aquifer. That resulted in another red patch that represent nitrate concentrations in excess of 10.0 mg/l and coincides with areas within and near Masama settlement (Figure 5.20 b).

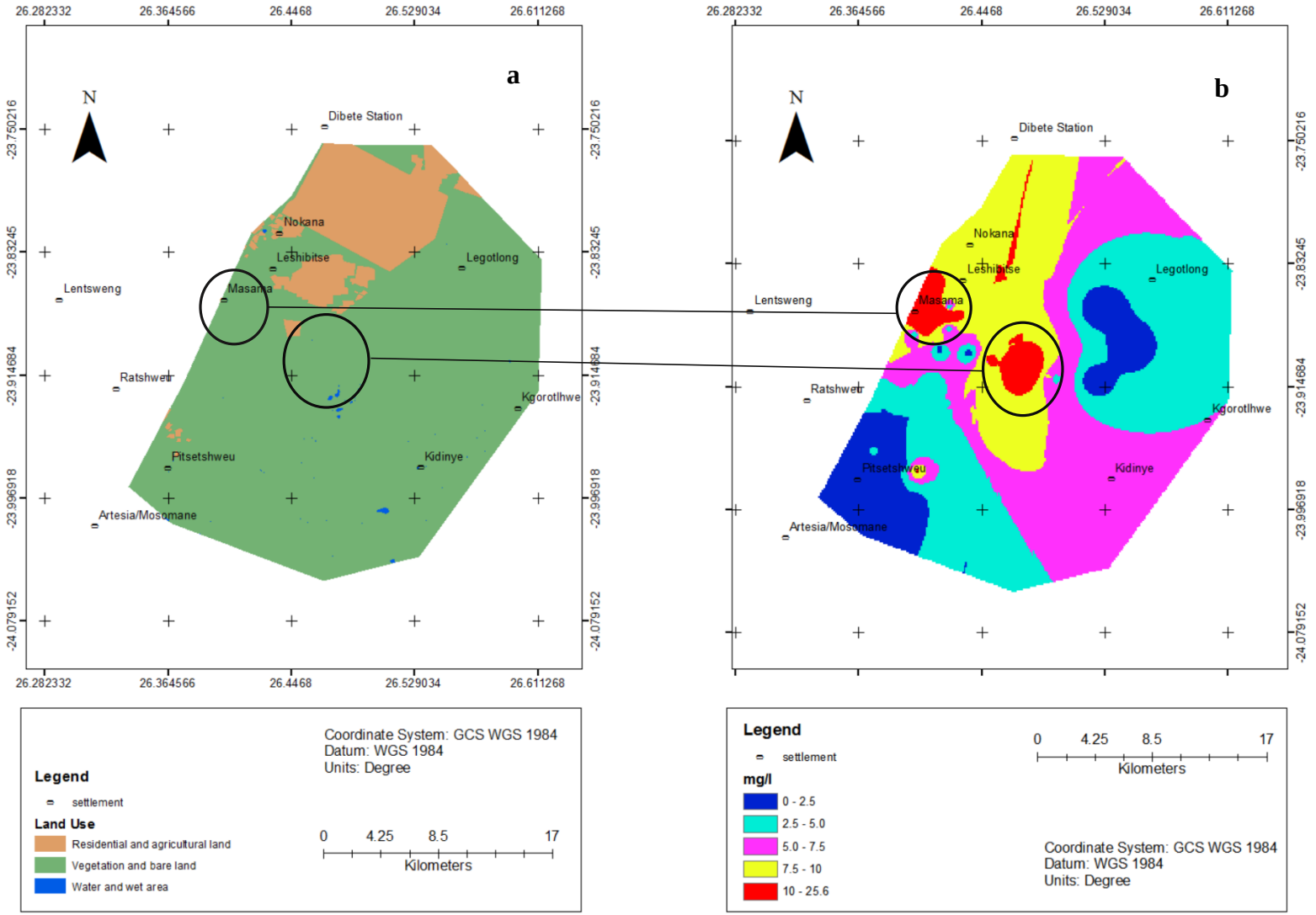

Figure 5.20. Comparison of the Land use map (a) and the nitrate distribution map (b) of the study area.

5.7.2 *Use of Spearman rank correlation coefficient*

The second validation procedure involved the use of the Spearman rank correlation coefficient to establish the statistical relationship between the land use map and nitrates distribution map. The outcome was a Spearman's rank correlation coefficient, r_s equal to 0.52 from a sample size equal to 33. This indicates that an intermediate direct correlation exists between the land use and nitrates distribution map. Basing on the above correlation coefficient and the visual comparison of land use and nitrate distribution maps, one can conclude that the nitrate content in the groundwater is slightly influenced by the type of land use in the study area. Therefore the occurrence of nitrate concentration in the groundwater in excess of 10 mg/l can be attributed to human impact and the integration of the land use parameter into the final groundwater pollution vulnerability map is justified.

6. CONCLUSION AND RECOMMENDATIONS

6.1 Conclusion

Intrinsic groundwater pollution vulnerability assessment provided a platform to assess and identify groundwater resources that are vulnerable and subsequently need protection from anthropogenic sources of pollution within Masama east well field. The outcome serves as a guideline for land use planners and decision makers to promote sustainable land use and enforce water quality protection within the well field. This partially fulfills the objectives of the water quality protection strategy in Botswana that was commissioned in 1992 by the Department of Water Affairs with the intention of protecting water resources by formulating and enforcing policies that prohibit pollution (WSB, 1993). Borehole records, geologic maps, pumping test data and information obtained from literature were compiled and reviewed in a GIS environment to produce a groundwater pollution vulnerability map of the well field. The fractured porous aquifers of the Karoo Supergroup and the fractured aquifers of the Waterberg Group make up the well field. The Karoo aquifers are confined by the massive Stormberg flood basalts along the western portion of the well field and unconfined in the absence of the basalt towards the ENE direction.

These are the most significant aquifers in the study area with regard to groundwater yield, particularly the Ntane sandstone aquifer of the Lebung Group that exhibits the highest transmissivity along fault zones. In some instances, the Mmamabula sandstone aquifer of the Ecca Group underlies the Ntane sandstone aquifer and form a multi-layered aquifer system with a 200m thick aquiclude separating the two aquifers (Masike, 2008). The Waterberg aquifers are less developed and bore significantly lower groundwater yields in comparison with the Karoo aquifers due to low primary porosity and complex hydrogeologic conditions caused by block faulting.

The net groundwater recharge in the well field as indicated by the chloride mass balance method is very low with an average of 15.49 mm/annum. Although this may be a negative impact during times of high groundwater abstraction, it also reduces the groundwater pollution vulnerability of the well field. Apart from the Stormberg Basalt Group, the vadose zone is dominated by the Kalahari Group that may increase the likelihood of pollutants reaching the groundwater. However, deep groundwater levels in the well field provide longer residence time for attenuation of pollutants, more especially the microbial pathogens.

Groundwater quality analysis indicates that some portions of the study area recorded nitrate concentration exceeding 10 mg/l, which is considered as a signature of human impact on the groundwater system. Other constituents of groundwater such as chloride ions were present at the time of analysis but in non-toxic concentrations. The overall current state of the groundwater quality in the well field is good and would not have any health implications when consumed by both human beings and livestock. The outcome of sensitivity analysis justified the use of all seven DRASTIC parameters in the standard DRASTIC map. The application of effective weights in combination with the addition of land use parameter to the standard DRASTIC map also improved the accuracy of the groundwater pollution vulnerability map and reflected the direct impact of human activities on the well field.

Very low groundwater vulnerability zones occur in the western portion and constitute 39.0% of the total well field area. These zones overlie a thick, massive Stormberg basalt confining layer and loamy sands. The deepest water levels and the highest elevation points in the well field were also observed within very low groundwater vulnerability zones. All these conditions offer very limited access, if not none for pollutants to migrate from the ground surface into the aquifer leading to very low to negligible groundwater vulnerability. Low groundwater vulnerability zones occur in patches throughout the well field and cover 19.9% of the overall study area. Such zones are characterized by low transmissivity, the absence of confining layer in some parts and existence of residential and agricultural land overlying the confining layer.

Moderate groundwater vulnerability zones cover 27.5% of the total well field area. The soil and vadose zone comprise of the Kalahari Group sands and both the depth to groundwater and transmissivity in such areas are moderate. The topography and hydrogeologic conditions of these zones favor infiltration rather than increased run-off, and are more likely to allow groundwater pollution in comparison to the zones discussed above. High groundwater vulnerability zones are the least abundant zones constituting 13.6% of the well field area and majority of them are confined to the south eastern portion. These zones are generally found in localized flat areas and in gravel soils underlain by unconsolidated sand that altogether offer very limited resistance against groundwater pollution.

6.2 Recommendations

Radioactive isotope data analysis should be incorporated into the outcome of this study in future to produce a more accurate and detailed groundwater pollution vulnerability map. This kind of analysis is essential for mapping groundwater pollution vulnerability since it is capable of estimating the residence time and pin-pointing the source of contaminants in a given aquifer with higher accuracy. The lineament density parameter should also be incorporated into the groundwater pollution vulnerability map as an additional parameter but only after lineaments contribution towards groundwater recharge has been verified using isotope data analysis (Abiye, 2013).

Microbial pathogens have detrimental effects on human health upon their ingestion and therefore, a review of microbial pathogens content in the groundwater within the study area is recommended in future. The very low and low groundwater vulnerability zones are recommended for urban and industrial development, residential and agricultural utilization. However, caution should be taken along fault zones as they might be preferential pathways for groundwater recharge and pollutants migration into the aquifer.

Moderate to high groundwater vulnerability zones are not recommended for extensive agricultural development, waste disposal and industrial sites. These zones, particularly the high groundwater vulnerability zones should be prioritized when implementing measures to protect groundwater resources in the well field. The public should also be sensitized about the groundwater pollution vulnerability state of such zones and the human activities that may lead to deterioration of groundwater resources.

This study has provided a relative evaluation of groundwater pollution vulnerability of Masama east well field but it is worth noting that the outcome is merely a general guide to the degree of groundwater pollution vulnerability within the area. It is therefore advisable to conduct further detailed studies prior to any form of agricultural, residential and industrial development. That is necessary to attain full comprehension of the groundwater processes and movement of potential contaminants and subsequently protect the groundwater resources in the well field.

7. REFERENCES

Abdullah, T., Ali, S., Al-Ansari, N., & Knutsson, S. (2015). Groundwater Vulnerability Mapping Using Lineament Density on Standard DRASTIC Model: Case Study in Halabja Saidsadiq Basin, Kurdistan Region, Iraq. Engineering, 7, 644-667. Retrieved from http://dx.doi.org/10.4236/eng.2015.710057

Abiye, T. (2013). The Use of Isotope Hydrology to Characterize and Assess Water Resources in South(ern) Africa. University of the Witwatersrand, School of Geosciences. Water Research Commission.

Acquah, B. (2007). The Impact of Drought on Household Food Security in the Limpopo Basin of Semi-Arid Southern Africa: The Case of Kgatleng District in Botswana. AAAE Conference Proceedings, (pp. 555-558).

Al-Adamat, R. A., Foster, I. D., & Baban, S. M. (2003). Groundwater Vulnerability and Risk Mapping for the Basaltic Aquifer of the Azraq Basin of Jordan Using GIS, Remote Sensing and DRASTIC. Applied Geography, 23(4), 303-324. doi:10.1016/j.apgeog.2003.08.007

Albinet, M., & Margat, J. (1970). Cartographie de la vulnérabilité à la pollution des nappes d'eau souterraine (Mapping of groundwater pollution vulnerability). Bull. BRGM 2ème Série, 3(4).

Alemaw, B., Shemang, E., & Chaoka, T. (2004). Assessment of groundwater pollution vulnerability and modelling of the Kanye Wellfield in SE Botswana – A GIS approach. Physics and Chemistry of the Earth, 29, 1125-1128.

Aller, L., Bennet, T., Leher, J. H., Petty, R. J., & Hackett, G. (1987). DRASTIC: A Standardized System For Evaluating Ground Water Pollution Potential Using Hydrogeological Settings. EPA.

Alwathaf, Y., & El Mansouri, B. (2011). Assessment of Aquifer Vulnerability Based on GIS and ARCGIS Methods: A Case Study of the Sana'a Basin (Yemen). Journal of Water Resource and Protection, 3, 845-855. doi:10.4236/jwarp.2011.312094

Amri, E. (2010). Germination of Terminalia sericea Buch ex Dc. Seeds: Effects of Temperature Regime, Photoperiod, Gibberellic Acid and Potassium Nitrate. American-Eurasian J. Agric. & Environ. Sci., 8(6), 722-727.

Anornu, G., Kabo-Bah, A., & Kortatsi, B. (2012). Comparability studies of high and low resolution digital elevation models for watershed delineation in the tropics: Case of Densu River Basin of Ghana. International Journal of Cooperative Studies, 1(1), 9-14.

Ashton, P., Love, D., Mahachi, H., & Dirks, P. (2001). An Overview of the Impact of Mining and Mineral Processing Operations on Water Resources and Water Quality in the Zambezi, Limpopo and Olifants Catchments in Southern Africa. Contract Report to the Mining, Minerals and Sustainable Development (SOUTHERN AFRICA), Project, by CSIR-Environmentek, Pretoria, South Africa, University of Zimbabwe, Geology Department, Harare, Zimbabwe.

Babiker, I., Mohamed, M., Hiyama, T., & Kato, K. (2005). A GIS-based DRASTIC model for assessing aquifer vulnerability in Kakamigahara Heights, Gifu Prefecture, central Japan. Science of the Total Environment, 345(127–140).

Bordy, E. M., Segwabe, T., & Makuke, B. (2010). Sedimentology of the Upper Triassic–Lower Jurassic (?) Mosolotsane Formation (Karoo Supergroup), Kalahari Karoo Basin, Botswana. Journal of African Earth Sciences, 58, 127–140.

Civita, M. (2004). Contamination Vulnerability Mapping of the Aquifer: Theory and Practice. Quaderni di Tecniche di Protezione Ambientale.

Colins, J., Sashikkumar, M., Anas, P., & Kirubakaran, M. (2016). GIS-based assessment of aquifer vulnerability using DRASTIC Model: A case study on Kodaganar basin. Earth Sciences Research Journal, 20(1), H1-H8. doi:http://dx.doi.org/10.15446/esrj.v20n1.52469

Cook, P. (2003). A guide to regional groundwater flow in fractured rock aquifers. 108.

Daly, D., Dassargues, A., Drew, D., Dunne, S., Goldscheider, N., Neale, S., . . . Zwhalen, F. (2002). Main concepts of the "European Approach" for (karst) groundwater vulnerability assessment and mapping. Hydrogeology Journal, 10(2), 340–345.

Davidson, L., Holysh, S., & Mayes, J. (2002). An Assessment of Aquifer Vulnerability Mapping Methods for the Oak Ridges Moraine. Ground and Water: Theory to Practice. Southern Ontario Section of the Canadian Geotechnical Society.

de Vries, J., Selaolo, E., & Beekman, H. (2000). Groundwater recharge in the Kalahari, with reference to paleo-hydrologic conditions. Journal of Hydrology, 238, 110–123.

El-Gamal, H. (2013). Tritium/Helium-3 Dating of River Infiltration: An Example from the Oderbruch Area, Berlin, Germany. Journal of Water Resource and Protection, 5, 46-53. Retrieved from http://dx.doi.org/10.4236/jwarp.2013.51006

Eriksson, E., & Khunakasem, V. (1969). Chloride concentration in groundwater recharge rate of deposition of chloride in the Israel coastal plain. Journal of Hydrology, 7, 178-197.

FAO, IFAD, & WFP. (2015). The State of Food Insecurity in the World 2015. Meeting the 2015 international hunger targets: taking stock of uneven progress, Rome.

Focazio, v., Reilly, T., Rupert, M., & Helsel, D. (2002). Assessing groundwater vulnerability to contamination: providing scientifically defensible information for decision makers. U.S. Geological Survey Circular, 1224. Retrieved from http://pubs.usgs.gov/circ/2002/circ1224/

Foster, S. (1987). Fundamental concepts in aquifer vulnerability, pollution risk and protection strategy, InVulnerability of Soil and Groundwater to Pollutants. (W. van Duijvenboden, & H. van Waegeningh, Eds.) TNO Comm. on Hydro. Research Hague, Proceeding and Information, 38, 69–86.

Fraga, C. M., Fernandes, L., F.A.L., P., Reis, C., & Moura, J. (2013). Exploratory assessment of groundwater vulnerability to pollution in the Sordo River Basin, Northeast of Portugal. Engenharia Civil, Civil Engineering, 66(1), 49-58.

Fritch, T. G., McKnight, C. L., Yelderman, J. C., & Arnold, J. G. (2000). An Aquifer Vulnerability Assessment of the Paluxy Aquifer, Central Texas, USA, using GIS and a modified DRASTIC approach. J. Environ. Manage., 25, 337–345.

Ghazavi, R., & Ebrahimi, Z. (2015). Assessing groundwater vulnerability to contamination in an arid environment using DRASTIC and GOD models. Int. J. Environ. Sci. Technol., 12, 2909–2918. doi:DOI 10.1007/s13762-015-0813-2

Gogu, R., & Dassargues, A. (2000). Current Trends and Future Challenges in Groundwater Vulnerability Assessment Using Overly and Index Methods. Environmental Geology, 36(6), 549-559. doi:10.1007/s002540050466

Goldscheider, N., Klute, M., Sturm, S., & Hotezl, H. (2000). The PI Method: A GIS-Based Approach to Mapping Groundwater Vulnerability with Special Consideration of Karst Aquifers. Zeitschrift für Angewandte Geollgie, 46(3), 157-166.

Gupta, N. (2014). Groundwater Vulnerability Assessment using DRASTIC Method in Jabalpur District of Madhya Pradesh. International Journal of Recent Technology and Engineering (IJRTE), 3(3).

Hao, J., Zhang, Y., Jia, Y., Wang, H., & Niu, C. (2017). Assessing groundwater vulnerability and its inconsistency with groundwater quality, based on a modified DRASTIC model: a case study in Chaoyang District of Beijing City. Arab J Geosci, 10(144), 1-16. doi:DOI 10.1007/s12517-017-2885-4

Hauke, J., & Kossowski, T. (2011). Comparison of values of Pearson's and Spearman's correlation coefficient on the same sets of data. Quaestiones Geographicae, 30(2), 87-93. doi:DOI 10.2478/v10117-011-0021-1

Javadi, S., Kavehkar, N., Mousavizadeh, & Mohammadi, K. (2011). Modification of DRASTIC model to map groundwater vulnerability to pollution using nitrate measurements in agricultural areas. Journal of Agricultural Science and Technology, 13(2), 239–249.

Jonker, B. (2016). Assessment of Groundwater Potential in the Eastern Kalahari Region, South Africa. MSc Dessertation, University of Witwatersrand, School of Geosciences, Johannesburg.

Joshua, W. (1991). Physical properties of soils of Botswana. UNDP Project, Field document 33, FAO, Soil mapping and Advisory Services.

Jovanovic, N., Thomas, A., & Saayman, I. (2006). Improved DRASTIC method for assessment of groundwater vulnerability to generic aqueous-phase contaminants. Conference Paper in WIT Transactions on Ecology and the Environment. doi:DOI: 10.2495/WM060421

Kinzelbach W., A. W.-H. (2002). A Survey of Methods for Groundwater Recharge in Arid and Semi-arid regions. Early Warning and Assessment Report Series,UNEP/DEWA/RS.02-2. United Nations Environment Programme.

Knox, R. C., Sabatini, D. A., & Canter, L. W. (1993). Subsurface transport and fate processes.

Lewis, W., Farr, J., & Foster, S. (1978). A Detailed Evaluation of the Pollution Hazard to Village Water-Supply Boreholes in Eastern Botswana. Report GS 10/4.

Li, R., & Merchant, J. W. (2013). Modeling vulnerability of groundwater to pollution under future scenarios of climate change and biofuels-related land use change: A case study in North Dakota, USA. Papers in Natural Resources, 368, 32-45. doi:10.1016/j.scitotenv.2013.01.011

Liggett, J., & Gilchrist, A. (2013). Technical Summary of Intrinsic Vulnerability Mapping Methods in the Regional Districts of Nanaimo and Cowichan Valley, British Columbia (2010). 64. doi:10.4095/287315

Lin, J., Ganesh, A., & Singh, M. (2012). Microbial pathogens in the Umgeni River, South Africa. WRC Report No. KV 303/12, Water Research Commission, Pretoria.

Lindhe, A., R. L., Johansson, P., & Norberg, T. (2014). Increase of Water Supply Safety by Managed Aquifer Recharge along the North-South Carrier – A pre-feasibility study. Final Report, Chalmers University of Technology, Department of Civil and Environmental Engineering, Göteborg, Sweden.

Lindhe, A., Rosen, L., Johansson, P., & Norberg, T. (2014). Final Report; Increase of Water Supply Safety by Manage Aquifer Recharge along the North-South Carrier-a prefeasibility study. Chalmers University of Technology.

Lindström, R. (2005). Groundwater Vulnerability Assessment Using Process-Based Models. TRITA-LWR PhD Thesis 1022, Stockholm.

Lodwick, W., Monson, W., & Svoboda, L. (1990). Attribute error and sensitivity analysis of map operations in geographical information systems: suitability analysis. Int J Geogr Inf Syst, 4(4), 413– 428.

Manyarara, T., J. Chifamba, J., & Tarugarira, F. (2016). Antifungal Activity of Ziziphus mucronata and Erythrina abyssinica Bark Crude Extracts on Cryptococcus neofomans and Candida albicans Species. (B. C.-Q. Rafik Karaman, Ed.) British Journal of Pharmaceutical Research, 10(3), 1-11. doi:10.9734/BJPR/2016/23843

Masike, S. (2008). The impact of climate change on cattle water demand and supply in Khurutshe, Botswana. PhD Thesis, University of Waikato, International Global Change Institute.

Mclaren, D. A., Hazell, R. T., & Gyopari, M. C. (1996). Water quality protection strategy in Botswana. Geoscience and Development, 4(5).

Mirbagheri, S. A. (2004). Modeling contaminant transport in soil column and ground water pollution control. International Journal of Environmental Science & Technology, 1(2), 141-150.

Modie, B. (2007). The Palaeozoic Palynostratigraphy of the Karoo Supergroup and palynofacies insight into palaeoenvironmental interpretations, Kalahari Karoo BasinBasin, Botswana. PhD thesis, unpublished.

Modie, B. N. (2000). The Karoo Supergroup of the Kalahari Basin: Report on a field visit to exposures in the Kalahari Karoo Basin of Botswana. Internal report, Geological Survey, Botswana.

Mongalo, N. (2013). Review: Peltophorum africanum Sond [Mosetlha]: A review of its ethnomedicinal uses, toxicology, phytochemistry and pharmacological activities. Journal of Medicinal Plants Research, 7(48), 3484-3491. doi:10.5897/JMPR2013.5302

Muhammad, A. M., Zhonghua, T., Dawood, A. S., & Earl, B. (2015). Evaluation of local groundwater vulnerability based on DRASTIC index method in Lahore, Pakistan. Geofísica Internacional, 54(1), 67-81.

Mweso, E. (2003). Evaluating the Importance of Soil Moisture Availability (as Land Quality) on Selected Rainfed Crops in Serowe Area, Botswana. MSc Thesis, International Institute for Geo-Information Science and Earth Observation.

Napolitano, P., & Fabbri, A. (1996). Single parameter sensibility analysis for aquifer vulnerability assessment using DRASTIC and SINTACS. In Proceedings of the HydrolGis application of geographic information systems in hydrology and water resources management. (a. H. K. Kova, Ed.) 559–566.

NRC. (1993). Groundwater vulnerability assessment, contamination potential underconditions of uncertainty. Washington DC: National Academy Press.

Oh, H., Kim, Y., Choi, J., Park, E., & Lee, S. (2010). GIS mapping of regional probabilistic groundwater potential in the area of Pohang City, Korea. (G. Syme, & T. Simmons, Eds.) Journal of Hydrology, 339, 158–172.

Oke, S. (2015). Evaluation of the Vulnerability of Selected Aquifer Systems in the Eastern Dahomey Basin, South Western Nigeria. PhD Thesis, University of the Free State, Institute for Groundwater Studies, Bloemfontein.

Panagopoulos, G. P., Antonakos, A. K., & J., L. N. (2000). Optimization of the DRASTIC Method for Groundwater Vulnerability Assessment via the Use of Simple Statistical Method and GIS. Hydrogeology Journal, Vol. 14(6), 894-911. doi:10.1007/s10040-005-0008-x

Petrie, B., Chapman, A., Midgley, A., & Parker, R. (2015). Risk, Vulnerability & Resilience in the Limpopo River Basin; Climate change, water and biodiversity – a synthesis. For the USAID Southern Africa "Resilience in the Limpopo River Basin" (RESILIM) Program, OneWorld Sustainable Investments, Cape Town, South Africa.

Piscopo, G. (2001). Groundwater vulnerability map, explanatory notes, Castlereagh Catchment, NSW. Department of land Water Conservation, Australia. Retrieved from

http://www.dlwc.nsw.gov.au/care/water/groundwater/reports/pdfs/castlereagh_map_notes.pdf

Porcel, D., Schuth, C., De Leon-Gomes, H., Hoppe, A., & Lehne, R. (2014, October 21). Land-Use Impact and Nitrate Analysis to Validate DRASTIC Vulnerability Maps using a GIS Platform of Pablillo River Basin, Linares, N.L., Mexico. International Journal of Geosciences, 1468-1489.

Reichhardt, F. J. (1994). The Molopo Farms Complex, Botswana: History, Stratigraphy, Petrography, Petrochemistry and Ni-Cu-PGE Mineralization. Exploration and Mining Geology, 3, 263-284.

Research, C. f. (2005). Draft Botswana country water report: Prepared for UN ECA as part of the preparation of the African water Development Report.

Robins, N., Chilton, P., & Cobbing, J. (2007). Adapting existing experience with aquifer vulnerability and groundwater protection for Africa. Journal of African Earth Sciences, 47, 30-38. Retrieved from http://www.elsevier.com/locate/jafrearsci

Saidi, S., Bouri, S., & Dhia, H. (2011). Sensitivity analysis in groundwater vulnerability assessment based on GIS in the Mahdia-Ksour Essaf aquifer, Tunisia: a validation study. Hydrological Sciences Journal, 56(2), 288-304. doi:10.1080/02626667.2011.552886

Secunda, S., Collin, M., & Melloul, A. (1998). Groundwater vulnerability assessment using a composite model combining DRASTIC with extensive agricultural land use in Isael's Sharon region. Journal of Environmental Management, 54: 39-57.

Seeyan, S., & Merkel, B. (2015). Groundwater Recharge Estimation for Shaqlaw-Harrir Basin in Kurdistan Region, Iraq. Journal of Environmental Hydrology, 23(4).

Segwabe, T. (2008). The Geological Framework and Depositional Environments of the Coal-Bearing Karoo Strata in the Central Kalahari Karoo Basin, Botswana. Theisis, Rhodes University.

Selaolo, E. (1998). Tracer studies and groundwater recharge assessment in the eastern fringe of the Botswana Kalahari: the Letlhakeng-Botlhapatlou area.

Setianto, A., & Triandini, T. (2013). Comparison of Kriging and Inverse Distance Weighted (IDW) Interpolation Methods in Lineament Extraction and Analysis. J. SE Asian Appl. Geol, 5(1), pp. 21–29.

Shiklomanov, I. (1993). World freshwater resources. In: Water in crisis: A guide to the world's fresh water resources. (G. P.H., Ed.) 67, 13-24.

Smith, R. A. (1984). The Lithostratigraphy of the Karoo Supergroup in Botswana. Bulletin 26, Geological Survey, Botswana.

Sophocleous, M. (2007). Groundwater Recharge. Encyclopedia of Life Support Systems (EOLSS).

Sorichetta, A. (2010). Groundwater vulnerability assessment using statistical methods. PhD Thesis, Universita degliStudidi Milano, Scuola di Dottorato in Terra, Ambiente e Biodiversita.

Stephenson, D., Shemang, E., & Chaoka, T. (2004). Water Resources of Arid Areas: Proceedings of the International Conference on Water of Arid and Semi-Arid Regions of Africa. In T. &. Francis (Ed.)., (pp. 714-718). Gaborone, Botswana.

Theis, C. V. (1935). The Relation Between the Lowering of the Piezometric Surface and the Rate and Duration of Discharge of a Well Using Groundwater Storage. Transactions of the American Geophysical Union, 16, 519-524.

Tombul, M., Koparal, A. S., & Ögˇütveren, Ü. B. (2005). Transport Modelling of Copper Contamination in Groundwater Caused by a Wood Preservation Plant. Water Quality Research Journal of Canada, Volume 40(No. 4), 469–475. doi:DOI: 10.2166/wqrj.2005.050

UNESC. (2007). Africa Review Report on Drought and Desertification. Fifth Meeting of the Africa Committee on Sustainable Development (ACSD-5), Regional Implementation Meeting (RIM) for CSD-16, Addis Ababa.

Van Stempvoort, D., Evert, L., & Wassenaar, L. (1993). Aquifer vulnerability index: a GIS compatible method for groundwater vulnerability mapping. Canadian Water Research Journal, 18, 25-37.

Van Stempvoort, D., Ewert, L., & Wassenaar, L. (1993). Aquifer Vulnerability Index (AVI): A GIS Compatible Method gor Groundwater Vulnerability Mapping. Canadian Water Resource Journal, 18(1), 25-37.

Verbeek, K. (1990). Soil Mapping and Advisory Services Botswana; Revised General Soil Legend of Botswana. Food and Agriculture Organization, United Nations Development Programme, Gaborone.

Verma, S. (2016). A Review Study on Acacia Tortillis. International Journal of Life Science & Pharma Research, 6(2).

Vias, J. M., Andreo, B., Perles, M. J., & Carrasco, F. (2005). A Comparative Study of Four Schemes for Groundwater Vulnerability Mapping in a Diffuse Flow Carbonate Aquifer Under Mediterranean Climatic Condition. Environmental Geology, 47(4), 586-595. doi:10.1007/s00254-004-1185-y

Vias, J. M., Andreo, B., Perles, M. J., & Carrasco, F. (2005). A Comparative Study of Four Schemes for Groundwater Vulnerability Mapping in a Diffuse Flow Carbonate Aquifer Under Mediterranean Climatic Condition. Environmental Geology, 47(4), 586-595.

Vias, J., Andreo, B., Perles, M., & Carrasco, F. (2004). A comparative study of four schemes for groundwater vulnerability mapping in a diffuse flow carbonate aquifer under Mediterranean climatic conditions. Environmental Geology, 47(4), 586–595.

Vrba, A., & Zoporozec, J. (1994). Guidebook on Mapping Groundwater Vulnerability. IAH International Contribution for Hydrogeology, 16, 131.

WHO. (2006). Protecting Groundwater for Health: Managing the Quality of Drinking-water Sources. London: IWA Publishing, Alliance House, 12 Caxton Street, London SW1H 0QS, UK.

Wigley, R. (1995). The Geochemistry of the Karoo Igeneous Volcanic and Intrusive Rocks of Botswana. University of Cape Town, Department of Geological Sciences. University of Cape Town.

Williamson, I. (1996). The geology of the area around Mmamabula and Dibete: including an account of the Greater Mmamabula Coalfield. District Memoir 6, Geological Survey, Botswana.

Wingqvist, G. Ö., & Dahlberg, E. (2008). Botswana Environmental and Climate Change Analysis.

WSB. (1993). Protection Zones and Guidelines for Major Wellfields, Aquifers and Dams in Botswana. Site-Specific Reports.

WSB. (2015). Drilling And Test Pumping Of 22 Replacement Production Boreholes at Masama-Makhujwane Wellfield. Final Report.

APPENDIX I: SAMPLES OF TEST PUMPING DATA ANALYSIS

Aquifer Thickness, b (m)	Discharge Rate, Q (m^3/h)	Transmissivity, T (m^2/day)	Hydraulic Conductivity, C (m/day)	Radial Distance to Pumping Well, R_{PW} (m)
85.0	90.0	2550.0	30.0	13.3

Recovery Method on an Observation Well

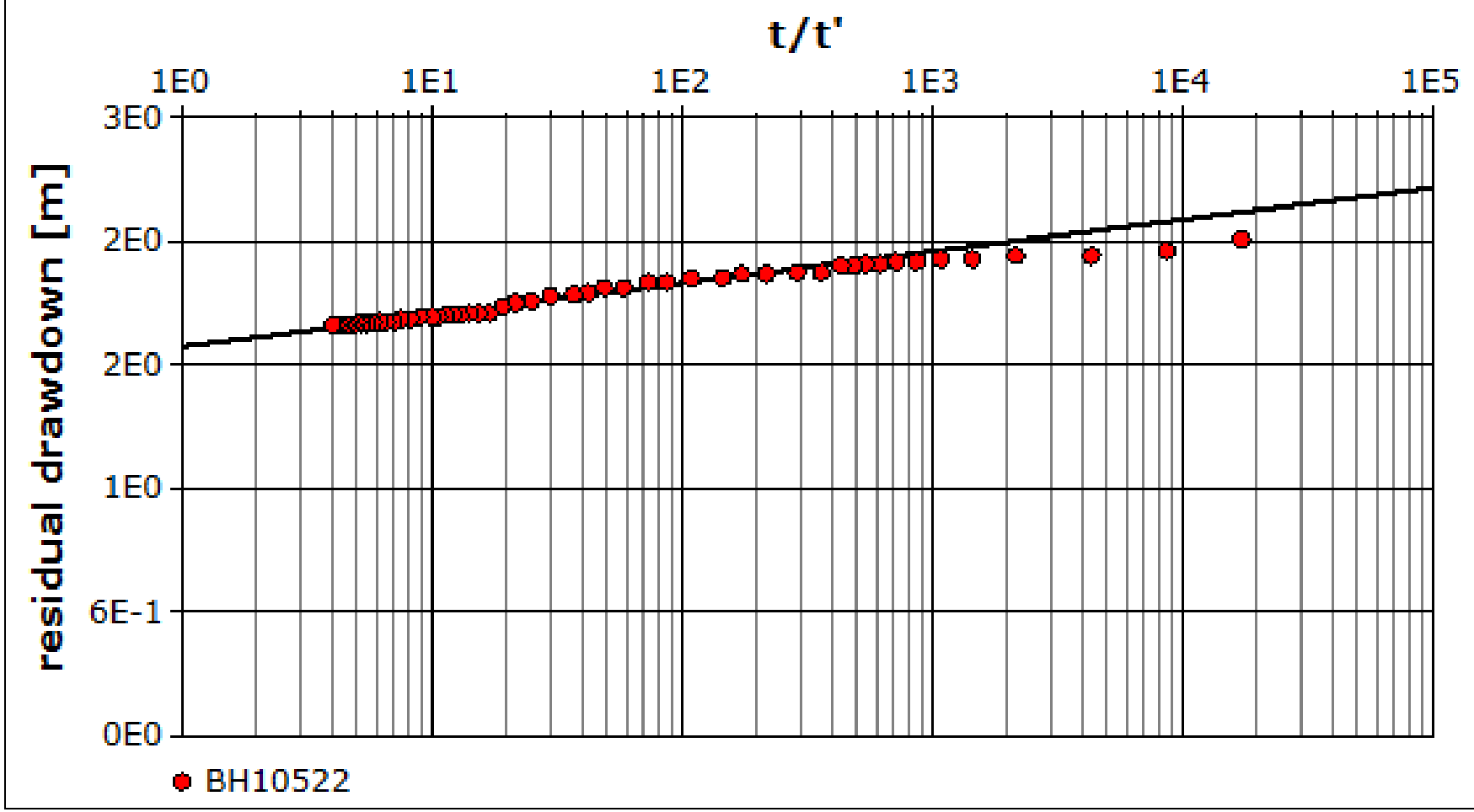

Aquifer Thickness, b (m)	Discharge Rate, Q (m^3/h)	Transmissivity, T (m^2/day)	Hydraulic Conductivity, C (m/day)	Radial Distance to Pumping Well, R_{PW} (m)
126.0	130.0	119.0	0.942	0

Recovery Method on a Pumping Well

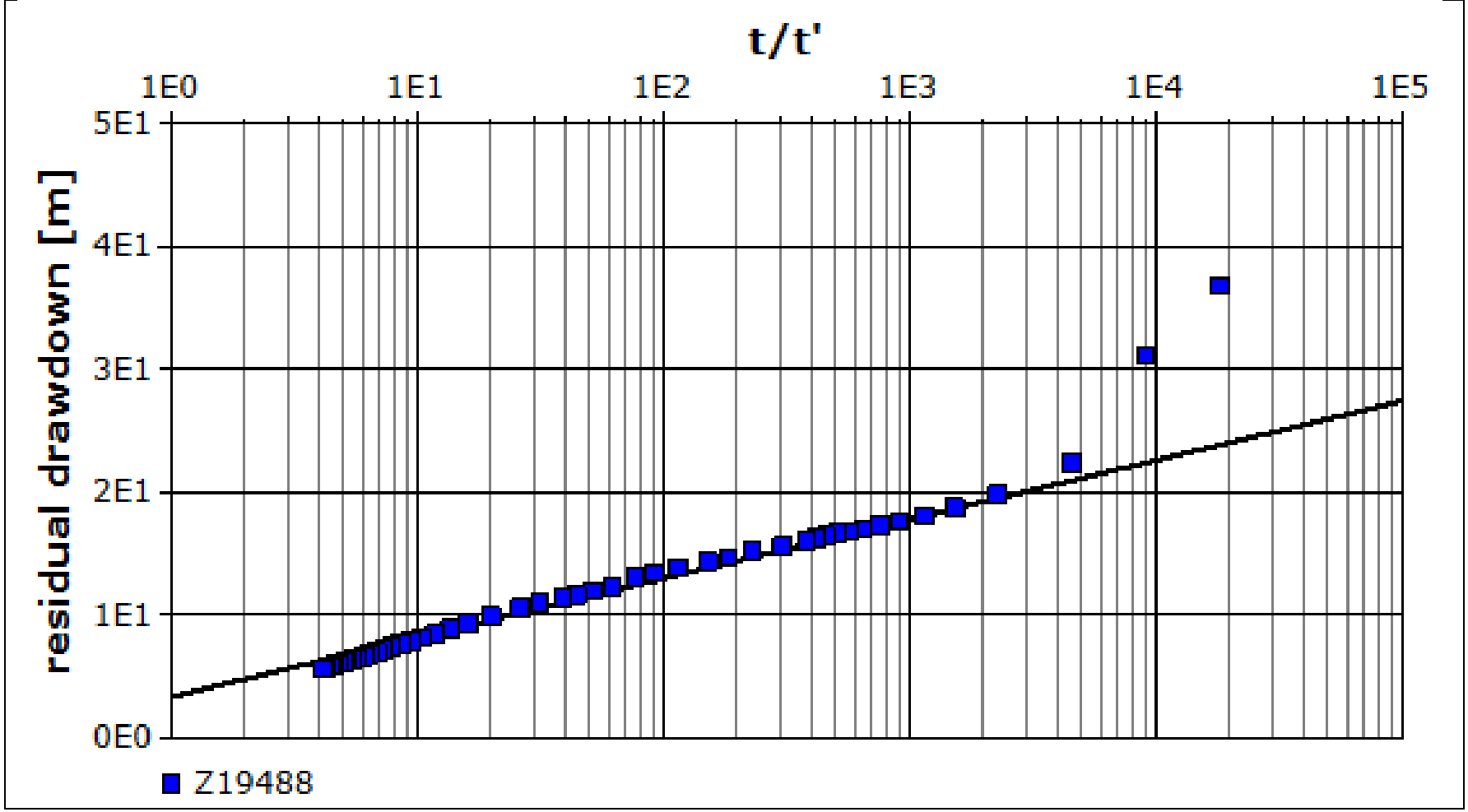

Aquifer Thickness, b (m)	Discharge Rate, Q (m^3/h)	Transmissivity, T (m^2/day)	Storativity	Hydraulic Conductivity, C (m/day)	Radial Distance to Pumping Well, R_{PW} (m)
142.0	60.0	22.79	7.23E-04	0.160	18.08

CRT Method on a confined aquifer (BH8321) for 148 hours

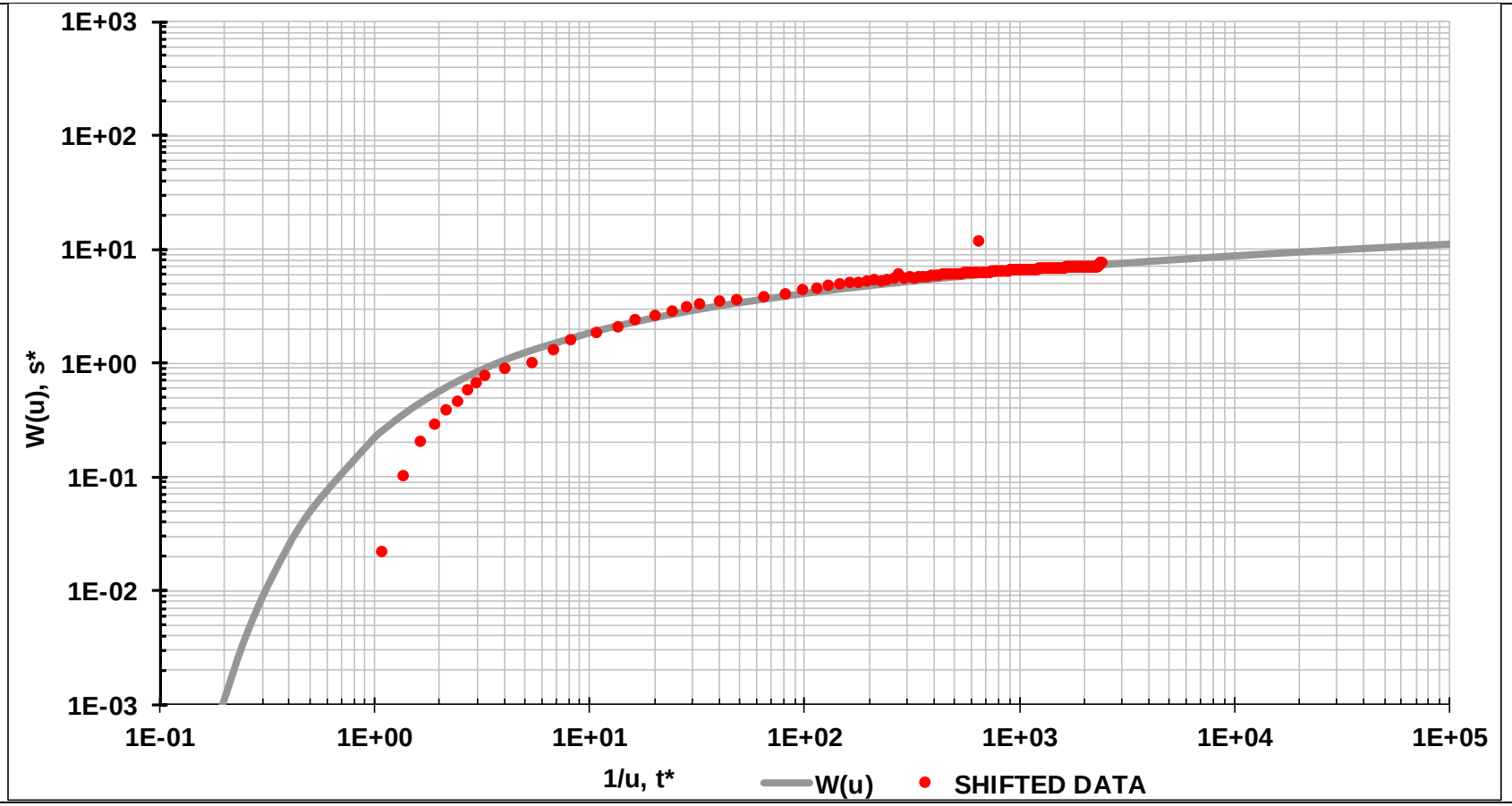

Aquifer Thickness, b (m)	Discharge Rate, Q (m^3/h)	Transmissivity, T (m^2/day)	Specific Yield	Hydraulic Conductivity, C (m/day)	Radial Distance to Pumping Well, R_{PW} (m)
137.0	15.0	87.8	0.173	0.641	18.2

CRT Method on an unconfined aquifer

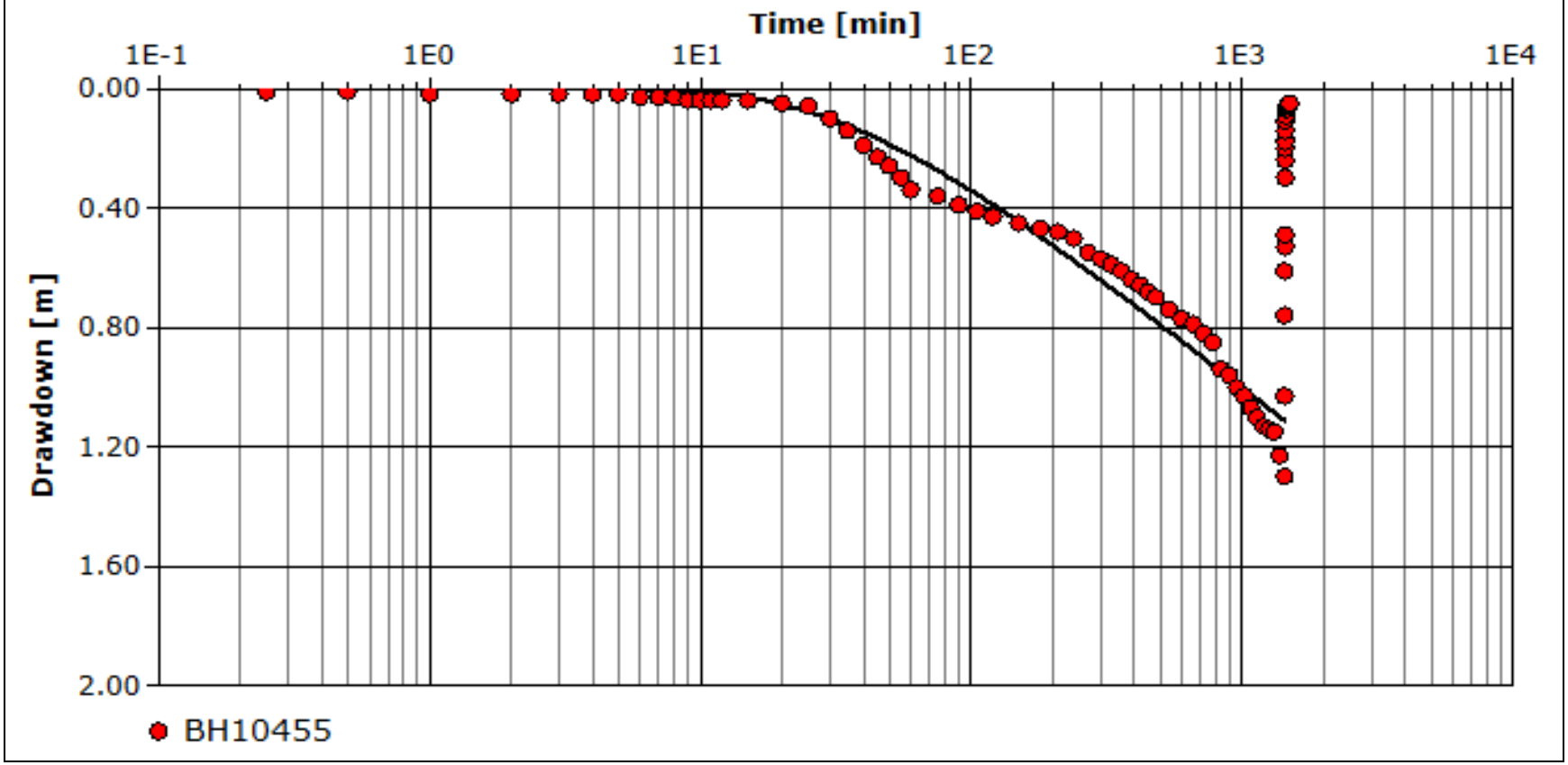

APPENDIX II: NET RECHARGE DEDUCTIONS

Borehole Number	Longitude	Latitude	Cl in Groundwater (mg/l)	Recharge			Average Recharge (mm/annum)
				TD-400	TD-525	TD-750	
Z19484	26.4924721403	-23.9087348164	44.68	8.95	11.75	16.79	12.50
Z20137	26.4510292683	-23.8977719672	77.2	5.18	6.80	9.72	7.23
Z20135	26.4383900620	-23.8923161023	66.81	5.99	7.86	11.23	8.36
Z20131	26.4249269280	-23.8757195304	29.55	13.54	17.77	25.38	18.89
Z20133	26.4253551514	-23.8610348776	40.23	9.94	13.05	18.64	13.88
Z20130	26.4182160485	-23.8828567800	20.35	19.66	25.80	36.86	27.44
Z20132	26.4022312900	-23.8793362294	12.05	33.20	43.57	62.24	46.33
Z20134	26.4059238840	-23.8751596302	21.79	18.36	24.09	34.42	25.62
Z20129	26.4138601691	-23.9143622379	39.7	10.08	13.22	18.89	14.06
Z20148	26.4037638552	-23.9712974301	26.12	15.31	20.10	28.71	21.38
Z19489	26.4019132092	-23.9910521982	41.13	9.73	12.76	18.23	13.57
Z19493	26.3838390033	-23.9777127106	43.55	9.18	12.06	17.22	12.82
Z19491	26.3755502131	-23.9659647496	28.37	14.10	18.51	26.44	19.68
Z19488	26.3749664151	-23.9586193819	31.07	12.87	16.90	24.14	17.97
Z20014	26.3939963815	-23.9664993162	26.7	14.98	19.66	28.09	20.91
Z19485	26.4641914814	-23.8674309434	49.93	8.01	10.51	15.02	11.18
Z19490	26.4226904689	-23.8661912945	33.34	12.00	15.75	22.50	16.75
Z19486	26.5796906887	-23.873668928	114.75	3.49	4.58	6.54	4.87
Z20149	26.3852522376	-23.9831144339	50.39	7.94	10.42	14.88	11.08
Z20768	26.4513538654	-23.8976737718	56.3	7.10	9.33	13.32	9.92
Z20147	26.3656609553	-23.9660598500	38.8	10.31	13.53	19.33	14.39
Z20146	26.3852810758	-23.9638182899	28.95	13.82	18.13	25.91	19.29
Z20145	26.5443584040	-23.8884122522	58.4	6.85	8.99	12.84	9.56
Z20144	26.4956238675	-23.9092419551	43.6	9.17	12.04	17.20	12.81
Z20143	26.5259137118	-23.8632921047	50.4	7.94	10.42	14.88	11.08
Z20142	26.4924511863	-23.9090689370	34.02	11.76	15.43	22.05	16.41
Z20141	26.5226078810	-23.9104119589	49.35	8.11	10.64	15.20	11.31
Z20140	26.4796148063	-23.9030648155	66.1	6.05	7.94	11.35	8.45

Borehole Number	Longitude	Latitude	Cl in Groundwater (mg/l)	Recharge			Average Recharge (mm/annum)
				TD-400	TD-525	TD-750	
Z20138	26.4792702059	-23.9032533243	54.92	7.28	9.56	13.66	10.17
Z20136	26.4786800033	-23.9034410000	45.14	8.86	11.63	16.61	12.37
Z20128	26.4189038372	-23.8894076567	28.19	14.19	18.62	26.61	19.81
Z13771	26.3106717670	-23.8713213640	51	7.84	10.29	14.71	10.95
Z13769	26.2882849246	-23.8414139469	42.5	9.41	12.35	17.65	13.14
Z13768	26.3208037342	-11.5322983755	25.83	15.49	20.33	29.04	21.62
Z13772	26.3039032677	-23.8568939063	63	6.35	8.33	11.90	8.86
Z13770	26.3171248750	-23.8506487402	28.5	14.04	18.42	26.32	19.59
Z13676	26.3537447065	-23.8326251285	81.75	4.89	6.42	9.17	6.83
Z13675	26.3668949335	-23.8986770563	22.25	17.98	23.60	33.71	25.09
Z13677	26.3449872467	-23.8910526276	45.5	8.79	11.54	16.48	12.27
Z13674	26.3346343380	-23.9024517446	24	16.67	21.88	31.25	23.26
Z13673	26.3473158935	-23.9183301438	38.5	10.39	13.64	19.48	14.50

APPENDIX III: CALCULATION OF HYDRAULIC PARAMETERS

Borehole ID	Type of Well	Aquifer Thickness (m)	Discharge (m^3/h)	Test Pumping Method	Method of Analysis	Transmissivity (m^2/day)	Hydraulic Conductivity (m/day)	Radial Distance to Pumping Well (m)
BH7152	Observation well	133	50	constant rate test	Neumann	527	3.962	20.7
BH7152	Observation well	133	50	recovery	Theis & Jacob	522	3.925	20.7
BH8325	Observation well	223	75	constant rate test	Theis	76.86	0.345	10
BH8325	Observation well	223	75	recovery	Theis & Jacob	80.8	0.362	10
BH7364	Observation well	85	90	constant rate test	Theis	5299.24	62.344	43.7
BH7364	Observation well	85	90	recovery	Theis & Jacob	4090	48.118	43.7
BH8321	Observation well	142	60	constant rate test	Theis	22.79	0.160	18.08
BH8321	Observation well	142	60	recovery	Theis & Jacob	19.2	0.135	18.08
BH8319	Observation well	129	80	constant rate test	Theis	52.12	0.404	15
BH8319	Observation well	129	80	recovery	Theis & Jacob	61	0.473	15
BH10448	Observation well	180	80	recovery	Theis & Jacob	123	0.683	14
BH10449	Observation well	162	45	constant rate test	Theis	66.29	0.409	12
BH10449	Observation well	162	45	recovery	Theis & Jacob	32.4	0.200	12
BH10450	Observation well	148	50	constant rate test	Theis	119.65	0.808	15
BH10450	Observation well	148	50	recovery	Theis & Jacob	35.6	0.241	15
BH10451	Observation well	169	30	constant rate test	Theis	104.51	0.618	18.55
BH10451	Observation well	169	30	recovery	Theis & Jacob	43.2	0.256	18.55
BH10452	Observation well	133	100	constant rate test	Theis	419.82	3.157	15
BH10452	Observation well	133	100	recovery	Theis & Jacob	486	3.654	15
BH10455	Observation well	137	15	constant rate test	Neumann	87.8	0.641	18.2
BH10455	Observation well	137	15	recovery	Theis & Jacob	160	1.168	18.2
BH10456	Pumping well	167	15	constant rate test	Theis	58.19	0.348	0
BH10456	Pumping well	167	15	recovery	Theis & Jacob	176	1.054	0
BH10515	Observation well	152	35	constant rate test	Theis	46.36	0.305	12
BH10515	Observation well	152	35	recovery	Theis & Jacob	42	0.276	12
BH10522	Observation well	85	90	constant rate test	Theis	177.06	2.083	13.3
BH10522	Observation well	85	90	recovery	Theis & Jacob	2550	30.000	13.3
Z19484	Pumping well	85	90	recovery	Theis & Jacob	128	1.506	0

Borehole ID	Type of Well	Aquifer Thickness (m)	Discharge (m^3/h)	Test Pumping Method	Method of Analysis	Transmissivity (m^2/day)	Hydraulic Conductivity (m/day)	Radial Distance to Pumping Well (m)
Z19485	Pumping well	131	85	recovery	Theis & Jacob	253	1.931	0
Z19486	Pumping well	133	50	recovery	Theis & Jacob	625	4.699	0
Z19488	Pumping well	126	130	constant rate test	Theis	29.97	0.238	0
Z19488	Pumping well	126	130	recovery	Theis & Jacob	119	0.944	0
Z19489	Pumping well	142	60	recovery	Theis & Jacob	17.9	0.126	0
Z19490	Pumping well	133	100	recovery	Theis & Jacob	522	3.925	0
Z19491	Pumping well	168	100	recovery	Theis & Jacob	51.2	0.305	0
Z19493	Pumping well	108	80	recovery	Theis & Jacob	35.4	0.328	0
Z20014	Pumping well	114	120	recovery	Theis & Jacob	41.3	0.362	0
Z20129	Pumping well	137	15	recovery	Theis & Jacob	3.08	0.022	0
Z20130	Pumping well	180	80	recovery	Theis & Jacob	250	1.389	0
Z20131	Pumping well	148	50	recovery	Theis & Jacob	49.4	0.334	0
Z20132	Pumping well	152	35	recovery	Theis & Jacob	40.9	0.269	0
Z20133	Pumping well	169	30	recovery	Theis & Jacob	55.1	0.326	0
Z20134	Pumping well	162	45	recovery	Theis & Jacob	27.4	0.169	0
Z20135	Pumping well	157	25	recovery	Theis & Jacob	29	0.185	0
Z20137	Pumping well	223	75	recovery	Theis & Jacob	131	0.587	0
Z20137	Pumping well	223	75	constant rate test	Theis	48.66	0.218	0
Z20148	Pumping well	129	80	recovery	Theis & Jacob	55.7	0.432	0

APPENDIX IV: GROUNDWATER LEVELS IN THE STUDY AREA

Borehole Number	Longitude	Latitude	SWL
Z19484	26.4924721403	-23.9087348164	51.50
BH7364	26.4931102056	-23.9063524313	51.80
BH10522	26.4930152981	-23.9063281832	52.25
BH8325	26.4593694318	-23.8877948854	50.42
Z20137	26.4510292683	-23.8977719672	51.56
Z20135	26.4383900620	-23.8923161023	59.70
BH10456	26.4387155491	-23.8897341029	60.35
BH10450	26.4252237508	-23.8730054006	64.94
Z20131	26.4249269280	-23.8757195304	63.20
Z20133	26.4253551514	-23.8610348776	61.33
BH10451	26.4255629975	-23.8584434273	62.80
Z20130	26.4182160485	-23.8828567800	65.90
Z20132	26.4022312900	-23.8793362294	68.67
BH10515	26.4025780519	-23.8765466570	70.08
Z20134	26.4059238840	-23.8751596302	64.30
BH10449	26.4061224060	-23.8725501170	66.69
Z20129	26.4138601691	-23.9143622379	53.42
BH10455	26.4142365516	-23.9115095378	54.60
Z20148	26.4037638552	-23.9712974301	52.00
BH8319	26.4041392498	-23.9686218050	50.00
Z19489	26.4019132092	-23.9910521982	51.50
Z19493	26.3838390033	-23.9777127106	59.00
Z19491	26.3755502131	-23.9659647496	51.75
Z19488	26.3749664151	-23.9586193819	48.50
Z20014	26.3939963815	-23.9664993162	55.00
Z19485	26.4641914814	-23.8674309434	49.00
Z19490	26.4226904689	-23.8661912945	58.00

Borehole Number	Longitude	Latitude	SWL
Z19486	26.5796906887	-23.873668928	33.30
BH10452	26.4230453326	-23.8636816906	58.20
BH8321	26.4020952133	-23.9882342109	51.38
BH7152	26.5791198816	-23.8744132535	34.80
BH10448	26.4184634103	-23.8802564665	70.08
Z20149	26.3852522376	-23.9831144339	49.56
BH10519	26.3856149515	-23.9804655487	49.56
Z20768	26.4513538654	-23.8976737718	50.00
BH8323	26.4512480911	-23.8951531594	50.00
BH10520	26.3660091036	-23.9634147535	46.00
Z20147	26.3656609553	-23.9660598500	46.00
Z20146	26.3852810758	-23.9638182899	41.85
Z20145	26.5443584040	-23.8884122522	45.10
BH8324	26.5446837825	-23.8822543455	45.10
Z20144	26.4956238675	-23.9092419551	51.60
BH10457	26.4958209041	-23.9065690819	51.60
Z20143	26.5259137118	-23.8632921047	49.17
BH10521	26.5588722019	-23.8608339119	49.17
Z20142	26.4924511863	-23.9090689370	58.00
Z20141	26.5226078810	-23.9104119589	44.34
BH10517	26.5229518648	-23.9077033714	44.34
Z20140	26.4796148063	-23.9030648155	50.00
Z20138	26.4792702059	-23.9032533243	52.00
BH8326	26.4795334015	-23.9004542482	50.00
Z20136	26.4786800033	-23.9034410000	58.10
Z20128	26.4189038372	-23.8894076567	63.45
BH10453	26.4193672193	-23.8868262237	63.45

Borehole Number	Longitude	Latitude	SWL
Z20139	26.4383666982	-23.8977262558	50.00
BH7155	26.5936890692	-23.9140070072	40.46
BH7183	26.5120856086	-23.7740660869	51.50
BH7275	26.4552125090	-23.9104530397	56.70
BH7287	26.4266380771	-23.9748755576	38.38
BH7294	26.4733559850	-23.8237506351	69.50
BH8373	26.4365102342	-23.9755854640	41.30

APPENDIX V: BOS 32: 2009 DRINKING WATER SPECIFICATIONS

Parameter	Units	BOS 32:2009 CLASS I (Ideal)	BOS 32:2009 CLASS II (Acceptable)
pH		5.5 – 9.5	5 - 10
Conductivity	Us/cm	1500	3100
TDS	mg/l	1000	2000
Sulphate	mg/l	250	400
Chloride	mg/l	200	600
Nitrate	mg/l	50	50
Fluoride	mg/l	1	1.5
Calcium	mg/l	150	200
Magnesium	mg/l	70	100
Potassium	mg/l	50	100
Sodium	mg/l	200	400
Iron	ug/l	300	2000
Manganese	ug/l	100	500
Turbidity	NTU	1	5
Zinc	mg/l	5	10
Alkalinity	mg/l	-	-
Nickel	ug/l	70	70
Chromium	ug/l	50	50
Cobalt	ug/l	500	500

Parameter	Units	BOS 32:2009 CLASS I (Ideal)	BOS 32:2009 CLASS II (Acceptable)
Cadmium	ug/l	3	3
Bromide	mg/l	-	-
Aluminium	ug/l	200	200
Copper	ug/l	2000	2000